Hydraulic and physical properties of alpine soils in relation to terrain and vegetation

How are soil hydraulic and soil physical properties related to vegetation and topography in an alpine environment (Meretschibach catchment, Valais, Switzerland)?

D.J.H. (Dick) van de Lisdonk

Utrecht University

Utrecht University, Faculty of Geosciences, MSc thesis Earth Surface and Water (GEO4-1520)

Author:	D.J.H. (Dick) van de Lisdonk
Student number:	6431917
1st supervisors:	T. (Thomas) Giesecke and J. (Jana) Eichel
2nd supervisor:	E.A. (Esther) Brakkee
ECTS Credits:	30 ECTS
Date:	31-12-2023

Abstract

High-mountain areas are hotspots of biodiversity and provide critical ecosystem services. These high-mountain areas are very sensitive to climate change. This causes temperature rise and strong changes in precipitation patterns, which leads to glacier retreat and snow cover reduction. Another consequence of climate change is greening, which is an increase in productivity of vegetation. This causes enhanced growth and spreading of vegetation. Besides the climatic conditions, greening depends on interactions between soil, vegetation and topography. This research aims to improve the insights in the relationships between soil, vegetation and topography in an alpine environment.

Data was collected on a field research in the Meretschibach catchment in Valais, Switzerland. Five different vegetation classes (bare, pioneer, grass, shrub and forest) were defined previously, from which 42 locations were randomly selected based on spectral characteristics using NDVI images. At these 42 locations plots of 2x2 m were installed. In these plots, various measurements of the surface cover, topography and soil characteristics were executed. Also, soil samples were collected, which were used to derive additional soil characteristics using experiments in the laboratory. To find out whether there are relationships between the measured soil, vegetation and topographic parameters a statistical analysis was executed, which consist of a correlation, boxplot, cluster, PCA and NMDS analysis. In the PCA and NMDS ordinations, the topographic and surface cover parameters were plotted passively as explanatory variables and the soil parameters as response variables.

One of the main findings is that the predefined vegetation classes are no good predictor for the soil characteristics. However, the correlation and boxplot analyses show that several soil characteristics can be related to vegetation. Moreover, vegetation cover has a large explanatory power for the variance in the soil parameters. This is also the case for rock cover, which has a negative association with vegetation cover.

From the different topographic parameters (elevation, slope angle, aspect and slope form), only elevation has a strong explanatory power on the variance of the soil data. This is mainly caused by climatic conditions which vary with elevation. Generally, slope angle and aspect cause an mosaic of microclimates that result in a strong variation in soil characteristics. However, the outcomes of the statistical analysis did not show the impacts of slope angle and aspect. The elevation dependent climatic conditions influence plant growth and consequently, several soil characteristics like the organic matter content and the soil depth. Besides, the soil microbial activity depends soil temperature and moisture, which is also influenced by the elevation dependent climatic conditions. This controls the soil nutrient cycle and therefore, the soil development. All together, they cause elevation to have a large explanatory power on the variance in soil data.

It is expected that greening will intensify in the Meretschibach catchment due to climate change. Upward migration of vegetation is likely to occur at locations where the snow cover duration shrinks due to climate change. Furthermore, stable soils that are relatively developed are the most favorable conditions for plant colonization. Greening causes increased evapotranspiration rates in the catchment. Therefore, decreased precipitation together with increased evapotranspiration during summer in the future, will cause a reduction in runoff from the catchment. This may result in browning, which is a decrease in productivity of vegetation. Greening is also beneficial for increasing soil depth and the water holding capacity of soils. Consequently, it will reduce the runoff from the catchment and therefore, greening may have a dampening effect on the increased runoff in the winter due to climate change.

Table of contents

1 Introduction

High-mountain areas are hotspots of biodiversity and provide critical ecosystem services (Alewell et al., 2015; Donhauser & Frey, 2018; Hagedorn et al., 2019; Körner, 2004; Y. Yang et al., 2018). These high-mountain areas are very sensitive to climate change (Castelli, 2021; Giaccone et al., 2019; Rosbakh et al., 2014; Siles et al., 2016; Xu et al., 2020), where the European Alps have experienced a temperature rise of 0.3 °C (± 0.2°C) per decade over the last few decades, which is 0.2 ± 0.1°C higher than global average (Intergovernmental Panel On Climate Change (Ipcc), 2022). Also, annual precipitation in the European Alps is likely to increase with 5-20% at 2100.

Under pressure of climate change, the ecosystems in high mountain areas are changing fast: glaciers are likely to lose more than 80% of their mass in 2100 for RCP8.5, and low elevation snow depth will decrease 10-40% in 2031-2050 in comparison to 1986-2005 (Intergovernmental Panel On Climate Change (Ipcc), 2022). The snow cover retreat is mainly caused by temperature rise at all elevations, and by enhanced rainfall in comparison to snowfall during winter (Intergovernmental Panel On Climate Change (Ipcc), 2022; Kotlarski et al., 2023; Viviroli et al., 2011). The snow cover reduction in combination with the expected increase in precipitation will change the discharge and regimes of the rivers flowing out of the Alps (Gobiet et al., 2014; Kotlarski et al., 2023). All these changes will affect the water cycle and therefore, the entire hydrological system in the Alps.

Simultaneously with the decline of snow cover, plant species are shifting upwards and greening occurs, which is mainly caused by temperature rise (Rosbakh et al., 2014). This "greening" means an increase in productivity of vegetation, which results in enhanced growth and spreading of vegetation (Carlson et al., 2017; Hagedorn et al., 2019; Heijmans et al., 2022; Rumpf et al., 2022). Long-term changes in greening can be measured using NDVI images (Rumpf et al., 2022). Over the last four decades, greening occurred in 77% of the area above the tree line in the European Alps (Rumpf et al., 2022). Greening has a positive feedback on snow cover reduction, because larger vegetation can trap snow that is blown up by the wind, which leads to increased radiation exchanges and consequently, enhanced snowmelt (Rumpf et al., 2022).

A thinner snow pack can cause a decreased thermal insulation and lower amounts of meltwater. This can have a negative effect on vegetation growth, especially in times of droughts, which will occur more frequently under increasing pressure of climate change (Heijmans et al., 2022; Rumpf et al., 2022). Eventually, browning of the vegetation can occur, which is a decrease in vegetation productivity. However, this is only the case in less than 1% of the area for short events (Rumpf et al., 2022). The decrease in snow cover and the increase in greening both result in a lower albedo, which will enhance the effects of climate change (Rumpf et al., 2022). Greening counteracts the effects of climate change by CO_2 sequestration, but the vegetation productivity in mountainous areas has only small effects on a global scale (Rumpf et al., 2022).

The characteristics and functioning of soils are also changing fast under pressure of climate change (Martinez-Almoyna et al., 2020). Soils have a parallel development with vegetation. Hence, vegetation provides organic matter to the soil by the turnover of litter and fine roots (Y. Yang et al., 2018). The decomposition of organic matter by microbes provides nutrients to the soil, which are beneficial for plant growth and soil development (Donhauser & Frey, 2018; Hagedorn et al., 2019; Martinez-Almoyna et al., 2020; Siles et al., 2016; Wu et al., 2016; Y. Yang et al., 2018; Yimer et al., 2006). Microbial activity is controlled by the local climate since it depends on soil temperature and soil moisture (Donhauser & Frey, 2018; Siles et al., 2016; Tyagi et al., 2023; Wu et al., 2016). Mountain areas contain a large variation in topography, which in turn, causes a large variation in climatic variables like air temperature,

precipitation and solar radiation. This causes a large variety of soils and vegetation in mountain areas (Aalto et al., 2013; Alewell et al., 2015; Donhauser & Frey, 2018; Hörsch, 2003; Yimer et al., 2006).

Furthermore, soils are important water storages, which makes them crucial components in the water cycle (Gao & Shao, 2012). The available soil moisture for vegetation and microbes, is controlled by soil characteristics and the local hydrological fluxes like infiltration, surface runoff and percolation. Vegetation also determines several hydrological fluxes: evapotranspiration transfers 60-80% of precipitation back into the atmosphere (Castelli, 2021). In addition, infiltration of atmospheric water into the soil is partly controlled by vegetation. Hence, interception and succeeding evaporation can prevent water to infiltrate (Oki et al., 2004; Wang et al., 2013). Furthermore, plants extract water from deeper soil layers for transpiration (Oki et al., 2004). On the contrary, roots create preferential flow paths which can accelerate infiltration rates of soils (Maier et al., 2020).

Thus, soil is a critical factor in the distribution of vegetation and the hydrological cycle in alpine environments, which is in turn, related to the local topography. The aim of this research is to get better understanding in the relationships between soil, vegetation and topography. The goal of this research can be expressed by the following research question:

> *How are soil hydraulic and soil physical properties related to vegetation and topography in an alpine environment (Meretschibach catchment, Valais, Switzerland)?*

To answer this question, three sub-questions must be considered:

1. *What are the relationships between soil and topographic properties?*
2. *What are the relationships between soil and vegetation properties?*
3. *What are the relationships between topographic and vegetation properties?*

To better understand the interdependence of soil, hydrology, topography and vegetation, first a literature study was executed. Thereafter, data were derived and soil samples were collected during a field work in the Meretschibach catchment in Valais, Switzerland. The samples were analyzed in the lab by various experiments. Afterwards, a statistical analysis was executed with the data from the field and the lab.

In the next chapter, the most important background information is described. Chapter 3 outlines the study area. In the Methodology, the most important steps of the field and lab work, and statistical analysis are explained. Chapter 5 provides the most important results of the statistical analysis. These results will be evaluated and discussed in chapter 6. Chapter 7 concludes the main findings of this research. The last two chapters are the references and appendix.

2 Background information

2.1 Characteristics of alpine soils

Mountain soils are typically shallow, rocky, acidic, infertile, immature and have poorly developed horizons (Donhauser & Frey, 2018; Kirkpatrick et al., 2014; Tyagi et al., 2023). Soil formation is mainly controlled by the factors time, climate, lithology, organisms and topography (Alewell et al., 2015; Egli et al., 2014; Kirkpatrick et al., 2014). The shallow and relatively undeveloped soils in alpine environments are the result of not very appropriate climatic conditions and a relatively young geological age of the parent material (Alewell et al., 2015; Donhauser & Frey, 2018). Well-developed soil horizons are uncommon in mountainous areas because they require long-lasting stable conditions (Donhauser & Frey, 2018).

Quantitatively, soil formation is equal to soil production minus denudation (Alewell et al., 2015). Where soil production is the sum of the amount transformed from parent material into soil, the lowering of bedrock and a supply of atmospheric deposition (Alewell et al., 2015; Egli et al., 2014). The denudation rate is controlled by erosion/deposition rate and the weathering rate (Alewell et al., 2015). The rate of erosion depends on several soil characteristics like soil texture, organic matter content, soil structure and root density (Alewell et al., 2015).

2.2 Physical and hydraulic soil properties

As mentioned in the introduction, soils play an important role in the hydrological cycle (Gao & Shao, 2012). The soil water storage and many hydrological fluxes are controlled by various soil physical and hydraulic properties like soil texture, saturated hydraulic conductivity, porosity, soil depth, bulk density, organic matter content (Hartmann et al., 2020). On the other hand, the behavior of a hydrological system influences the formation of soils (Alewell et al., 2015).

One of the most important soil hydraulic properties is the saturated hydraulic conductivity (k_{sat}), which is the water flux or seepage velocity per unit area for a constant water potential gradient and a saturated soil (Gupta et al., 2021; Zuo & He, 2021). It is a critical component in the water balance as it determines the partitioning between infiltration and overland flow at the soil surface (Gupta et al., 2021; Maier et al., 2020). Consequently, k_{sat} affects soil erosion by surface runoff, because surface runoff depends on this partitioning of water. Groundwater flow in the saturated and in the unsaturated zone is controlled by k_{sat}, which makes it a major determining factor of water distribution in the subsurface. Plant water availability, soil development and weathering rates are affected by the distribution of soil water, and consequently by k_{sat} (Maier et al., 2020; Y. Yang et al., 2020; Zuo & He, 2021). It is also one of the variables in Darcy's Law for saturated flow, and in Richards equation for unsaturated flow (Zuo & He, 2021). Therefore, k_{sat} is an important input parameter for many hydrological models (Zuo & He, 2021).

Vegetation, soil development and weathering influence the k_{sat} (Maier et al., 2020). Root density and soil organic matter are positively correlated with k_{sat}, which leads to preferential flow and the presence of macropores (Li et al., 2007; Zuo & He, 2021). Furthermore, aggregate stability and organic matter content are beneficial for k_{sat}, because they improve the soil and pore structure (Li et al., 2007; Zuo & He, 2021). An improved soil and pore structure means that the tortuosity of the soil becomes smaller and the connectivity larger, which enhances the k_{sat} (Kia et al., 2017). Also the soil texture affects the k_{sat}, which generally decreases for fine textured soils and increases for gravel content (Gupta et al., 2021; Maier et al., 2020; Y. Yang et al., 2020). Moreover, soil development causes decreasing permeability and consequently, decreasing k_{sat} values (Maier et al., 2020). All in all, the strong heterogeneity of soils in mountain areas results in relatively large variations of k_{sat} in horizontal and vertical direction (Y. Yang et al., 2020).

Another important soil hydraulic property is the water holding capacity, which controls the soil water storage, redistribution and availability, and potential evaporation (F. Yang et al., 2014). Many soil physical properties and climatic variables influence the soil moisture content: particle size distribution (soil texture), soil structure, porosity, specific surface area, depth of the soil, mineralogical composition, salinity, pore fluid characteristics, degree of compaction, presence of contaminants, organic content, temperature and humidity (Aalto et al., 2013; Dai et al., 2020; Hartmann et al., 2020; Li et al., 2007; S.U. et al., 2014; Wang et al., 2013). Of course, the soil moisture content depends on influxes like infiltration of precipitation, and effluxes like percolation and evapotranspiration.

The other relevant soil hydraulic properties, wilting point and field capacity, can be the best explained using the soil water retention curve (Figure 1), which expresses the relation between the soil moisture content and the soil suction (Cianfrani et al., 2019; S.U. et al., 2014). The parameter that represents the soil suction is the matric potential (F), which is the force that is required to extract water from the soil (Cianfrani et al., 2019). The logarithm of the absolute value of the matric potential is commonly used to calculate the suction, which is the pF value. A pF value of 4.2 is the permanent wilting point, which means that most plants will not survive these circumstances (Cianfrani et al., 2019). The field capacity has a pF value of 2.7, which is the soil water content in the soil after gravitational drainage has stopped (Cianfrani et al., 2019). The plant available water in a soil is amount of water between the difference field capacity and permanent wilting point (Cianfrani et al., 2019; S.U. et al., 2014). The field capacity and permanent wilting point differ per soil and vegetation type, because they depend on soil and vegetation characteristics (Cianfrani et al., 2019).

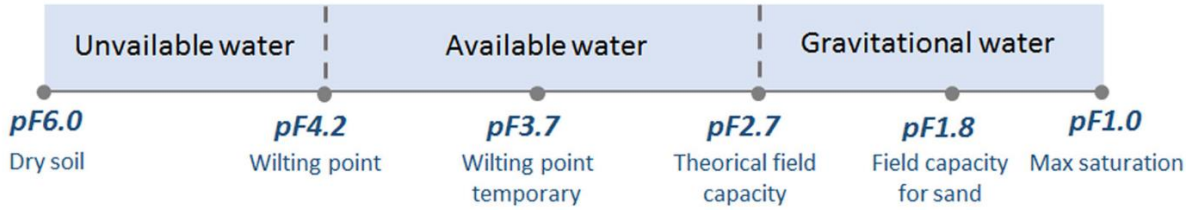

Figure 1: Soil water availability in relation to the corresponding points on the water retention curve. The soil water content at different values of pF characterizes the soil water holding capacity (Cianfrani et al., 2019).

2.3 Soil-topography interactions

Mountains have a strongly varying topography on a short spatial scale due to many geological and geomorphological processes (Donhauser & Frey, 2018; Tyagi et al., 2023; Yimer et al., 2006). Topographic variables like slope angle (Kirkpatrick et al., 2014), slope form, aspect, elevation, and erodibility of parent material influence the development of soils (Aalto et al., 2013; Yimer et al., 2006). The local mountain climate is a major determining factor for soil development, which is strongly affected by topography (Kirkpatrick et al., 2014). Climatic variables like water fluxes, incident radiation, air flow, temperature, heat flow and relative humidity vary largely on a relatively small spatial scale in mountain areas (Aalto et al., 2013; Donhauser & Frey, 2018; Hörsch, 2003; Yimer et al., 2006). This results in a large variation in microclimates in mountainous areas, which leads to a large variation in pedogenic processes (Aalto et al., 2013; Donhauser & Frey, 2018; Yimer et al., 2006). These pedogenic processes are affected by changes in chemical, physical and biological processes, and the distribution of vegetation (Donhauser & Frey, 2018; Yimer et al., 2006). This influences the plant health and plant species composition, weathering rates and leaching intensity, which results in changes in organic matter content, clay content, mineralogy, cation exchange capacity, and hydrology (Yimer et al., 2006). As a result, there is a strong soil heterogeneity in mountainous areas.

Soil heterogeneity is caused by erosion and deposition of soil material, which has a larger contribution than the supply from the underlying parent material (Donhauser & Frey, 2018). The rate of erosion and deposition also depends on topography (Alewell et al., 2015; Donhauser & Frey, 2018). For example, fine sediments end up predominantly in depressions (Aalto et al., 2013). Soils are more likely to form on weathered material than directly on bedrock (Donhauser & Frey, 2018). Also nutrients can be accumulated in depressions or downslope areas, which is beneficial for soil development (Donhauser & Frey, 2018). Thus, soils on relatively steep or convex slopes are prone to erosion, while relatively gentle or concave slopes are likely to gain sediments and nutrients from above and therefore, more favorable for soil development (Alewell et al., 2015; Donhauser & Frey, 2018; Sabzevari & Talebi, 2019).

The local hydrology has also large variations due to the mountain topography. For example, the topography determines whether a location receives or loses water by affecting the flow path of surface runoff and the drainage of soil moisture along a slope (Aalto et al., 2013). Moreover, the distribution and thickness of snow is affected by the topography, which mostly accumulates in depressions (Aalto et al., 2013; Rumpf et al., 2022).

The soil moisture content and soil temperature are controlled by incident radiation, which is strongly influenced by the slope aspect (Aalto et al., 2013; Wang et al., 2013). Generally, south facing slopes receive the most incident radiation on the northern hemisphere, which will result in relatively large evapotranspiration rates (Wang et al., 2013). However, Penna et al., (2009) concluded that topography is a relatively poor predictor for the spatial variability of soil moisture content.

2.4 Soil-vegetation interactions

As explained in section 1.1, the rate of soil erosion strongly depends on soil characteristics. Besides this, vegetation cover plays also a crucial role in this process (Alewell et al., 2015; Meusburger et al., 2010). Hence, soil detachment by raindrops is decreased by vegetation by reducing the impact of raindrops, the strength and velocity of surface runoff are reduced (Alewell et al., 2015; Isselin-Nondedeu & Bédécarrats, 2007; Meusburger et al., 2010). Moreover, the infiltration rate of soils increases due to the presence of vegetation and the soil stabilizes by improved physical, chemical and biological properties (Caviezel et al., 2014; Isselin-Nondedeu & Bédécarrats, 2007; Meusburger et al., 2010). Besides preventing soil erosion, vegetation can also trap sediments (Isselin-Nondedeu & Bédécarrats, 2007). Plant length and a complete canopy are crucial factors for sediment trapping (Isselin-Nondedeu & Bédécarrats, 2007).

The presence of vegetation can change some soil physical properties. For example, the litter production of vegetation results in accumulation of organic material at the soils surface (Y. Yang et al., 2018). This affects the soil and pore structure, which can enhance the soil stability (Y. Yang et al., 2018). Moreover, the organic matter can be decomposed by microbes, which leads to an increase in bioavailability of nutrients. This is a positive feedback on vegetation (Hagedorn et al., 2019; Yimer et al., 2006). Vegetation affects the pore structure also by their roots (Li et al., 2007; Zuo & He, 2021). These changes in soil physical properties due to vegetation have also an impact on the soil hydraulic properties, like the k_{sat} (Li et al., 2007; Zuo & He, 2021).

Several hydrologic fluxes are affected by vegetation, and therefore, the soil moisture content will change. Hence, the soil moisture content can be reduced by the extraction of water for transpiration (Aalto et al., 2013; Kemppinen et al., 2021), and preventing infiltration of precipitation by interception and succeeding evaporation (Wang et al., 2013). On the other hand, vegetation can enhance the infiltration capacity of soils by improving pore networks with their roots (Li et al., 2007; Zuo & He, 2021), and due to relatively large soil organic matter contents (Wang et al., 2013). The presence of vegetation provides shading of the soil, which will reduce the soil surface temperature during summer, and therefore, can reduce the bare soil evaporation (Aalto et al., 2013; Hagedorn et al., 2019; Kemppinen et al., 2021). All in all, vegetation mediates the fluctuations in soil moisture content (Aalto et al., 2013).

On a large scale, air temperature plays a major role in the vegetation distribution in mountains. As explained in the introduction, greening occurs in the Alps due to temperature rise, which caused an upward shift of vegetation (Rumpf et al., 2022). However, the upward shift of vegetation lags behind the rising air temperature, because the soil temperature has a delayed increase from the air temperature rise (Hagedorn et al., 2019). In turn, this leads to a delayed increase in pedogenic processes which are crucial for the upward shift of vegetation. So, soil development is a key limiting factor for the upward vegetation shift and greening in mountains (Hagedorn et al., 2019).

3 Study area

The Meretschibach catchment is with 9.2 km^2 a relatively small catchment, which flows out into the valley of the Rhône river in southwestern Switzerland. On the western side of the Meretschibach catchment is the Illgraben catchment located. The Meretschibach catchment extents from the top of the Bella Tolla in the South (3025 m a.s.l.) to the outlet into the Rhône valley in the North (619 m a.s.l.) (Frank et al., 2016). So, the catchment faces to the North. The study area has a surface area of approximately 4.9 km^2 (Figure 2) and is located between approximately 2000 and 2750 m.

The catchment is named to the main stream of the basin: the Meretschibach. In the upper part of the catchment, four lakes, of which the Oberer and Unterer Meretschisee are the largest, interrupt the stream (Figure 3). Downstream of the fourth lake, a hydropower station located. The outlets of the three lowest lakes are regulated by the hydropower company. There is also a small farm located study area, which is used for grazing during the summer months. Besides the hydropower device and the farm, there are two houses located close to the hydropower station.

Swiss national soil information system (NABODAT), created a national soil catalog (*Bodenkartierungskatalog - NABODAT*, z.d.). However, the most soil data is derived for the northern part of the country. So, there was a lack of soil information about the study area before this research.

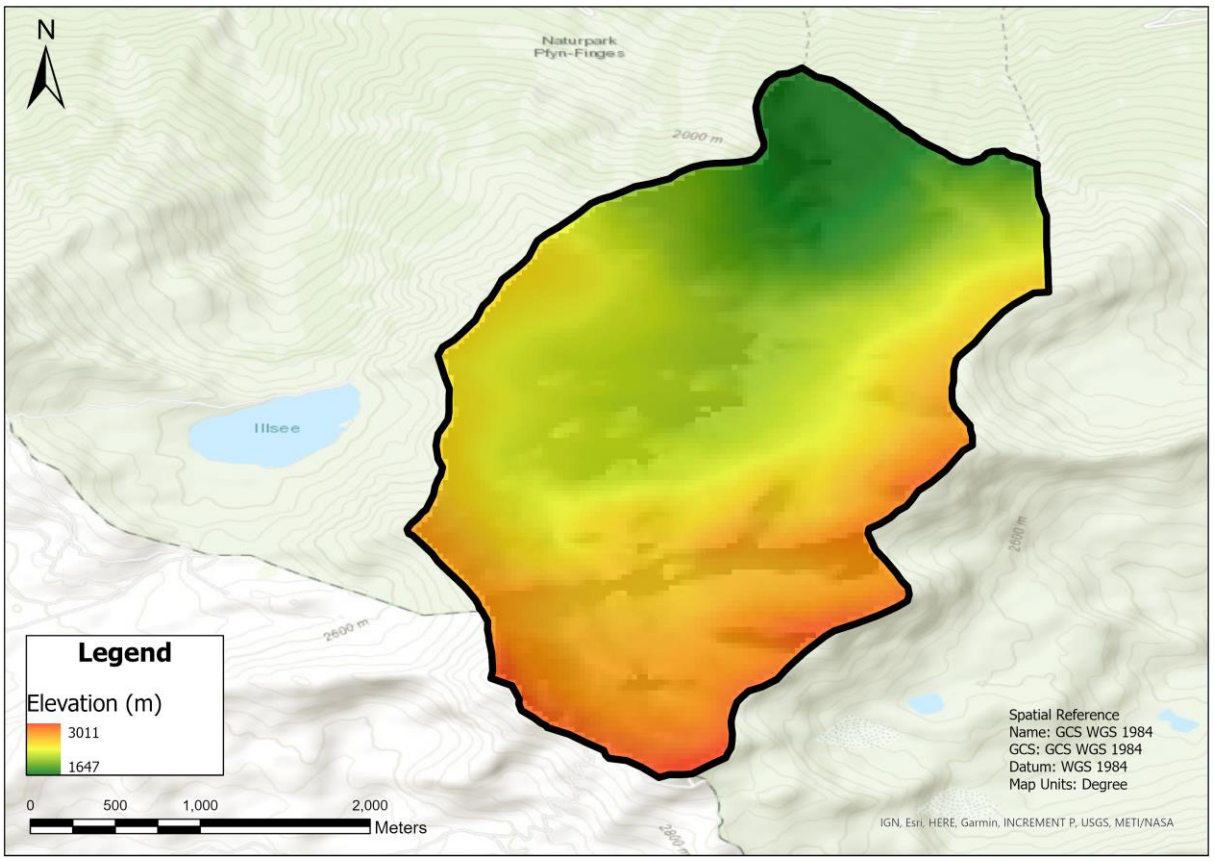

Figure 2: Elevation map of the study area (Berrick, 2023).

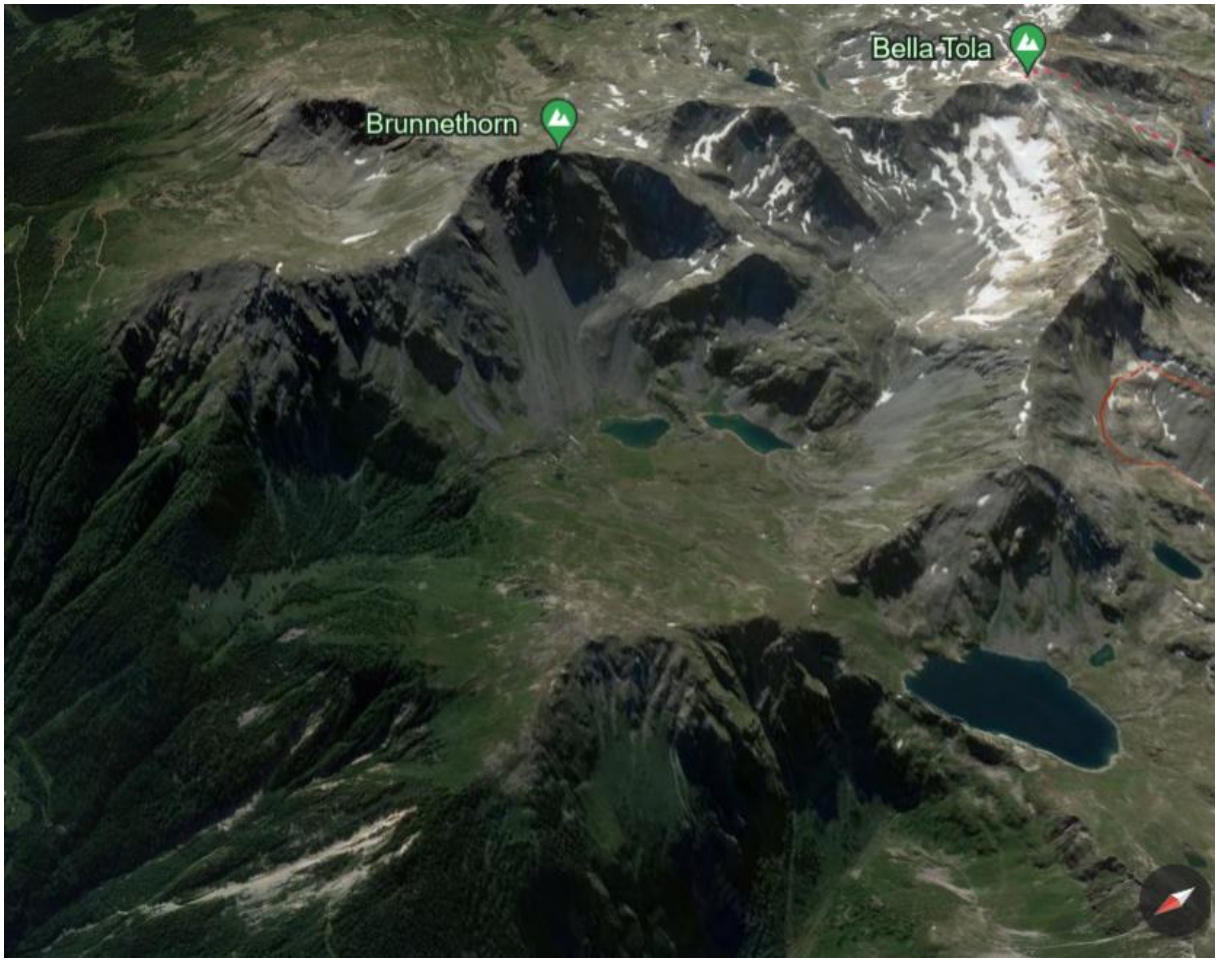

*Figure 3. Study area overview (North arrow in bottom-right corner), including the Bella Tolla glacier in the south, and the Oberer and Unterer Meretschisee in the middle (west of the Brunnerhorn) (*Google Earth*, z.d.).*

In the very upper part of the study area, a relatively small glacier is present: the Bella Tola glacier. A little downstream of the glacier is a moraine deposit located. The study area contains more moraine deposits at lower elevations. Around the Bella tola summit (South) and the Meretschihorn (West), the main outcrops are sandstone and quartzite. Gneiss outcrops can be found all over the catchment, especially at the eastside of the catchment, where these outcrops are the largest. Amphibolite is present in the southern part. Granite has some outcrops in the northern part. Several debris slopes and talus slopes are located all over the catchment. Furthermore, a (relict) rock glacier is present in the center of the catchment (Figure 4) (*Swiss Geoportal*, z.d.).

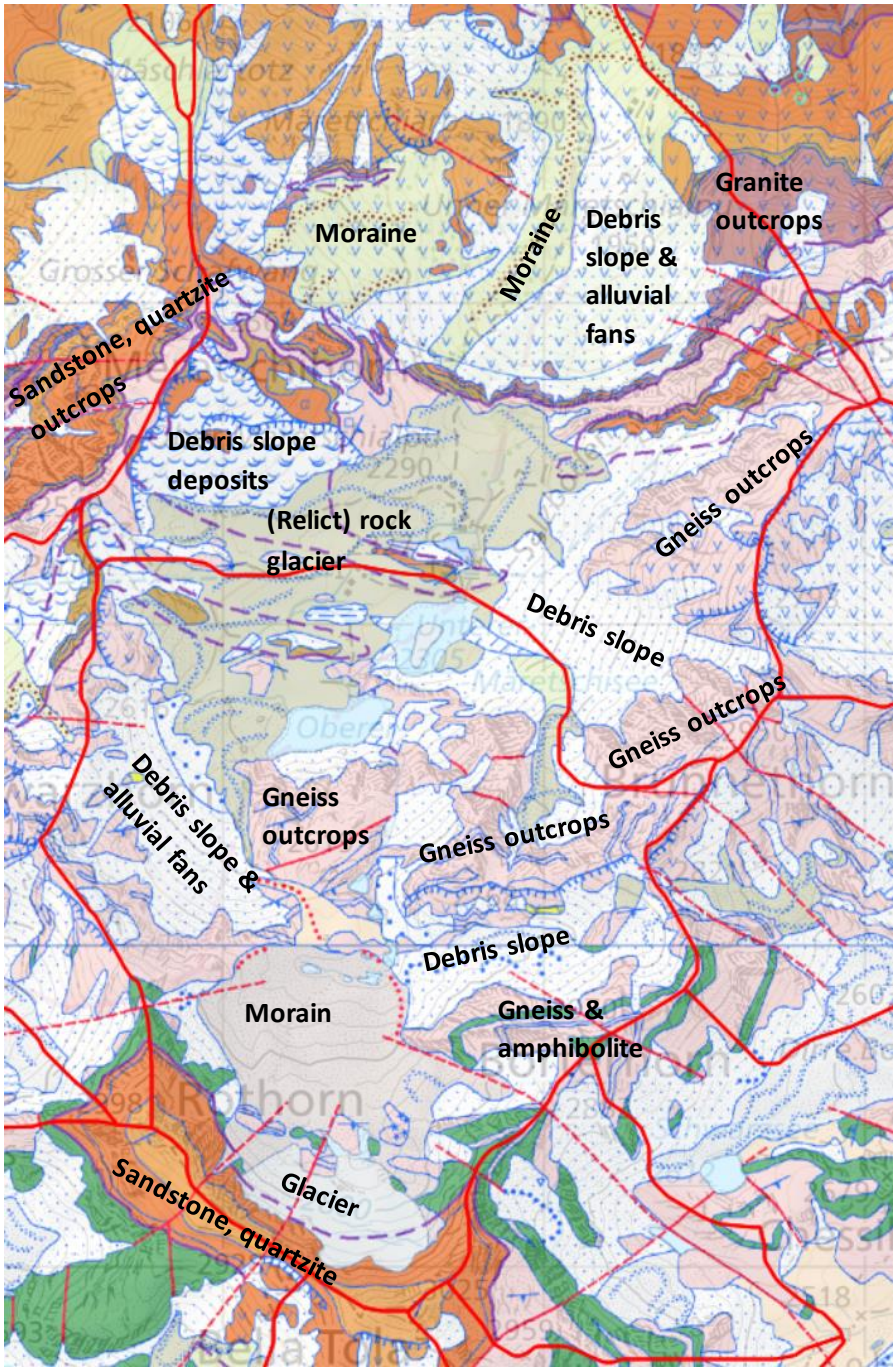

*Figure 4: Geology and geomorphology cover map of the study area (*Swiss Geoportal*, z.d.). The red lines indicate the boundaries of the catchment. The Meretschibach catchment is divided into two catchments in this case.*

In Leukerbad, a climate station is located, which is at the other side in the Rhône valley, at an elevation of 1286 m. The annual precipitation varied between 913 and 1739 mm the last 30 years. This climate station is located the closest to the Meretschibach catchment. The closest located climate station that measures the air temperature is located in Grächen at an elevation of 1605 m. The mean annual air temperature has risen from 5.0 °C to 7.4 °C during the last 30 years. It is expected that the research area has a little higher annual precipitation value and a little lower annual temperature value, because it is located at a higher elevation than these weather stations and because it is located at a north facing catchment instead of facing southwards (*Swiss National Basic Climatological Network - MeteoSwiss*, z.d.).

4 Methodology

This research requires data from soil physical, soil hydraulic, vegetation and topographic properties to find out whether there are relationships between them. The majority of the required data was collected in the field. Therefore, three weeks (08-07-2023 to 29-07-2023) of field research were conducted in the Meretschibach catchment. The field research is executed by several researchers, who have shared the collected data. The main goals of the field research are:

- Collect data of the soil physical, soil hydraulic, vegetation and topographic properties, which can be used in the statistical analysis;
- understanding the relationships between soil, vegetation, topography and hydrology;
- and help the other researchers with their experiments and data collections.

The different soil physical and hydrological, topographic and vegetation measurements were executed at 42 plots spread over the study area. First, five classes of plots were defined : bare, pioneer, grass, shrub and forest plots. Thereafter, based on NDVI images with a spatial resolution of 10x10 m, eight locations per class were randomly chosen. During the field research, two extra plot locations were chosen. Altogether, the plots should give a good representation of the variation in soils, vegetation topography and hydrology of the study area. Several measurements were done at every plot. In the next section (3.1), the most important measurements are described. Collected samples from the field were analyzed in the laboratory by executing several experiments. This is explained in section 3.2. Thereafter, a statistical analysis was executed, which is described in section 3.3. The workflow of the several steps in this research are visualized by Figure 5.

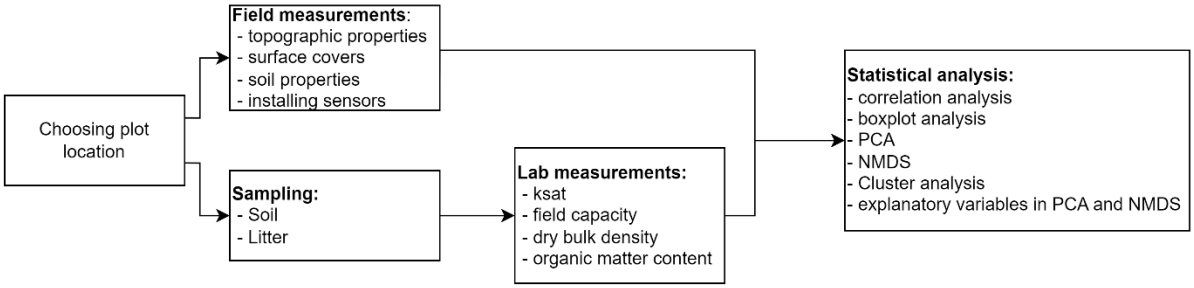

Figure 5: Workflow of this research.

4.1 Plot measurements

The predefined plot locations were added to a digital map. With a phone including GPS, this map was used to navigate to the plot locations, as far as these locations could be reached in safety. The plots of 2x2 m were installed using four rulers. The rulers are placed in a way that each side of the plot is facing to north, east, south and west. At the NE corner of every plot a magnet was buried. This is done to make sure that the plots will be installed at the exact same location for further field research by Utrecht University. After the installation, the exact location and elevation of the plot was determined using a DGPS-Rover. The final locations are represented in Figure 6.

Thereafter, the surface characteristics of each plot were described. This includes an estimation of the cover (%) of vegetation, litter, bare soil, rock outcrops and rock fragments within the plot. Also the geomorphology type and major vegetation type were evaluated and described.

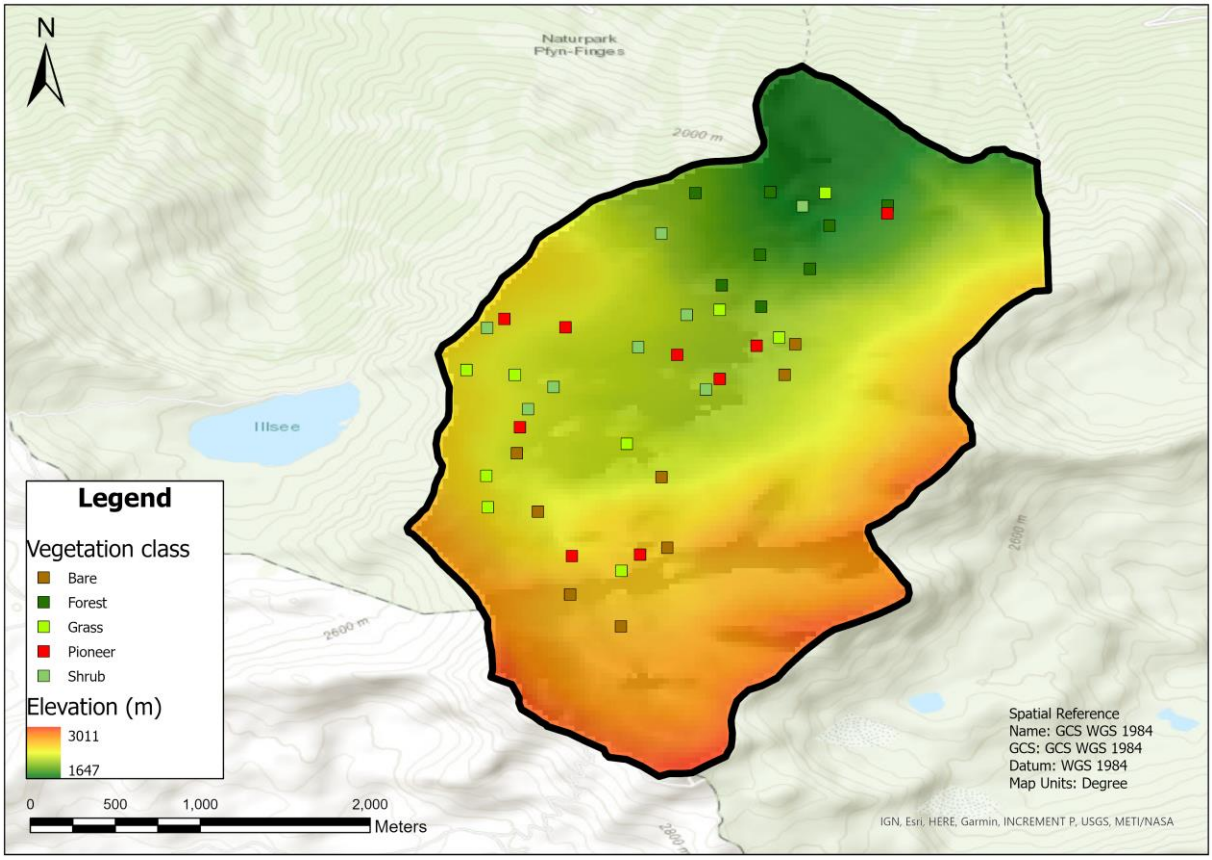

Figure 6: Elevation map (Berrick, 2023) of the study area, including the plot locations and the vegetation classifications of the plots.

4.1.1 Topography measurements

As explained above, the elevation of the plot was measured using a DGPS. The aspect of each plot was measured by placing a compass in the plot at a location which embodies the major aspect of the plot. Then, the azimuth was noted. The average slope angle of the plot was determined by placing the compass at three locations in a straight line along the main slope direction of the plot. The slope angle measurements were done at three locations, because the slope angle can vary within a plot. The slope form, which is mainly classified as concave, convex, straight or complex, was also described at every plot, at plot scale. However, the description was more elaborate than these four classes. The slope form was not described at a hillslope scale. The explanation of the topographic parameters and the description of the protocol can be found in Appendix 1 and 2.

4.1.2 Field soil measurements

Within 1 m downslope of each plot, pits of varying depths were dug (Figure 7). The pits were dug downslope of the plots to make sure that the plots will not be disturbed hydrologically. The reason for digging the pit within 1 m from the plot is that the soil characteristics of the soil profile should be representative for the soil under the plot. The pits vary in depth because they were dug as deep as possible with the available equipment. It was intended to make the pits perpendicular to the slope. However, due to the steep terrain, this was not possible at every location. After the pits were dug, they were used for the description of the soil characteristics, which are listed in Appendix 3 to 6. First, the characteristics over the entire profile were described, like the soil depth, rooting depth, amount of macropores etc. These depths were measured perpendicular to the soil surface. Then, several soil properties like soil texture and clast sorting were described at depths of 10, 20 and 30 cm. The measurements at 10, 20 and 30 cm depth were done find out whether soil characteristics vary with

depth. After that, the presence and thickness of soil horizons was evaluated (FAO, 2006). Appendix 3 to and 16 include the protocols and explanations that has the soil measurements.

Figure 7: Examples of soil measurement pits including a ruler for scale (picture by Dick van de Lisdonk).

In addition to the measurements in the pit, several soil and litter samples were taken at every plot (Figure 8). The maximum amount of samples per plot is: 2 surface soil samples, 2 litter samples, and 3 soil samples at depths of 10, 20 and 30 cm. The reason for taking samples at various depths is to investigate whether the soil properties vary with depth. The surface soil samples were taken within 1 m from the plot at both lateral sides of the plot. This will not cause hydrological disturbances in the plot. Before a surface soil sample could have been collected, first all the material upon the soil, generally litter and vegetation, had to be removed. Thereafter, a metal cylinder with a volume of 100 ml was placed into the soil by holding a small wooden plate on it and hitting it with a small hammer. Then, a knife was used to loosen the soil around the sample, which makes it easier to place a plastic lid on top of the sample. After that, the sample was dug out until a putty knife could be placed under the bottom of the sample. Together, the sample and the putty knife were taken out of the soil carefully, in a way that no soil was lost from the sample. Then the sample was turned upside down, the roots that were sticking out were cut using a scissors and the second lid was placed. Finally, the samples were sealed with tape and stored at a cool temperature (5 °C) to make sure that there was almost no water loss (vapor). After the soil description, the 5, 10 and 30 cm depth-samples were taken at a horizontal distance of 5 to 10 cm from the 'main-pit'. The 5 cm depth-samples were placed into the soil at 2,5 cm, because the middle of the metal cylinder is then at 5 cm depth when it is placed into the soil. So, the 10 and 30 cm depth-samples were taken at 7,5 and 27,5 cm, respectively. When a rock could not fit into the sample, the rock was either split or the rock was replaced by a smaller rock of the same material, which is more representative than leaving the rock out of the sample. There were also locations were the soil was not deep enough to fill the metal cylinder entirely. These samples are still useful for research. Although, the volume of these samples must be estimated. At locations where it could not be managed to get soil into the cylinder, representative loose soil material was taken (disturbed sample). The litter samples were taken using the putty knife, and are also disturbed samples.

The disturbed soil and litter samples were not used in the lab experiments, but they can be used for analyzing the soil texture in future research of Utrecht University.

Figure 8: Example of placing a soil sample cylinder into the soil (left) and when the soil sample was taken out of the soil (right) (picture by Dick van de Lisdonk).

4.1.3 Field hydrological measurements

The near surface temperature and soil moisture content is measured with a Temperature-Moisture-Sensor (TMS-4) (Wild et al., 2019) (Figure 9). The TMS-4-Dwarf has three independent sensors, which can monitor the air and soil temperature. The resolution of the temperature sensors is 0.0625 °C over a range from −55 °C to +125 °C (Wild et al., 2019). The implemented sensors will monitor the temperature and soil moisture for at least 4 years with a temporal resolution of 15 minutes.

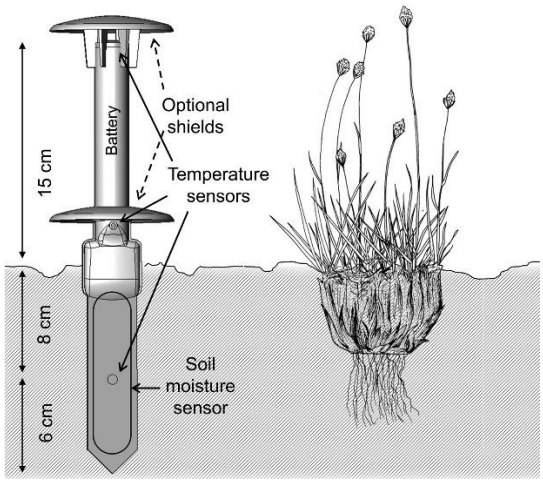

Figure 9. Schematic representation of a TMS data logger, which measures the air, soil surface and soil temperature with three different sensors. A TMS data logger also measures the soil moisture content (Wild et al., 2019).

The soil moisture content is measured over a range between -3 to -15 cm in the soil by the TMS-4-Dwarf. Generally, a TMS sensor monitors the soil moisture content according an electromagnetic method based on dielectric permittivity: Time-Domain-Transmission (TDT) (Wild et al., 2019). TDT sends high frequency-shaped electromagnetic pulses. When a pulse reaches a counting unit, another pulse is sent. The number of pulses is proportional to the soil moisture content (Wild et al., 2019). The TMS sensors that were used in the field look a bit different from the schematic representation of Figure 8, but they have equal functionalities.

Every plot contains one surface sensor inside the plot, which was implemented into the soil perpendicular to the soil surface, with the top of the sensor ca. 3 cm above the surface (Figure 10). Inside the walls of most pits, TMS sensors were placed parallel to the soil surface at depths of 5 and 30 cm. After that, the pit was filled up with the original material and is covered with the original vegetation and other material at the surface. Due to a lack of sensors, not every plot has both of these horizontally placed sensors.

The data of the TMS-sensor measurements can only be derived when connecting a laptop using a cable. Consequently, there is only a little data of the time span between the implementation and the read out time during the field work. Therefore, these soil moisture and temperature data is not analyzed in this research. However, the data will be used in further research of Utrecht University.

Figure 10: TMS-sensor, placed as surface sensor inside a plot (picture by Dick van de Lisdonk).

Besides the TMS-sensors, the soil moisture content was measured using the Theta-probe (Figure 11). This tool works the same as the TMS, but it provides directly a value in electro-Volt (eV). The Theta-probe has four pins which can be put into the soil, then it sends an electromagnetic pulse and the amount of eV can be measured. Using a conversion table the soil moisture content can be derived.

The soil moisture data of the Theta-probe are not really useful for this research, because the soil moisture data of the Theta-probe were only derived during the three weeks of the field research. Therefore, the soil moisture values really depend on the weather conditions during the days or hours before the measurement. However, these Theta-probe measurements were executed at every plot, and therefore, the data can be useful for comparing the outcomes of the TMS-sensors in further research.

Figure 11: Theta-probe measurement executed inside a plot (picture by Dick van de Lisdonk).

4.2 Laboratory soil hydraulic and soil physical measurements

The collected soil samples were used in various experiments to derive the saturated hydraulic conductivity (k_{sat}), field capacity, dry bulk density, and organic matter content. As mentioned in the background information (Chapter 1.2), the k_{sat} is an important soil property, because it determines infiltration rates of the soil. The field capacity of a soil controls the amount of water that can be hold by the soil, which is important for the water availability for vegetation. The organic matter content is crucial for microbial life and plant growth.

4.2.1 Saturated hydraulic conductivity

The k_{sat} can be calculated by Darcy's Law (Hendriks, 2010) (Equation 1). Therefore, the pressure head (dh, in cm), travel distance (dx, in cm) and surface area (A, cm^2) must be known. Moreover, during the measurements the amount of water flowing through the sample in a certain time must be measured. The pressure head is equal to the vertical distance between the air inlet of the plastic water cylinder and the top of the soil sample (Figure 12). The travel distance is equal to the height of the sample, which is 5 cm when the cylinder of the sample is filled entirely (Figure 12). The discharge (Q, in m^3/day) can be calculated by weighting the buckets that catch the water before and after each time span, keeping track of the time and dividing the volume of water by the time. To calculate k_{sat} using Darcy's Law, Q must be divided by the surface area (A, in m^2) of the sample which is 20 cm^2 and by dh/dx.

$$Q = -A\, k_{sat} \frac{dh}{dx} \qquad (1)$$

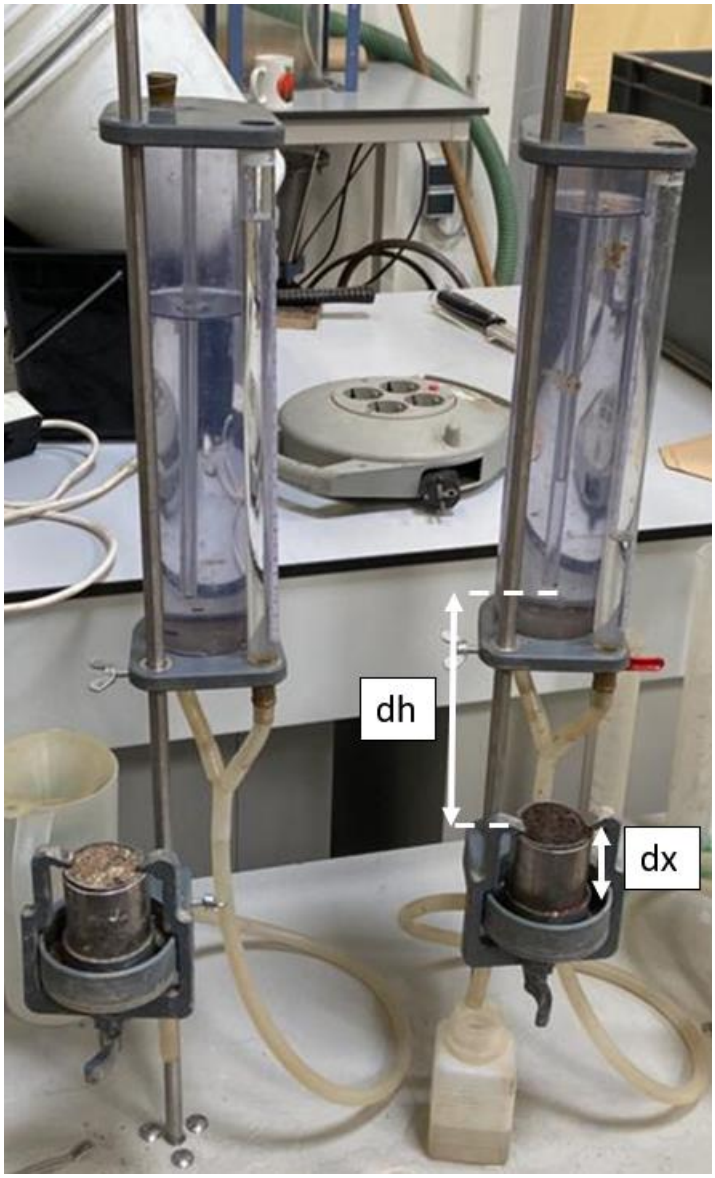

Figure 12: Photograph of the permeameter installation for the k_{sat} measurements of the soil samples, including the pressure head (dh in cm) and the travel distance (dx in cm) (picture by Dick van de Lisdonk).

Before the measurements started, all 142 collected soil samples were weighted, from which 14 samples were disturbed. Then, k_{sat} was measured using a permeameter (MD Sahadat Hossain et al., 2021). The first step was to connect the sample to the permeameter. Therefore, the lids and tape were removed, and at the top side of the samples, a plastic lattice was placed. This lattice had the function to reduce the loss of soil material during the experiment, because the water flowing through the sample takes up soil material which will be lost otherwise. The sample was installed on a rubber ring which surrounds a sponge. At the top of the sample, a plastic ring was placed upon the lattice to prevent that soil moves upwards by placing it on the permeameter. After that, the sample could be attached.

The permeameter consists of a small water cylinder with a volume of ca. 1200 ml, which is connected with a rubber tube to the sponge on which the soil sample was placed. During the measurement water flows from the cylinder, through the tube and sponge into the bottom of the sample. The sponge makes sure the water is distributed evenly into the sample. When the water flows out of the top of the sample, the water flows over the sides of the sample and drips into a small bucket.

Before, the measurements could start, the samples must be saturated. Hence, the k_{sat} is the water flux or seepage velocity per unit area for a constant water potential gradient and a saturated soil (Gupta et al., 2021; Zuo & He, 2021). The amount of water that is needed for saturation was calculated by subtracting the original weight of the sample from the weight of the saturated sample.

After being saturated, the k_{sat} of 65 samples (35 surface, 25 10 cm depth, and 5 5 cm depth-samples) was investigated using the permeameter. Due to a lack of time, a selection of the 142 soil samples was made for the k_{sat} measurements. For plots that did not have 10 cm depth-samples, but did have 5 cm depth-samples, these 5 cm depth-samples were used for the measurements.

4.2.2 Field capacity

After the k_{sat} measurements, the field capacity (FC, in %) of the samples was measured. This was executed by placing the samples on a metal lattice and let them leak for 48 hours at an air temperature of ca. 20 °C. Only the bottom lids were removed for these measurements. Also, thin plastic foil was laid over the samples. After 48 hours, the samples should be at field capacity, which means that all the soil moisture that could have been drained by gravity, should be out of the sample (Cassel & Nielsen, 1986). To calculate the field capacity (Equation 2), the weight of the oven dried samples had to be known.

$$FC = \frac{W_{gravitational\ drainage} - W_{oven\ dried}}{V_{sample}} \quad (2)$$

To determine the weights of the soil samples without moisture, the samples were dried in an oven with a duration of 48 hours and a temperature of 105 °C. Thereafter, the samples were weighted again. The field capacity (FC, (-)) was calculated by subtracting the weight of the oven dried samples ($W_{oven\ dried}$, in g) from the weight of the samples after gravitational drainage ($W_{gravitational\ drainage}$, in g) and dividing that by the volume of the sample (V_{sample}, in ml) (Equation 2) (Dingman, 2015). Since the difference between the weights is equal to the difference in ml of water, the field capacity can be expressed in a content or percentage of the volume of the sample.

4.2.3 Dry bulk density

The dry bulk density (ρ_b, in g/cm^3) is the density of the soil sample without soil moisture. This was calculated by dividing the weight of the oven dried samples ($W_{oven\ dried}$, in g) by the volume of the samples (V_{sample}, in cm^3) (Equation 3) (Hendriks, 2010).

$$\rho_b = \frac{W_{oven\ dried}}{V_{sample}} \quad (3)$$

4.2.4 Organic matter content

For determining the organic matter content, first the oven dried samples were removed from their metal cylinder and put in a bowl. In the bowl, the samples were broken down using a mortar and pestle until almost all soil aggregates were gone. This is beneficial for the combustion of the organic material, because the total surface of soil material exposed increases when breaking down the soil aggregates. Then, a representative part of the soil sample was taken, put into a ceramic cup and weighted. Thereafter, the ceramic cups were placed into an oven at a temperature of 550 °C. After 4 hours of combustion, all the organic matter should have been combusted (Heiri et al., 2001). Eventually, the combusted soil samples were weighted again. The organic matter content (OM, in %) was calculated by subtracting the weight of the sample after combustion ($W_{combusted}$, in g) from the sample before combustion ($W_{oven\ dried}$, in g) and dividing by the weight before combustion ($W_{oven\ dried}$, in g) (F. Yang et al., 2014).

$$OM = \frac{W_{oven\ dried} - W_{combusted}}{W_{oven\ dried}} * 100\% \quad (4)$$

4.3 Statistical analysis

For the statistical analysis, two set of variables are used: response (dependent) and explanatory (independent) variables (Borcard et al., 2011; Israels, 1984; Legendre & Legendre, 2012). The response variables are the soil parameters, and the explanatory variables are the topographic and surface cover parameters.

4.3.1 Data

The collected data consist of four types: nominal, ordinal, continuous and discrete data (Table 1). Every statistical analysis technique performs better for certain data, which is explained by the description of the different techniques.

Table 1: Data types of the different soil, topographic, surface cover and vegetation data.

Continuous	**Nominal**	**Discrete**	**Ordinal**
Soil depth (cm)	Matrix grading	Macropores (nr/dm^2)	Clast sorting
Organic layer depth (cm)	Soil texture	Fine root abundance (nr/dm^2)	
Rooting depth (cm)	Horizon class	Coarse root abundance (nr/dm^2)	
Litter depth (cm)	Munsell color		
Rock fragments (%)	Geomorphology		
Mean rock fragment size (mm)	Slope form		
Horizon thickness (cm)	Vegetation type		
Saturated hydraulic conductivity (m/day)			
Field capacity (-)			
Dry bulk density (g/cm^3)			
Organic matter content			
Elevation (m)			
Slope angle (°)			
Aspect (°)			
Surface covers (%)			

4.3.1.1 Data treatment

Before starting with the statistical analysis, a part of the data from the field and laboratory must be modified. For example, the soil texture classes were described quiet elaborate. Therefore, a description like “fine to coarse sand” is reclassified to “medium sand”. Moreover, mixed soils have been set into the soil class that has the largest proportion. So, a soil with the description “medium sand (25%), org. matter (75%)” is classified as “organic material”. The reclassification resulted eight soil texture classes: “medium sand”, “loamy sand”, “sandy loam”, “sandy clay loam”, “clay loam”, “sandy clay”, “silty clay”, and “organic material”.

In addition, the grading is set to three classes: “no grading”, “fining upwards” and “coarsening upwards”. The sorting is set to five classes: “very poorly sorted”, “poorly sorted", “moderately sorted", "well sorted” and “very well sorted”. The first soil horizon is also set to two classes: “O-horizon” and “C-horizon”. The second horizon has three classifications: “no horizon”, “A-horizon” and “E-horizon”, and the third horizon has only two classes: “no horizon " and "E-horizon”. The last soil data that has been modified for the statistical analysis is the rock fragment size. The rock fragment size was described in the field as a range of rock sizes that was found at a location (e.g. 2-250 mm). However, such a range is not preferable for the analysis. Therefore, the mean of this range was taken (e.g. mean of 2-250 mm is 126 mm).

For the topographic data, the aspect is set from wind directions into degrees to get continuous data instead of classes (e.g. E to 90°). Furthermore, the classification of slope form is sometimes a bid elaborate (e.g. straight, depression at SE corner). Therefore, the slope form descriptions are reclassified to the four major classes: "straight", "convex", "concave" and "complex". For example, "straight, depression at SE corner" is set to "straight".

All the surface cover data is in percentages. To make them comparable to each other, values larger than 100% were set to 100%. This was mostly the case for vegetation cover, where different layers of vegetation (ground vegetation, shrubs and trees) can cover more than 100% of the plot.

Some variables and some plots locations are not included in the analysis. This is due to the fact that some methods cannot handle missing values. Therefore, all the data of one plot or the data of a variable for all the plots were removed when there is a missing value. For example, from the eight investigated bare plots in the field are only three used in the analysis. This is mainly caused by the fact that these plots have (almost) no soil and consequently, they have many missing soil values. The soil measurements at 10, 20 and 30 cm depth have many missing values, because some plot locations have very thin soils. Therefore, all 20 and 30 cm depth measurements are missing in the PCA and NMDS (e.g. soil texture (20 cm depth) or rock fragments (%) (20 cm depth)). Moreover, there are many missing values for k_{sat}, field capacity and organic matter content of the 5 and 10 cm depth-samples. Therefore, these data are not included in the analysis. The missing values are caused by multiple reasons: (1) disturbed samples could not be used in the lab-experiments, (2) too shallow soil for taking a 5 or 10 cm depth-sample and (3) a lack of time to execute all field capacity and organic matter content experiments. Besides these soil parameters, also a topographic parameter is not included in the analysis: geomorphological unit. The reason for this is that there are many geomorphological units described, which provides too many classes, which is not favorable.

4.3.2 Univariate statistics

The first step in the statistical analysis applying univariate statistics. Various soil, surface cover and topographic parameters were plotted against each other in scatter plots. Also, their correlations and significance were evaluated. Thereafter, a correlation analysis was performed to create an overview of these correlations. Eventually, a boxplot analysis was executed for the nominal and ordinal data that could not be used in the correlation analysis.

4.3.2.1 Correlation analysis

Correlation plots were created to get an overview of all correlations between the different continuous and discrete parameters. These correlations were calculated by the Pearson's correlation coefficient (r). r is a measure of any linear trend between two variables (Puth et al., 2014; Schober et al., 2018). If r =1, the correlation is perfectly positively linear, and if r = -1, the correlation is perfectly negatively linear. The magnitude of r explains the amount of scatter in the data around the linear trend line. So, it is not the magnitude of the trendline itself (Puth et al., 2014). A correlation is strong when $r > 0.7$, and moderate when $0.4 < r < 0.7$. The Pearson's correlation coefficient cannot be used for nominal and ordinal data. Therefore, only the continuous and discrete data were used in the correlation analysis.

4.3.2.2 Boxplots, ANOVA and Bonferroni correction

Boxplots were used to analyze the variance of continuous or discrete data for different groups of nominal or ordinal data. An advantage of boxplots is that the values of the minimum, first quartile, median, third quartile and maximum can be derived.

To find out the statistical significance of grouped data in a boxplot, an ANOVA (ANalysis Of VAriance) was used, which uses univariate data (Ståhle & Wold, 1989). However, the p-value of the ANOVA is

about the statistical significance of all the classes together in the boxplot. To investigate whether the groups within the boxplot differ significantly, the pair-wise error rate is calculated, which is based on the Bonferroni correction (Equation 5) (Armstrong, 2014). The Bonferroni correction corrects for the chance of significance by the number of tests (T) for a certain critical p-value (a) (Armstrong, 2014). This Bonferroni correction is also used when examine the individual correlations and their p-value between different variables.

$$1 - \frac{1-a}{T} \qquad (5)$$

4.3.3 Multivariate statistics

4.3.3.1 Principal Component Analysis

A Principal Component Analysis (PCA) is chosen to use as first in the multivariate statistical analysis. It is mainly used to reduce a set of multidimensional data to lower dimensions while keeping the most information (Karamizadeh et al., 2013; Ringnér, 2008). This reduction is achieved through identifying directions, which are called principal components (PC), along which is a maximal variation in data (Ringnér, 2008). The principal components are linear combinations of the original variables (Ringnér, 2008). A requirement for PCA is that the correlation between variables should be linear and the data should be free of outliers. PCA is based on Euclidean distances, which are real distances (Legendre & Legendre, 2012). Therefore, nominal, ordinal and discrete data are not very suitable for PCA. So, PCA is typically applied to continuous data, which is also done for this research.

4.3.3.2 Nonmetric Multidimensional Scaling

Nonmetric multidimensional scaling (NMDS) tries to represent the position of objects in a multidimensional space in a reduced number of dimensions as well as possible (Borcard et al., 2011; Legendre & Legendre, 2012). NMDS tries to represent the position of objects in a multidimensional space in a reduced number of dimensions as well as possible (Borcard et al., 2011; Legendre & Legendre, 2012). It fails to maximize the variability of associated with the individual axes of the ordination. The axes of NMDS are arbitrary, which means that the plots can be rotated, centered or inverted arbitrarily (Borcard et al., 2011; Legendre & Legendre, 2012). It is more flexible than PCA, because it does not require linear data and it can handle data that is not normally distributed. NMDS allows the usage of any kind of distance instead of only Euclidean distances like PCA. Therefore, it can perform for continuous, discrete, ordinal and nominal data. In contrast to PCA, NMDS can be used to analyze the entire dataset of this research.

The positions of the soil parameters and the plots in the NMDS plot represent similarities or differences between them. The fit of an NMDS is typically evaluated by the stress. When the stress value is smaller than 0.2, the minimum number of dimensions in which a given dataset can be visualized without inducing unacceptable levels of distortion (Dexter et al., 2018).

4.3.3.3 Cluster analysis

In the cluster analysis, the plot locations are clustered in the PCA and NMDS plots. Since the PCA and NMDS use different soil data, the resulting clusters are different between them. The purpose of clustering is to put plot locations in a cluster group to identify distinctions between groups.

The first clustering is based on the predefined vegetation classes: bare (B), forest (F), grass (G), pioneer (P) and shrubs (S). The aim of this clustering is to investigate whether soil properties have a strong association with these vegetation classes.

Besides clustering per vegetation class, it can also be executed by first standardizing the data, compute a dissimilarity index, and eventually cluster the data in groups. Computing a dissimilarity index can be

executed using different methods, in this research only Ward's minimum variance method is applied. At the start of the clustering, each plot is its own cluster. Therefore, the distance of the centroid is equal to 0. As the clusters form, the centroids move away from the plots and the sums of the squared distances increases. "At each clustering step, Ward's method finds the pair of objects or clusters whose fusion increases as little as possible the sum, over all objects, of the squared distances between objects and cluster centroids" (Legendre & Legendre, 2012).

Different distances, like the "Canberra", "Manhattan", "Euclidean", "Bray", "Kulczynski" and "Gower", were applied to examine which distance provides the best clustering. The "Canberra" distance clustered the data the best, because it creates distinct clusters with minimal overlap. The Canberra distance is a weighted version of the Manhattan distance (Legendre & Legendre, 2012; Lengyel & Botta-Dukát, 2022), which is the sum of absolute values of the differences between ranks, divided by their sum (Jurman et al., 2009). The Canberra distance is typically applied when it is required to find the distance between points that are located around the origin in the vector space (Faisal et al., 2020). As a result, each cluster group consist of plot locations which have comparable soil properties.

4.3.3.4 Explanatory variables

In this research two set of variables were used: response (dependent) and explanatory (independent) variables (Borcard et al., 2011; Israels, 1984; Legendre & Legendre, 2012). The soil parameters are the response variables and the topographic and surface cover parameters are the explanatory variables.

The explanatory variables are plotted passively in the PCA plot. This means that the explanatory variables have no effect on the principal components (PC1 and PC2). Therefore, it is hard to examine precise correlations between the explanatory variables and the soil parameters. However, the direction of the vectors of the explanatory variables give still an overview of whether they have a positive or negative correlation with the soil parameters. Since the NMDS is executed for all the soil data, the explanatory variables are also analyzed for the NMDS. Again, they are plotted passively.

5 Results

5.1 Univariate statistics

5.1.1 Correlation analysis

Correlation analysis explores the relationships between the different soil data (5.1.1.1), topographic data (5.1.1.2), surface cover data (5.1.1.3), and topographic and surface cover data (5.1.1.4).

5.1.1.1 Soil data correlation analysis

The correlation plot (Figure 13) represents all the correlations between the different soil variables. On the right side of the correlation plot is the scale, indicating that blue squares have positive and red squares negative correlations. In the following, a correlation is considered strong when Pearson's correlation coefficient $r > 0.7$, moderate when $0.4 < r < 0.7$ and weak when $r < 0.4$.

From the correlations between the soil data (Figure 13), only one strong positive correlation can be found, which is between minimal soil depth and rooting depth (0.79). Soil depth is also moderately correlated with fine root abundance (0.48), which is not the case with coarse root abundance.

Rooting depth has three moderate correlations with fine and coarse root abundance and litter depth (0.54, 0.52 and 0.54, respectively). Coarse root abundance has also a moderate correlation with litter depth.

The k_{sat} of the surface samples has no moderate or strong correlations with the other soil data. However, its correlations with coarse root abundance, litter depth, rock fragment size and rock fragments are relatively large in comparison to the other correlations with k_{sat} surface.

Rock fragment size and the percentage of rock fragments have a moderate correlation (0.62). They are weakly correlated to the other soil data.

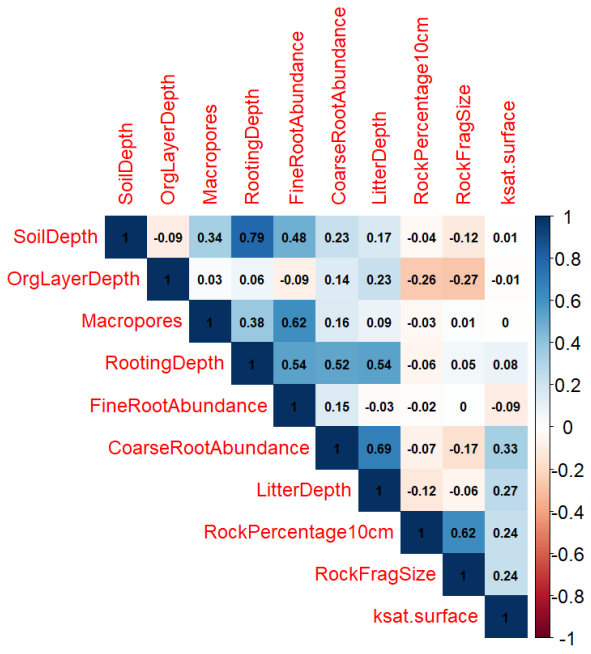

Figure 13: Correlations between the continuous and discrete soil parameters using Pearson's correlation coefficient, including the scale on the right side with a range of -1 to 1.

5.1.1.2 Soil and topographic data correlation analysis

There are no strong correlations between the topographic and soil parameters (Figure 14). Elevation has the most moderate (negative) correlations with soil, rooting and litter depth (cm) and coarse root

abundance (-0.47, -0.7, -0.54 and -0.66, respectively). Organic layer depth, fine root abundance, percentage of rock fragments and rock fragment size have weak correlations with elevation. Aspect has one moderate negative correlation with fine root abundance (-0.44). Slope angle has only weak correlations.

Figure 14: Correlations between the continuous and discrete soil parameters with the continuous topographic parameters using Pearson's correlation coefficient, including the scale on the right side with a range of -1 to 1.

5.1.1.3 Soil and surface cover data correlation analysis

Vegetation and rock cover have the strongest correlations with the soil data (Figure 15). The soil parameters to which vegetation cover has a positive correlation, have mostly a negative correlation to rock cover and vice versa. Rooting depth has a strong correlation with vegetation and rock cover (0.7 and -0.7, respectively). Soil and litter depth and fine and coarse root abundance are moderate correlations for both the vegetation and rock cover. Litter cover has less soil parameters to which it has a moderate correlation: litter and organic layer depth and coarse root abundance. The correlations of litter are mostly positive when correlations of vegetation cover are also positive and vice versa. Bare soil cover has only weak correlations.

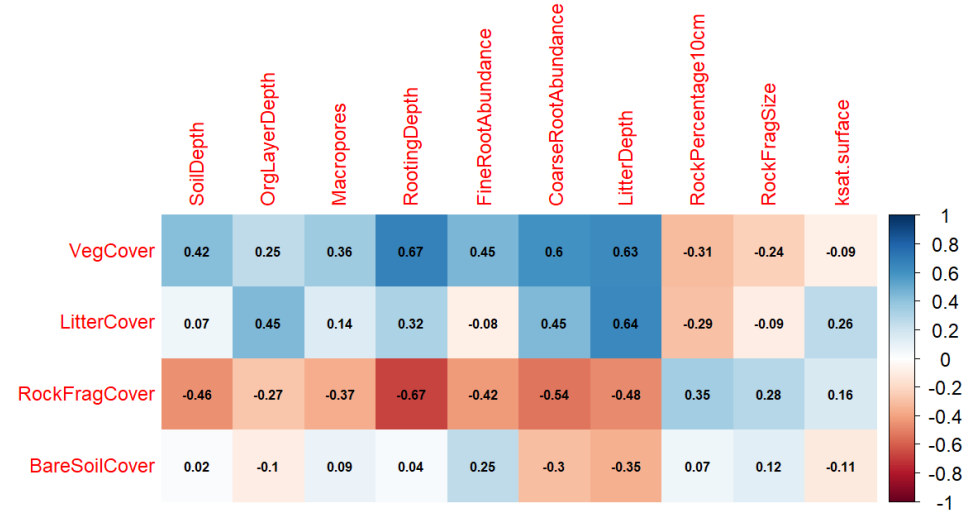

Figure 15: Correlations between the continuous and discrete soil parameters with the continuous surface cover parameters using Pearson's correlation coefficient, including the scale on the right side with a range of -1 to 1.

5.1.1.4 Topographic and surface cover data correlation analysis

Elevation has the highest correlations to surface cover data (Figure 16). Vegetation and litter cover are negatively correlated with elevation (-0.6 and -0.48, respectively) and rock cover is positively correlated with elevation (0.51). Slope angle and aspect have a minor influence on the surface covers. Although, aspect has a moderate negative correlation with rock cover (0.42).

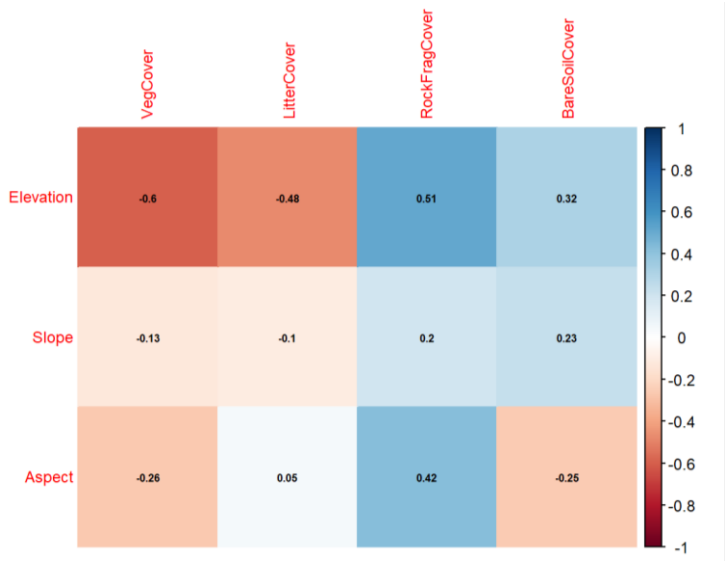

Figure 16: Correlations between the continuous topographic and surface cover parameters using Pearson's correlation coefficient, including the scale on the right side with a range of -1 to 1.

5.1.2 Boxplot analysis

The boxplots provide visual comparisons of continuous or discrete data for different groups of nominal or ordinal data. An ANOVA is used to test the significance of the boxplots, which is visualized with the red label. The pairwise comparisons between different groups are derived using a t-test, which is based on the Bonferroni method. The outcomes of these t-tests are p-values, which are given as codes in tables (- < 0.05, * = 0.05, ** = 0.01, *** = 0.001, **** = 0.0001 and ***** < 0.00001).

5.1.2.1 Vegetation classes

Forest plots extent between approximately 2050 to 2300 m elevation (median ca. 2150 m), which is much lower than the other vegetation classes (Appendix 19 and 20). Forests have generally the largest soil (Figure 17 and Table 2), litter (Appendix 23 and 24) and rooting depth (Figure 18 and Table 3). The spread of soil depth of forest is relatively small in comparison to pioneer and shrub plots (Figure 17). The spread of the litter depth is relatively large for forests in comparison to the other plots (Appendix 23 and 24). The median of the organic layer depth is slightly lower than those of pioneer and shrub plots (Appendix 21 and 22). The median of the coarse root abundance is the largest for forest plots (Appendix 27 and 28) and the median of the fine root abundance is only larger for grass plots (Appendix 25 and 26). The vegetation cover in forests is mostly 100% (Figure 19 and Table 4). Forests have also the largest litter cover (Appendix 29 and 30), with a median of ca. 95%. On the other hand, the rock cover of forest plots is approaching 0% (Figure 20 and Table 5).

Grass plots have the largest medians for fine root abundance (Appendix 25 and 26). The median of minimal soil and rooting depth (Figure 17 and 18 and Table 2 and 3) of the grass plots is the second largest after the forest plots. The organic layer depth is relatively low for grass plots (median ca. 2.5 cm) (Appendix 21 and 22) and they have normally no litter (Appendix 23, 24, 29 and 30). The vegetation cover is relatively high (median ca. 85%) (Figure 19 and Table 4). Similar to forests, the rock cover is relatively low (median ca. 5%) (Figure 20 and Table 5). Grass is the only vegetation class that has a small spread in k_{sat} surface values with a median of ca. 5 m/day (Appendix 31 and 32), which is relatively low.

Shrub plots have together with pioneer plots the largest median for organic layer depth (ca. 7.5 cm) (Appendix 21 and 22). Also their soil (medians ca. 25 cm) (Figure 17 and Table 2) and rooting depth (median shrubs ca. 20 cm and pioneer 18 cm) (Figure 18 and Table 3) are comparable. The rooting depths have moderate values compared to forest and bare plots.

There are also differences between shrubs and pioneer plots: the coarse root abundance (median ca. 7 coarse roots per dm^2) (Appendix 27 and 28) and litter cover (median 90%) of shrubs (Appendix 29 and 30) are the second largest after forests, where pioneer plots have a third place. Shrubs have also a smaller spread in elevation than pioneer and grass plots (Appendix 19 and 20). The vegetation cover of shrubs (median ca. 92%) (Figure 19 and Table 4) relatively high. The rock cover of pioneer plots is the second largest (median ca. 45%), where shrubs have generally almost no rock cover (Figure 20 and Table 5).

Bare plots are very different from the other vegetation classes. Their spreading is between 2350 and 2750 m (Appendix 19 and 20). All the vegetation related soil parameters (rooting depth, litter depth, fine root abundance etc.) are almost zero. Bare plots have the largest rock cover (median ca. 98%) (Figure 20).

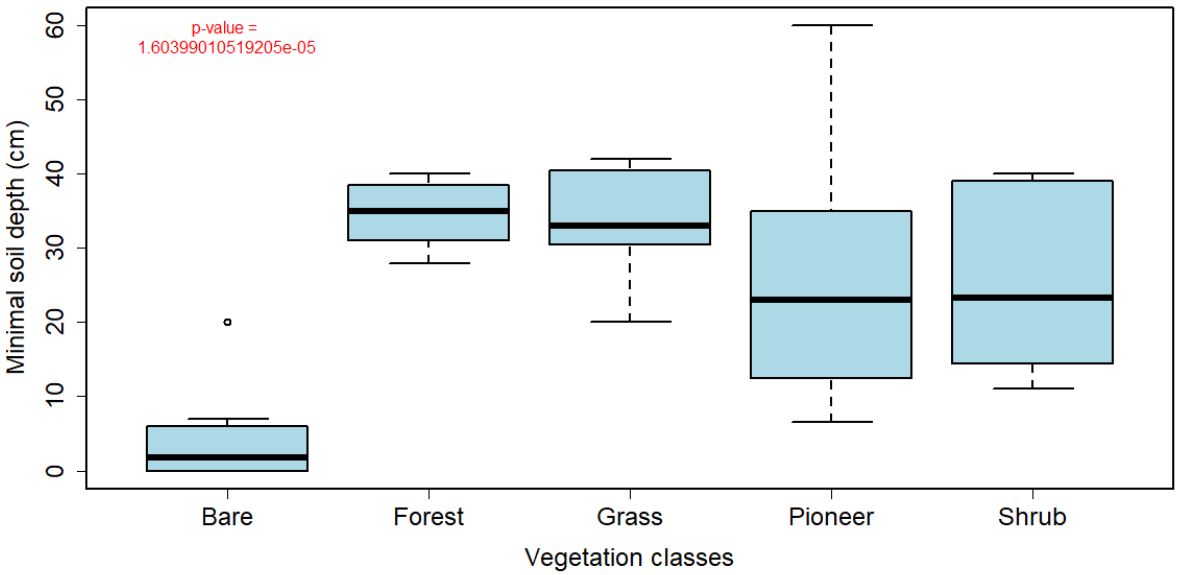

Figure 17: Boxplot of minimal soil depth (cm) for the five vegetation classes (bare, forest, grass, pioneer and shrub), including the overall p-value (red).

Table 2: p-values of the pairwise comparisons using a t-test between the different vegetation classes (bare, forest, grass, pioneer and shrub) for the boxplot against minimal soil depth (cm).

	Bare	**Forest**	**Grass**	**Pioneer**
Forest	*****			
Grass	*****	-		
Pioneer	***	-	-	
Shrub	***	-	-	-

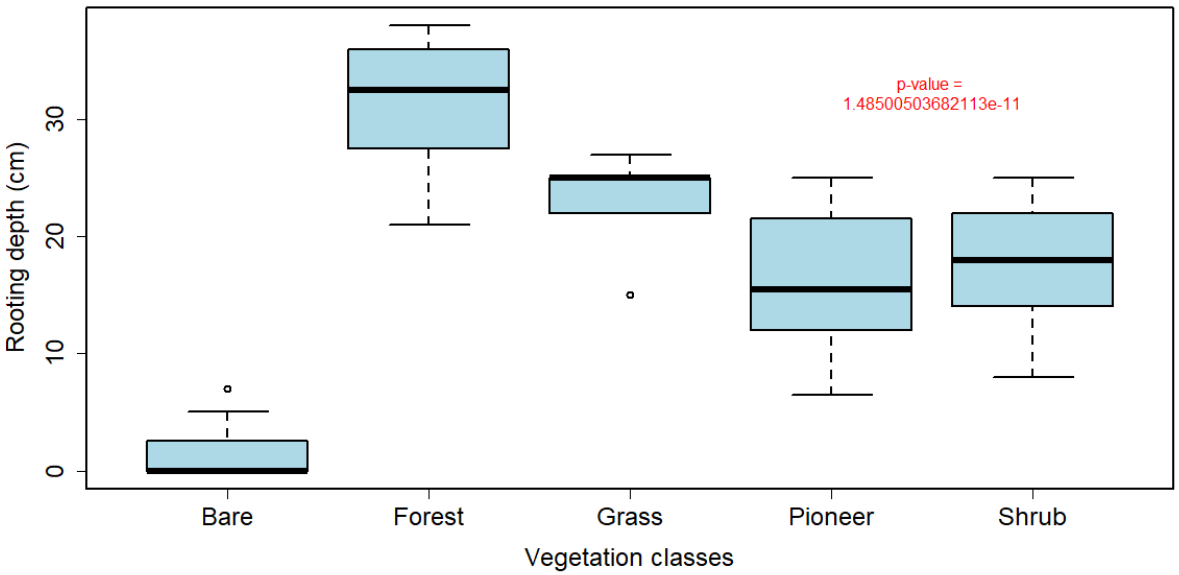

Figure 18: Boxplot of rooting depth (cm) for the five vegetation classes (bare, forest, grass, pioneer and shrub), including the overall p-value (red).

Table 3: p-values of the pairwise comparisons using a t-test between the different vegetation classes (bare, forest, grass, pioneer and shrub) for the boxplot against rooting depth (cm).

	Bare	Forest	Grass	Pioneer
Forest	*****			
Grass	*****	*		
Pioneer	*****	*****	-	
Shrub	*****	*****	-	-

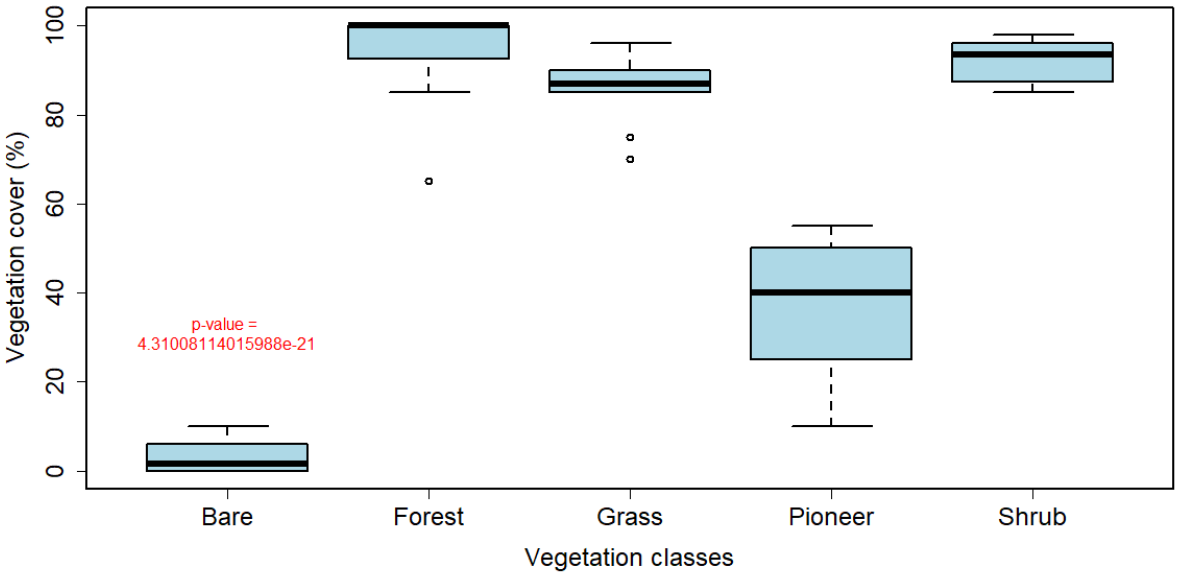

Figure 19: Boxplot of vegetation cover (%) for the five vegetation classes (bare, forest, grass, pioneer and shrub), including the overall p-value (red).

Table 4: p-values of the pairwise comparisons using a t-test between the different vegetation classes (bare, forest, grass, pioneer and shrub) for the boxplot against vegetation cover (%).

	Bare	Forest	Grass	Pioneer
Forest	*****			
Grass	*****	-		
Pioneer	*****	*****	*****	
Shrub	*****	-	-	*****

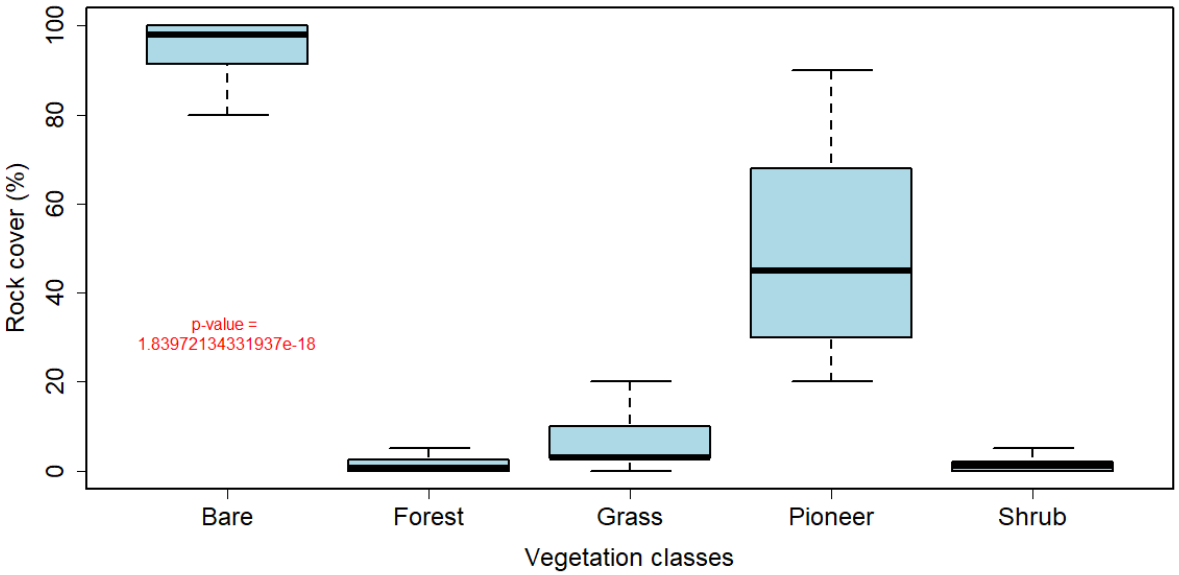

Figure 20: Boxplot of rock cover (%) for the five vegetation classes (bare, forest, grass, pioneer and shrub), including the overall p-value (red).

Table 5: p-values of the pairwise comparisons using a t-test between the different vegetation classes (bare, forest, grass, pioneer and shrub) for the boxplot against rock cover (%).

	Bare	**Forest**	**Grass**	**Pioneer**
Forest	*****			
Grass	*****	-		
Pioneer	*****	*****	*****	
Shrub	*****	-	-	*****

5.1.2.2 Soil texture classes relationship to k_{sat}

As explained before, the k_{sat} strongly depends on soil texture. The median of the soil texture class "medium sand" has an extremely large k_{sat} value (ca. 100 m/day) in comparison to the other soil texture classes (Figure 21). The k_{sat} value of organic material (ca. 20 m/day) is the closest to that of medium sand (Appendix 22). The median of silty clay (ca. 0.7 m/day) has the largest difference with medium sand. However, there is found only one sample of silty clay. Therefore, no spread is visible for this soil texture class.

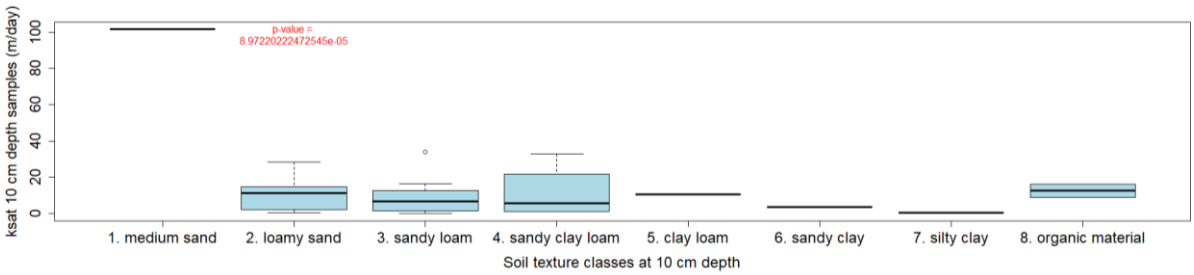

Figure 21: Boxplot of k_{sat} (m/day) of the soil samples taken at 10 cm depth for the eight soil texture classes measured at 10 cm depth, including the overall p-value (red).

5.1.1.3 Clast sorting

The boxplots of clast sorting (Figure 22 and 23) show that the clasts are better sorted for soils with a lower content of rock fragments and for soils with a lower mean rock fragment size. The classes moderately sorted and well sorted were found at only one location. Very poorly sorted has a median of ca. 70% for rock percentage and 125 mm for mean rock fragment size. The very well sorted soils contain generally almost no rock fragments.

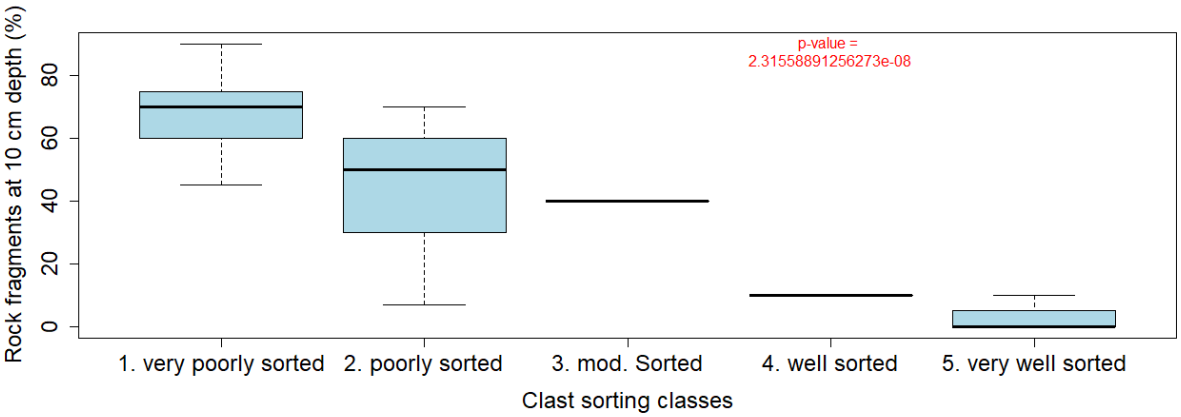

Figure 22: Boxplot of rock fragments (%) at 10 cm depth for the five clast sorting classes measured at 10 cm depth, including the overall p-value (red).

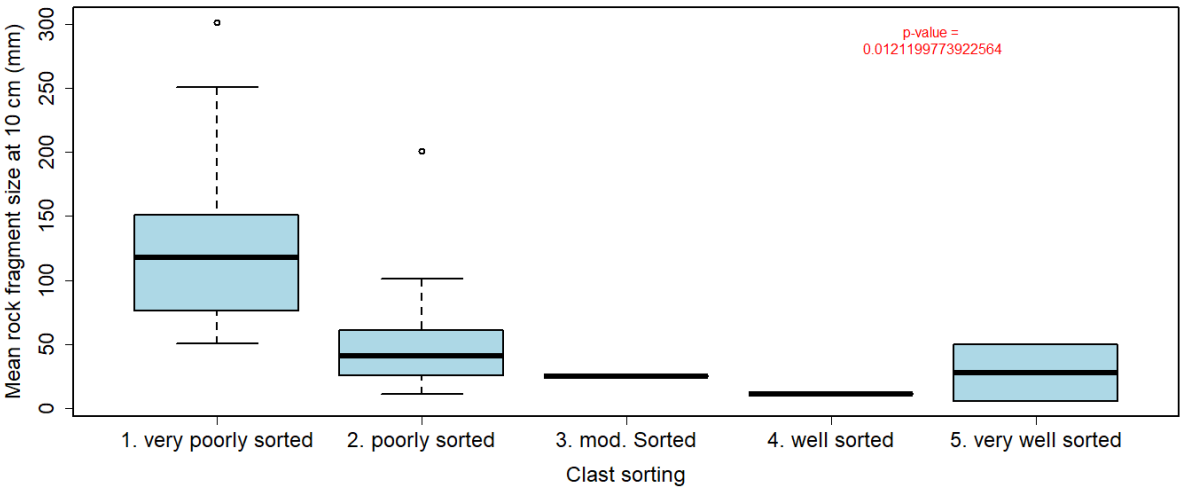

Figure 23: Boxplot of rock fragments (%) at 10 cm depth for the five clast sorting classes measured at 10 cm depth, including the overall p-value (red).

5.2 PCA and NMDS analysis

PCA performs best for continuous data and the inclusion of the nominal and ordinal data as pseudo variables resulted in a lower explanatory power of the first two axis (37%) compared to omitting them (42%). Further removal of discrete data and the soil horizon thicknesses yielded the first two principal components to capture 57% of the variance.

The plot locations are visualized as samples (sit1-31) and soil parameters are visualized as vectors. Appendix 18 shows which code corresponds to which original plot number. Distances between plot locations indicate similarities, and angles between parameters show the correlation between them. This means that parameters pointing in the same direction have a positive correlation, and parameters that have opposite directions a negative correlation. The PCA biplot (Figure 24) illustrates that the percentage rock fragments at 10 cm depth (RockPercentage10cm) and mean rock fragment size (mm) at 10 cm depth (RockFragSize) are positively correlated and negatively correlated to organic layer depth (cm) (OrgLayerDepth). Moreover, litter depth (cm) (LitterDepth) and coarse root abundance (nr/dm^2) (CoarseRootAbundance) are relatively strong positively correlated to each other. This is also the case for minimal soil depth (cm) (SoilDepth) and rooting depth (cm) (RootingDepth) and litter depth (cm) (LitterDepth).

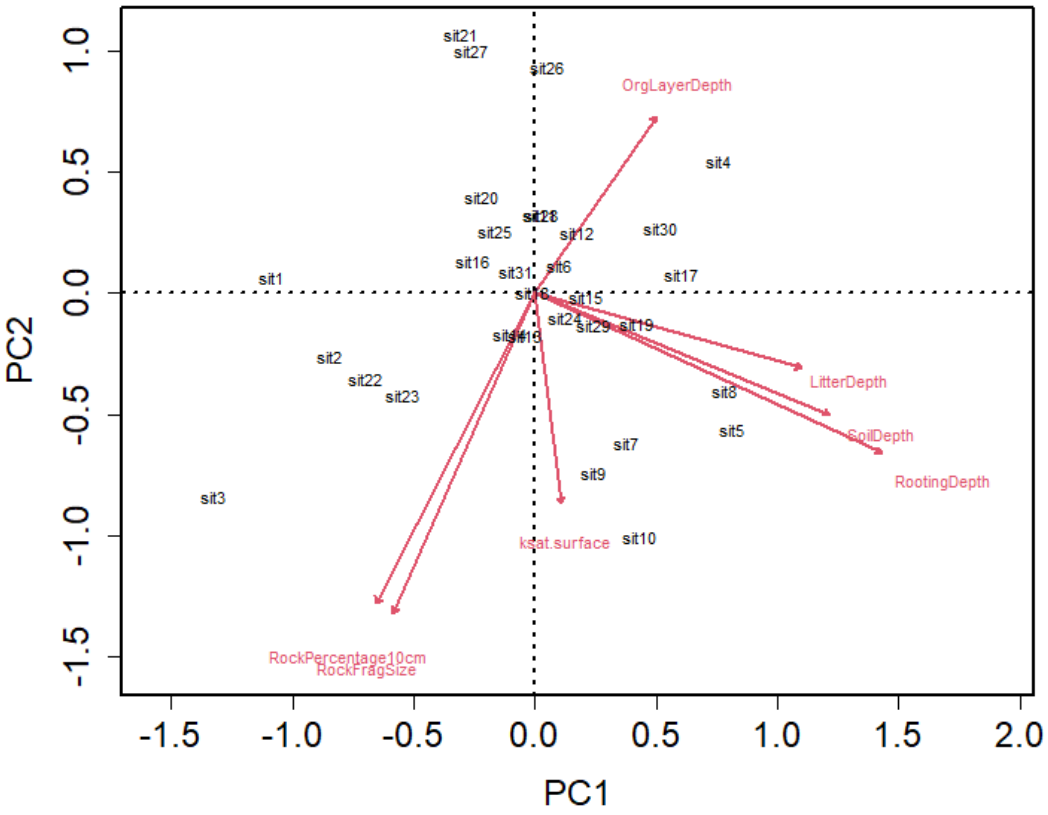

Figure 24: PCA plot of continuous soil parameters (red arrows) and plot locations (black codes (e.g. sit1) (variance explained by PC1 and PC2 = 57%).

Compared to PCA, NMDS performs better with a mix of data types and the soil data (nominal, ordinal, continuous and discrete) are therefore included here. The stress value is ca. 0.102. This is smaller than the limit of 0.2, which means that the NMDS found a good fit (Dexter et al., 2018). The plot gives an

overview of which soil parameters and plot locations are associated with each other (Figure 25). For example, rooting depth (RootingDepth), fine root abundance (FineRootAbundance), minimal soil depth (SoilDepth) and macropores (Macropores) have a positive association. The percentage of rock fragments at 10 cm depth (RockPercentage10cm), the mean rock fragment size at 10 cm depth (RockFragSize) and clast sorting class "very poorly sorted" (VeryPoorlySorted) have also a positive association. Moreover, litter depth (LitterDepth) and organic layer depth (OrgLayerDepth) have a positive association. Furthermore, coarse root abundance (CoarseRootAbundace) and O-horizon as first horizon (O.Hor1) have a positive association.

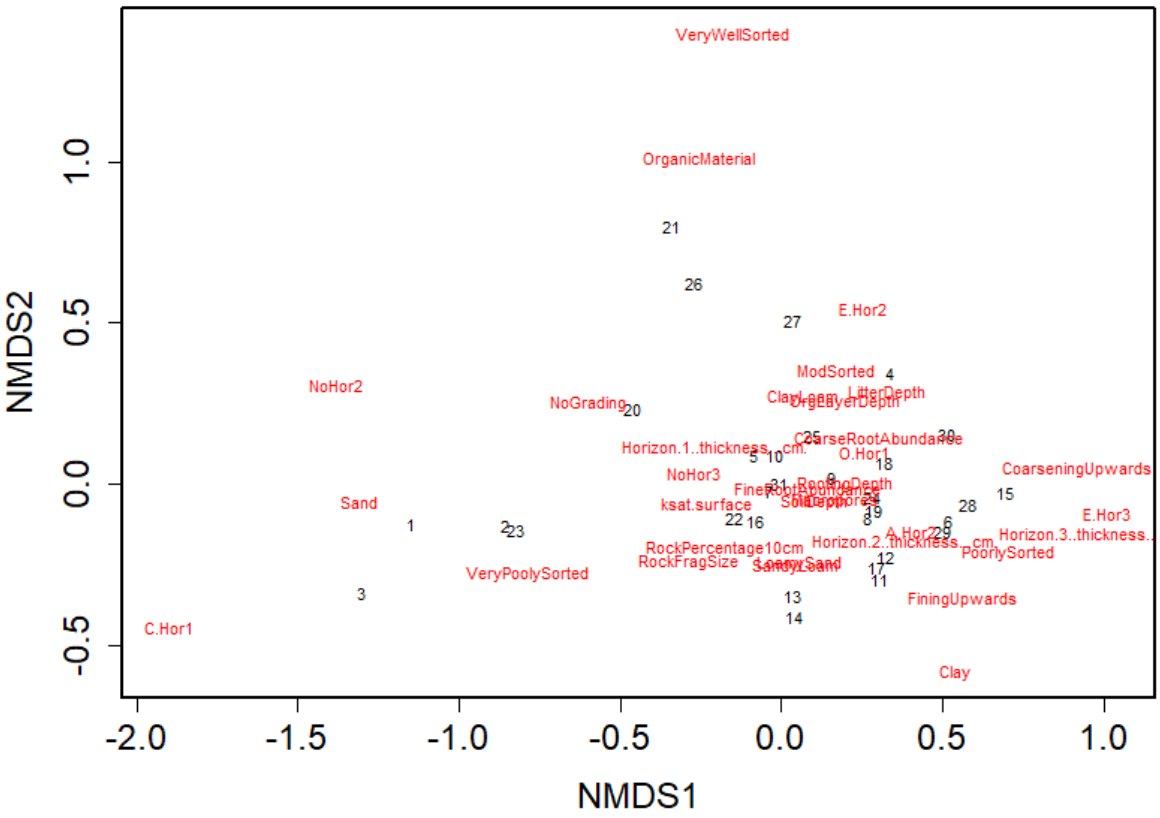

Figure 25: PCA plot of all soil parameters (red arrows) and plot locations (black codes (e.g. sit1).

5.3 Cluster analysis

5.3.1 Clustering by vegetation class

Plots were classified into five vegetation classes: bare (B), forest (F), grass (G), pioneer (P) and shrubs (S). The assignment of the plot locations to these vegetation classes is visualized in the PCA space (Figure 26). This provides an overview of which classes are associated with which soil parameters and which classes have common soil parameters to which they are strongly associated. Since the PCA and NMDS are executed with different data, the grouping of the plot locations differs between them. Moreover, NMDS is based on a different distance, which results in a different configuration. Therefore, both visualizations are presented in this section. The PCA plot shows that the bare plots have very different soil characteristics compared to all other plots. The other vegetation classes have relatively much overlap in the PCA, especially shrub, pioneer and grass plots have comparable soil parameters according to the PCA ordination. Forest plots are strongly associated to minimal soil depth (cm), rooting depth (cm) and litter depth (cm) in comparison to the other vegetation classes.

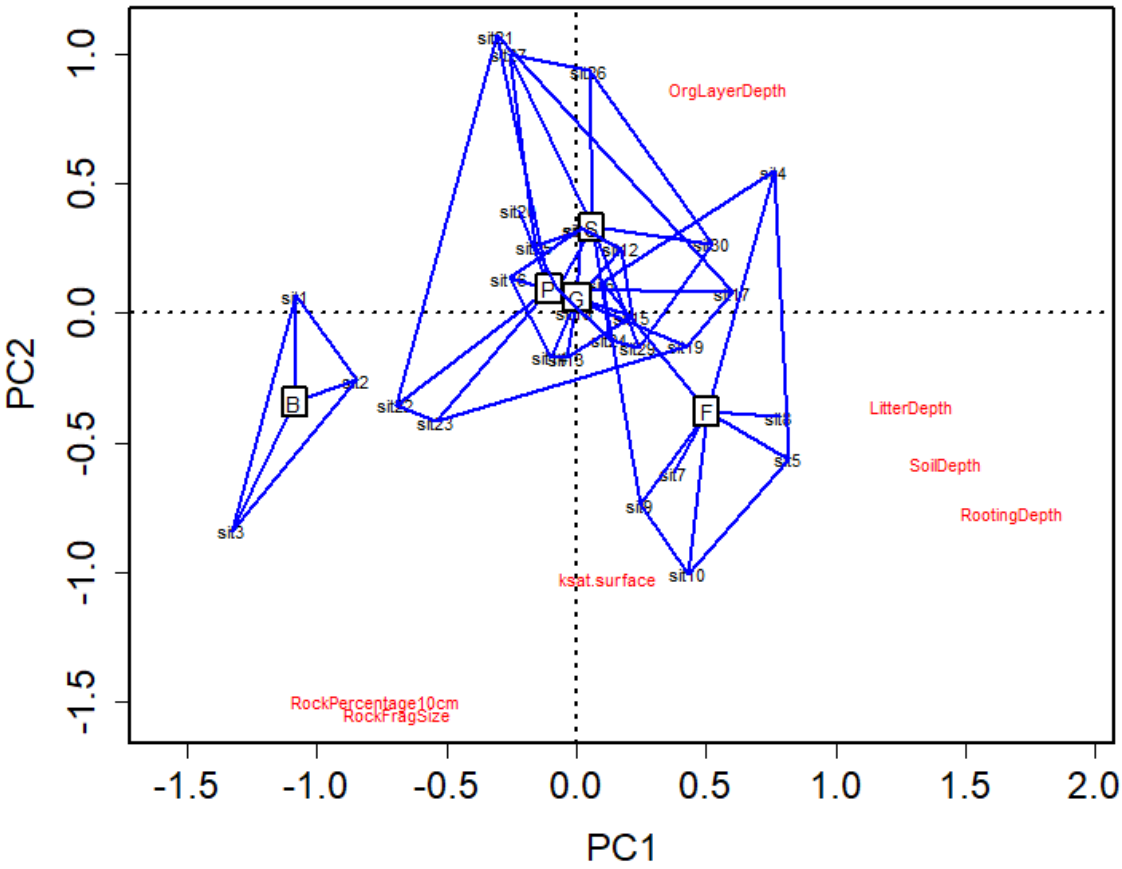

Figure 26: PCA plot of soil parameters (red) and plot locations (black), including clustering by vegetation class (B = Bare, F = Forest, G = Grass, P = Pioneer and S = Shrub). The vectors of the soil parameters are not included for a clearer visualization.

The grouping in the NMDS plot (Figure 27) shows also that bare plots form a distinct group with respect to soil parameters, which is in line with the PCA plot (Figure 26). Bare plots are relatively strong associated to C-Horizon 1, soil texture class “sand” and soil sorting class “very poorly sorted”. Different from the PCA vegetation clustering, the shrub and forest plot clusters are closely located to each other, and the grass cluster is located a little further from them. The pioneer cluster is located between the bare and the others, which is also different from the PCA.

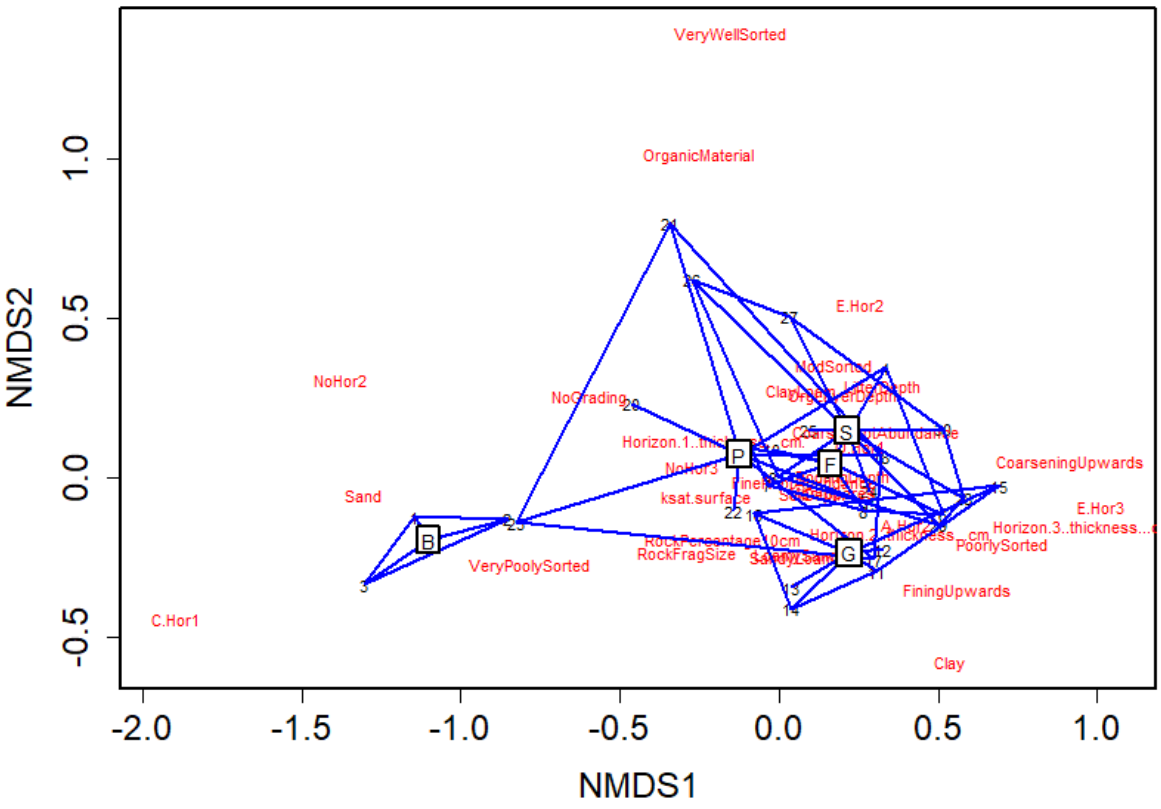

Figure 27: NMDS plot of all soil data (red) and plot locations (black), including the vegetation class clustering (B = Bare, F = Forest, G = Grass, P = Pioneer and S = Shrub).

All in all, it can be said that grouping the plot locations by their vegetation class provides an overview of which soil parameters are related to which vegetation classes. However, the most vegetation classes have overlap in their clusters, which means that this vegetation classification is not a good predictor for soil characteristics. Therefore, another clustering technique was used to find out whether some plot locations can be clustered based on their soil properties.

5.3.2 Cluster analysis

The results of cluster analysis were compared to the above to ordinations and their performance evaluated by their separation of samples in groups in ordination space. The best results were obtained using the Canberra distance.

The dendrogram (Figure 28) shows how the clusters are formed by the Ward's minimum variance linking method and the Canberra distance. The choice was made to create four groups, which are visualized by the red boxes in the dendrogram. The plot locations are also visualized in the dendrogram with the different colors.

Plots from pioneer vegetation class are placed in all groups. This indicates that the soil properties of pioneer plots are relatively variable. Group 1 comprises all the three bare plots and two pioneer plots. This indicates that P5 and P8 resemble the soil properties of bare plots. Three shrub plots are located in group 2 together with P6 and F1. Group 3 mainly consists of forest and grass plots. Group 4 has all vegetation classes except bare plots.

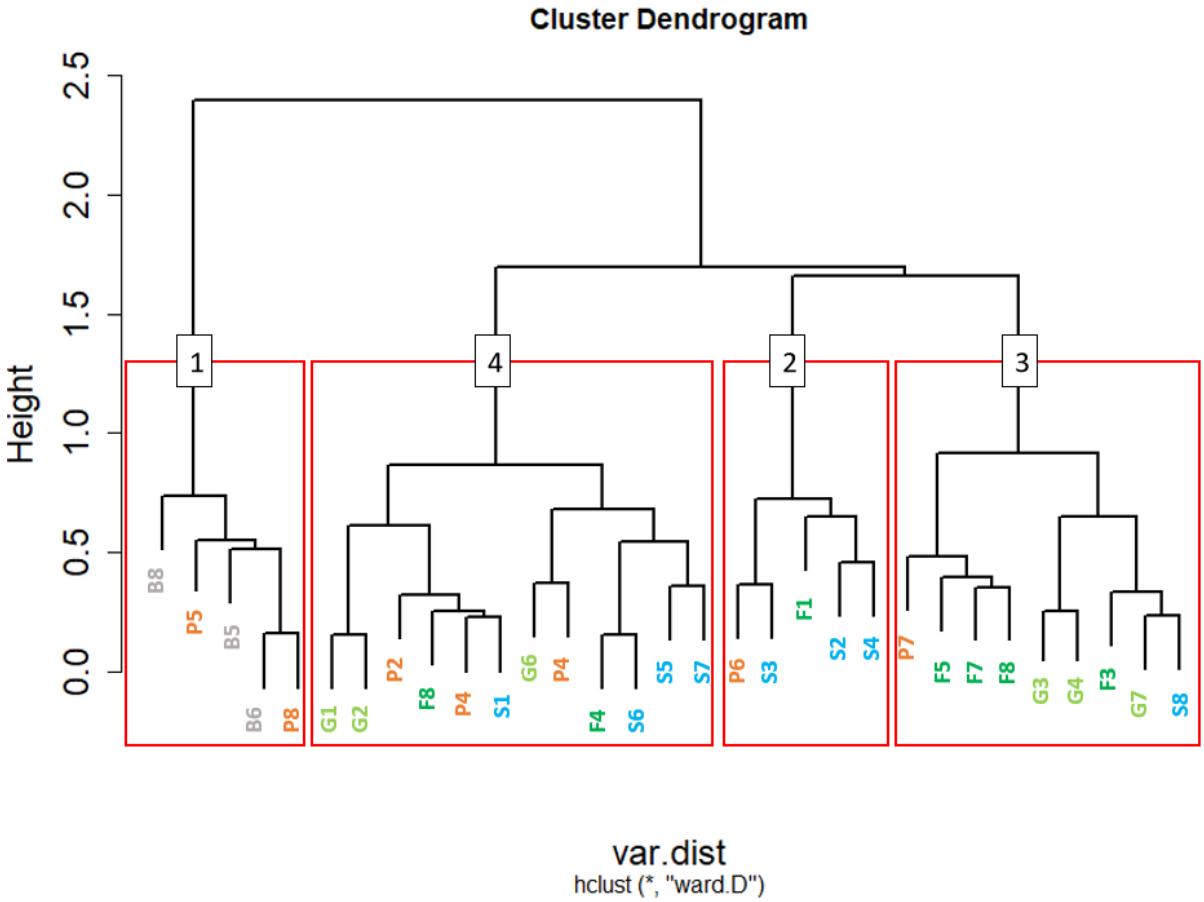

Figure 28: Dendrogram of all the soil data that is used in the NMDS analysis, clustered by Ward's minimum variance method and the Canberra distance. The colors indicate the vegetation classes: bare = grey, pioneer = orange, grass = light green, forest = dark green, shrub = blue.

All clusters are clearly separated in the NMDS space (Figure 29). This indicates that these clusters have different soil characteristics. For example, group 1 consists of plot locations that have associations with the soil texture class "sand", sorting class "very poorly sorted", no grading class and a C-Horizon 1. Group 2 is associated with sorting classes "moderately sorted" and "very well sorted", an E-Horizon 2, soil texture class "clay loam", organic layer depth, litter depth and soil texture class "Organic material". Group 3 has plot locations that are associated with among others high fine root abundance, soil texture classes "sandy loam" and "loamy sand" and minimal soil depth. Group 4 has associations with an A-Horizon 2 and horizon 2 thickness, E-Horizon 3 and horizon 3 thickness and the sorting class "poorly sorted". The soil parameters rooting depth and macropores are located in between group 3 and 4.

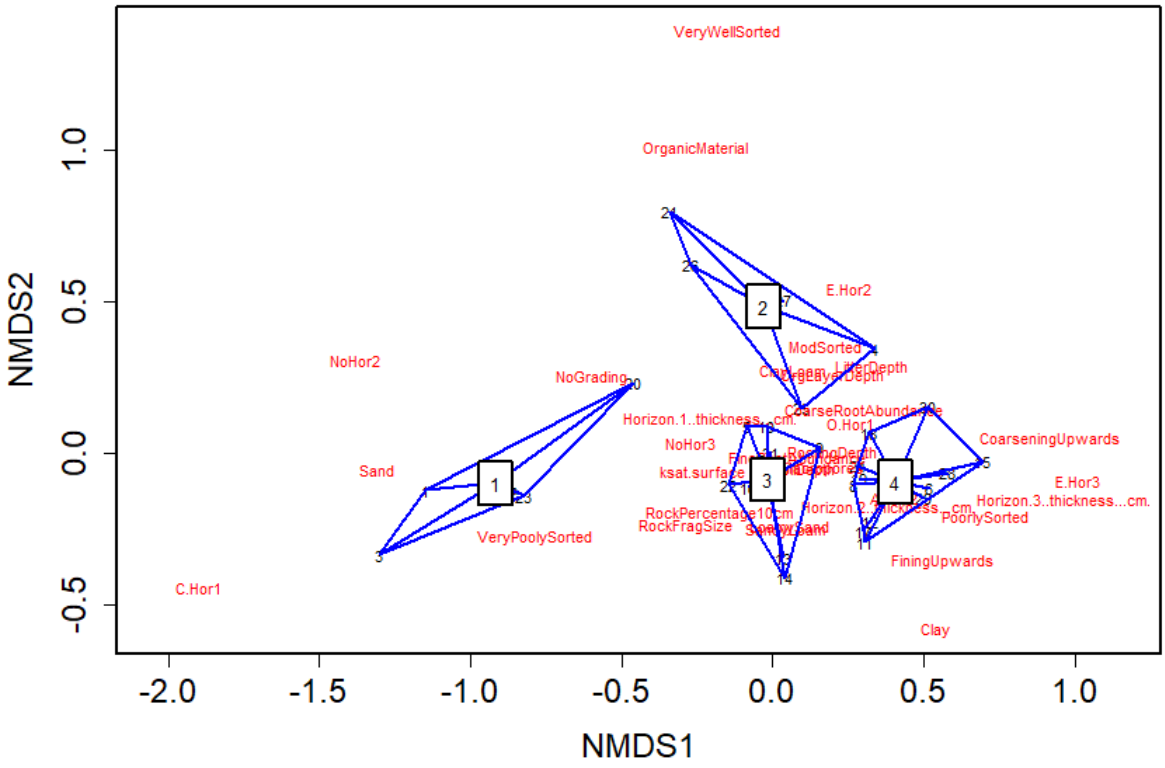

Figure 29: NMDS plot all soil data (red) and plot locations (black), including clustering by Ward's minimum variance method and the Canberra distance.

5.4 Explanatory variables

In this section, the explanatory variables are passively plotted as vectors in the PCA and NMDS plots. The directions of the explanatory variables show whether they have positive or negative correlations to soil parameters and plot locations. The r^2-value of every explanatory variable is equal to the partition of that explanatory variable to the total variance of the soil (response) variables in the PCA or NMDS plot.

5.4.1 Topographic explanatory variables

The topographic properties that have been determined in the field are elevation, slope angle, aspect and slope form. The slope form has four classes: straight, concave, convex and complex. All these topographic variables are used as explanatory variable and are plotted passively in the PCA as vectors (Figure 30).

Elevation and complex slope form have both a negative association with litter depth, soil depth and rooting depth. Slope angle has a positive association with rock fragments and rock fragment size and a negative association with organic layer depth. Convex slope form is negatively associated k_{sat} surface. Elevation (m) explains ca. 69.7% of the variance of the continuous soil parameters in the PCA. The r^2 values of the other topographic variables are not significant (Table 6).

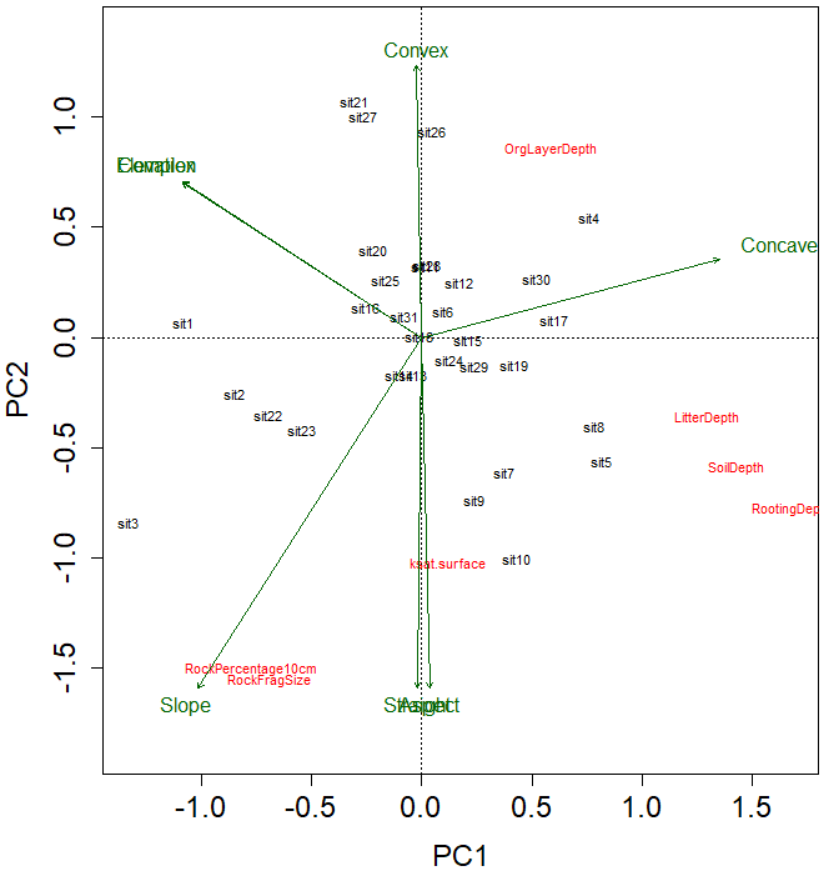

Figure 30: PCA plot of the continuous soil data (response variables, red) and plot locations (black), including the passively plotted topographic explanatory variables (green) and the clustering by Ward's minimum variance method and the Canberra distance (Note: elevation and complex pointing both to the upper-left corner and aspect and straight pointing both downwards).

Table 6: r^2 values of the topographic (explanatory) variables for the soil (response) variables in the PCA, including the p-values.

Topographic (explanatory) variable	r^2	Pr(>r)
Elevation (m)	0.6968	0.001
Slope (°)	0.0464	0.519
Aspect (°)	0.0504	0.536
Slope form class = "straight"	0.1118	0.213
Slope form class = "convex"	0.0723	0.353
Slope form class = "concave"	0.054	0.461
Slope form class = "complex"	0.0342	0.629

The NMDS plot (Figure 31) indicates that elevation has a positive association with plot locations from group 1 and the soil texture class "sand", no second horizon and a C-Horizon 2. Similar to the PCA plot (Figure 30), elevation has a negative association with rooting depth, litter depth and soil depth. Also, the positive association of slope form "convex" and the plot locations from group 4 is visible in the NMDS, like in the PCA. In addition, complex is also associated to group 4 in the NMDS plot. Furthermore, slope angle is still positively correlated with rock fragments percentage and mean rock fragment size. Table 7 provides the r^2 values of the different topographic variables and their corresponding p-values. None of r^2 values is significant.

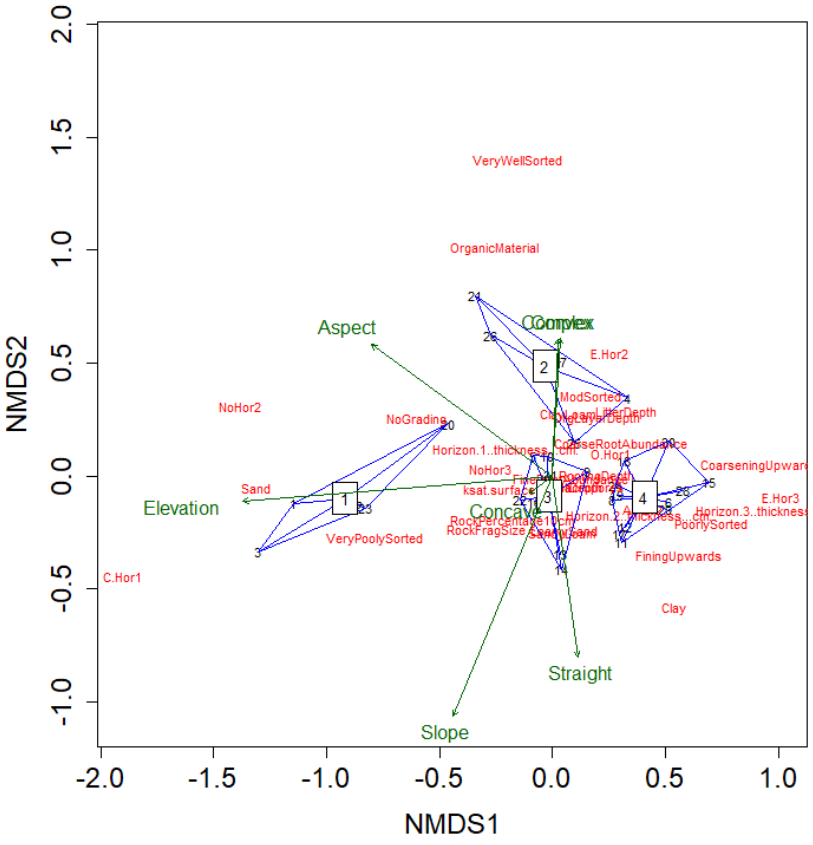

Figure 31: NMDS plot of all the soil data (response variables) (red) and plot locations (black) and the passively plotted explanatory (topographic) variables (green), the clustering by Ward's minimum variance method and the Canberra distance (Note: convex and complex point both in upward direction).

Table 7: r^2 values of the topographic (explanatory) variables for the soil (response) variables in the NMDS, including the p-values.

Topographic (explanatory) variable	r^2	Pr(>r)
Elevation (m)	0.1763	0.060
Slope (°)	0.1232	0.149
Aspect (°)	0.0916	0.263
Slope form class = "straight"	0.0612	0.423
Slope form class = "convex"	0.0350	0.612
Slope form class = "concave"	0.0016	0.972
Slope form class = "complex"	0.0341	0.630

5.4.2 Surface cover explanatory variables

There are four surface cover parameters used in this research: vegetation, bare soil, rock and litter cover, which are plotted passively as explanatory variables in the PCA space (Figure 32). Considering the site scores of the first two axis of the PCA, rock and bar soil cover are negatively correlated with litter and vegetation cover. These surface cover (explanatory) variables are correlated with the first PCA axis. This means that the PCA analysis can be interpreted as the gradient from no vegetation and litter cover, dense rock cover and bare soils to dense vegetation and litter cover.

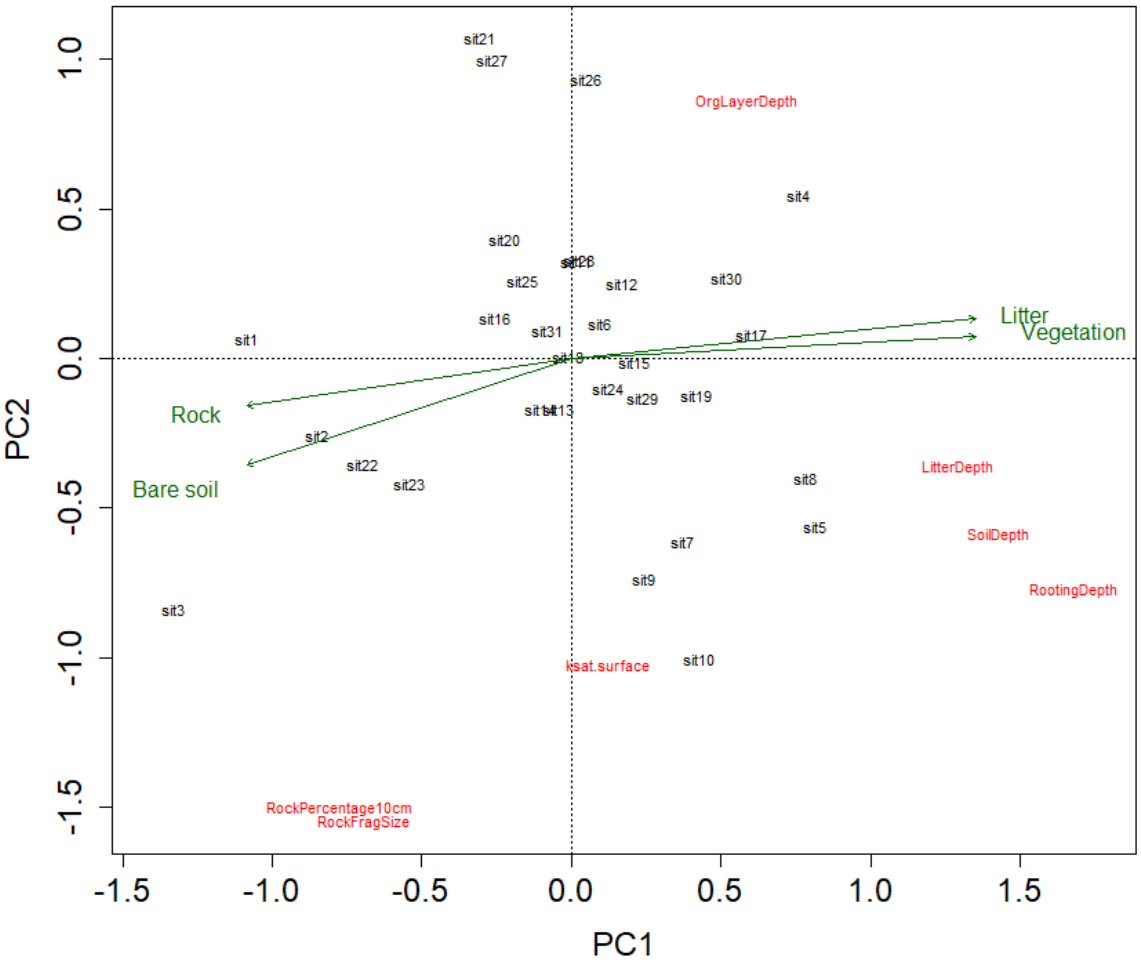

Figure 32: Numeric soil parameters (without horizon thicknesses) and plot locations PCA plot, including the surface cover explanatory variables and the Canberra clustering method.

Vegetation and rock cover explain a large part of the soil parameter variance which is ca. 56.9 and 54.8%, respectively (Table 8). So, their explanatory power is somewhat lower than that of elevation (ca. 69.7%, Table 6). Litter cover explains ca. 25.0%. The contribution of bare soil cover to the variance in soil parameters in the PCA is insignificant. Although, together, the surface cover parameters have probably a strong explanatory power.

Table 8: r^2 values of the surface cover (explanatory) variables for the soil (response) variables in the PCA, including the p-values.

Surface cover (explanatory) variable	r^2	Pr(>r)
Vegetation cover (%)	0.5689	0.001
Litter cover (%)	0.2498	0.031
Rock cover (%)	0.5479	0.001
Bare soil cover (%)	0.021	0.704

In the NMDS plot (Figure 39), rock cover (%) has a positive association with group 1. Similar to the PCA, rock and vegetation cover are negatively associated. The association between litter and vegetation cover (%) is smaller than in the PCA. This is also the case for rock and bare soil cover (%).

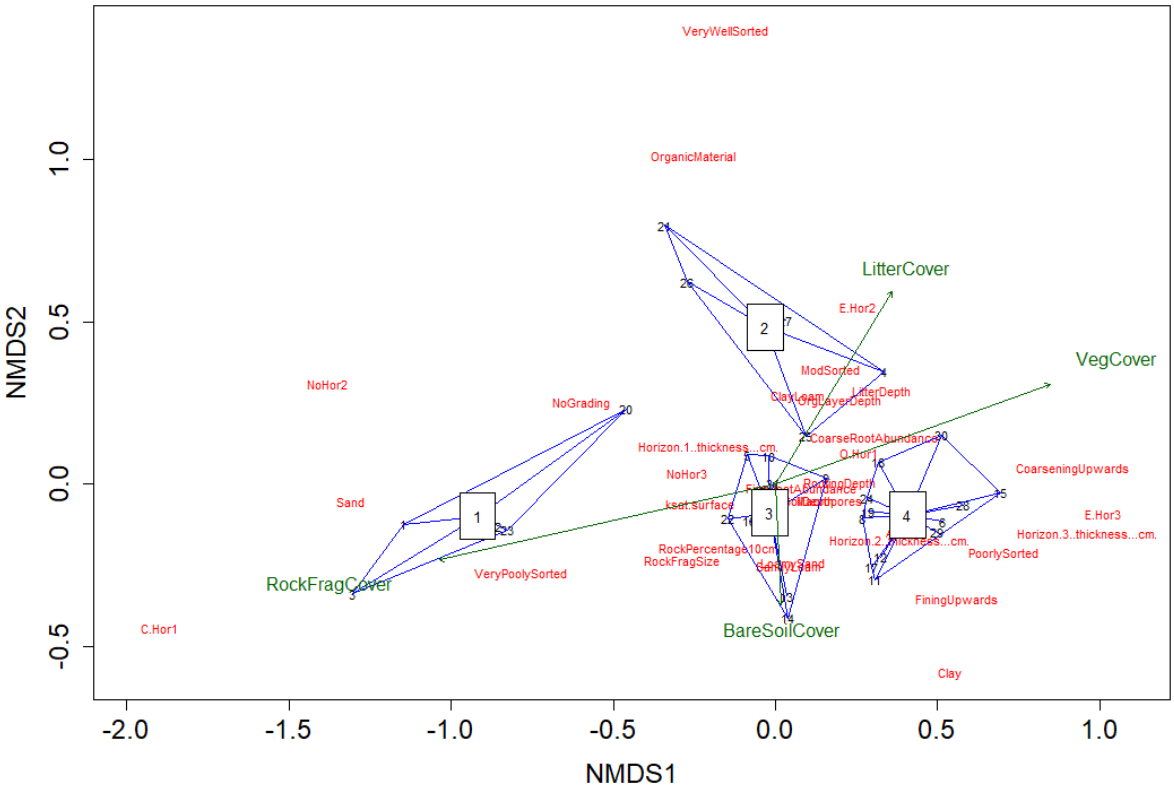

Figure 33: NMDS plot of numeric and ordinal soil data (response variables) (red) and plot locations (black) and the explanatory (surface cover) variables, including clusters derived by the Canberra clustering method.

Rock cover corresponds with ca. 70.3% of the configuration of the NMDS, which is a relatively large in comparison to vegetation and litter cover (ca. 50.6 and 29.9%). The r^2 value of the bare soil cover is insignificant (Table 9). The surface cover values of the NMDS cannot be compared to the topographic

(explanatory) variables of the NMDS, because of there were no significant topographic variables in the NMDS (Table 7).

Table 9: The r^2 values of the topographic (explanatory) variables for the soil (response) variables in the NMDS analysis.

Topographic (explanatory) variable	r^2	Pr(>r)
Vegetation cover (%)	0.5057	0.001
Litter cover (%)	0.2994	0.004
Rock cover (%)	0.7026	0.001
Bare soil cover (%)	0.0859	0.269

6 Discussion

The results document different correlations and relationships between soil, topographic and vegetation parameters. In this research the aim is to find out how the soil, topographic and vegetation parameters are related. This discussion aims to evaluate whether the correlations and relationships are caused by the interaction between soil, topography and vegetation or by external factors.

6.1 Effects of vegetation

The cluster analysis indicates that the predefined vegetation classes are not a good predictor of soil characteristics. Soil formation and development are controlled by multiple factors like time, climate, lithology, organisms and topography (Alewell et al., 2015; Egli et al., 2014; Kirkpatrick et al., 2014), which makes this a logical result.

However, the outcomes PCA and NMDS analyses show that vegetation cover explains a large amount of the variance of the continuous soil data and all soil data, respectively. This indicates that vegetation has a large influence on the soil characteristics.

The grouping assignment based on soil characteristics (Figure 28) also shows that vegetation classes have influence on the soil properties. Some groups consist of (mainly) two vegetation classes. For example group 1, which comprises all bare plots and two pioneer plots. This is a logical outcome, because four of these five plots have less than 10% vegetation cover (P5 has 40%) and many soil parameters that were measured are directly or indirectly related to vegetation. Measured soil properties that have a direct link to vegetation are rooting (Figure 18) and litter depth (Appendix 23 and 24) and fine and coarse root abundance (Appendix 25-28), and their values are very low for bare plots in comparison to the others.

6.1.1 Organic matter

A soil characteristic that is indirectly affected by vegetation is the soil organic matter content, which is measured in the laboratory for some soil samples. The values range from 0.49 to 31.34% (median = 1.31%). These values are party comparable with the data from a research in the Swiss Alps (Matteodo et al., 2018), which has organic matter contents from 0.45 to 59% (median = 6.2%). The maximum and median of Matteodo et al. (2018) much larger, which can be caused by differences in vegetation, climate and the decomposition by microbial activity.

Vegetation provides organic carbon to the soil by their litter and the turnover of fine roots (D'Amico et al., 2015; Siles et al., 2016; Y. Yang et al., 2018). However, no correlations were found for both the organic matter content of the surface and 10 cm depth-samples with vegetation cover. Besides the organic matter content, also the organic layer depth is measured for every plot location. However, vegetation cover has only a weak positive correlation with organic layer depth (0.25) (Figure 15). This result is different from Giupponi et al. (2023), who found a high positive correlation between vegetation cover and soil organic matter. The weak correlation in this research is probably caused by the differences in the amount of litter per vegetation class. The organic matter contents of the surface and 10 cm depth samples have no correlation with litter depth nor cover. For organic layer depth, there is a moderate correlation with litter cover (0.45) (Figure 15). Also the plotting of litter cover as explanatory variable in the NMDS plot (Figure 33) illustrates that litter cover has a positive association with the soil texture class "organic material" and with the organic layer depth. On the contrary, grass plots for example, have generally a large vegetation cover (median ca. 85%), almost no litter and relatively low organic layer depths. Moreover, the turnover of fine roots seems to have a minor impact on the soil organic matter, because grass plots have generally the largest amount of fine roots (median ca. 50 roots per/dm^2). Also the correlations between organic layer depth with litter cover (0.45) (Figure 15), litter

depth (0.23) and fine root abundance (-0.09) (Figure 13) show that organic matter is more likely to be produced by the turnover of litter than fine roots.

The boxplot analysis indicates that shrub and pioneer plots have generally the largest organic layer depths (Figure 21 and 22). This corresponds to the litter cover values of shrubs plots (median ca. 90%), but the median of pioneer plots is much lower (ca. 25%) (Appendix 29 and 30). This is probably caused by the fact that the soil measurements were executed at the locations were soil is present, which is mostly at the places where the litter is located. Forests have the largest litter cover and depth, but this does not result in larger organic layer depths.

6.1.2 Soil depth

Another process that is partly controlled by vegetation is denudation, because vegetation can prevent erosion and can capture soil material (Alewell et al., 2015; Caviezel et al., 2014; Isselin-Nondedeu & Bédécarrats, 2007; Y. Yang et al., 2018). Both of these effects are beneficial for an increasing soil depth.

Plant root density and root length can enhance the soil strength (Alewell et al., 2015; Giupponi et al., 2023; Meusburger et al., 2010; Vannoppen et al., 2015). Consequently, this will reduce the erosion-potential of soils (Alewell et al., 2015; Caviezel et al., 2014). This corresponds partly with the outcomes of the correlation analysis, where soil depth has a strong positive correlation with rooting depth (0.79), a moderate positive correlation with fine root abundance (0.48) and a weak correlation with coarse root abundance (0.23) (Figure 13).

Besides enhancing the soil strength, vegetation can prevent soil erosion by other processes. Rainfall can be intercepted by the canopy of vegetation, which reduces the amount of water reaching the surface of the soil (Wang et al., 2013). It also decreases the velocity of the falling raindrops, which reduces the impact (Ma et al., 2014). Therefore, the detachability of soil particles will decrease, which results in decreased sheet erosion rates (Ma et al., 2014; Talebi et al., 2016).

The erosion rate by sheet flow can decrease further due to friction by vegetation, which reduces the flow velocity and consequently, the strength to detach soil particles (Alewell et al., 2015; Isselin-Nondedeu & Bédécarrats, 2007; Meusburger et al., 2010; Talebi et al., 2016). The decrease in velocity of the sheet flow can eventually lead to deposition of soil particles (Talebi et al., 2016). This will increase the soil depth. Furthermore, plant canopy reduces wind velocities, which can result in the deposition of sediments that were transported by the wind (Isselin-Nondedeu & Bédécarrats, 2007).

So, vegetation cover and canopy completeness have a positive effect on sediment trapping (Giupponi et al., 2023) and erosion prevention (Isselin-Nondedeu & Bédécarrats, 2007), which should be beneficial for the soil depth. Vegetation cover has a moderate positive correlation with soil depth (0.42) (Figure 15), which is in line with the effects of vegetation cover to the processes explained above. However, this value is relatively low compared to the results of Giupponi et al. (2023), who found a correlation of more than 0.8.

Erosion by water like sheet erosion can be prevented by vegetation due to increased infiltration rates (Isselin-Nondedeu & Bédécarrats, 2007). Improved soil structure causes that water can flow easier through the soil, which enhances the infiltration rates. In turn, the supply of organic matter causes the formation of soil aggregates, which improves this soil structure (Wang et al., 2013). Furthermore, the presence of roots can create preferential flow paths for infiltrating water, which also can enhance the infiltration rates (Li et al., 2007; Zuo & He, 2021). However, no correlation between the k_{sat} of the surface samples and soil depth can be found (Figure 13).

Besides, sediment trapping and preventing erosion, vegetation can enhance soil formation by increasing the physical weathering of the parent material (Egli et al., 2014; Phillips et al., 2008). Roots can penetrate into rocks and accelerate rock wedging and fragmentation (Egli et al., 2014; Phillips et al., 2008).

The boxplot analysis shows that forests have the largest soil depths (median ca. 35 cm). This is a logical result, because forest plots have the largest rooting depth (Figure 18), coarse root abundance (Appendix 27 and 28) and vegetation cover (Figure 19). Moreover, forests have the most complete canopy. All these factors are favorable for preventing erosion and stimulating deposition and physical weathering. On the other hand, bare plots have generally no vegetation and soil, which also corresponds with the explanations from above.

The diagram below (Figure 34) gives an overview of three properties of vegetation (roots, canopy and the supply of organic matter) that cause an increase sedimentation and physical weathering, and a decreased erosion, which results in an increasing soil depth.

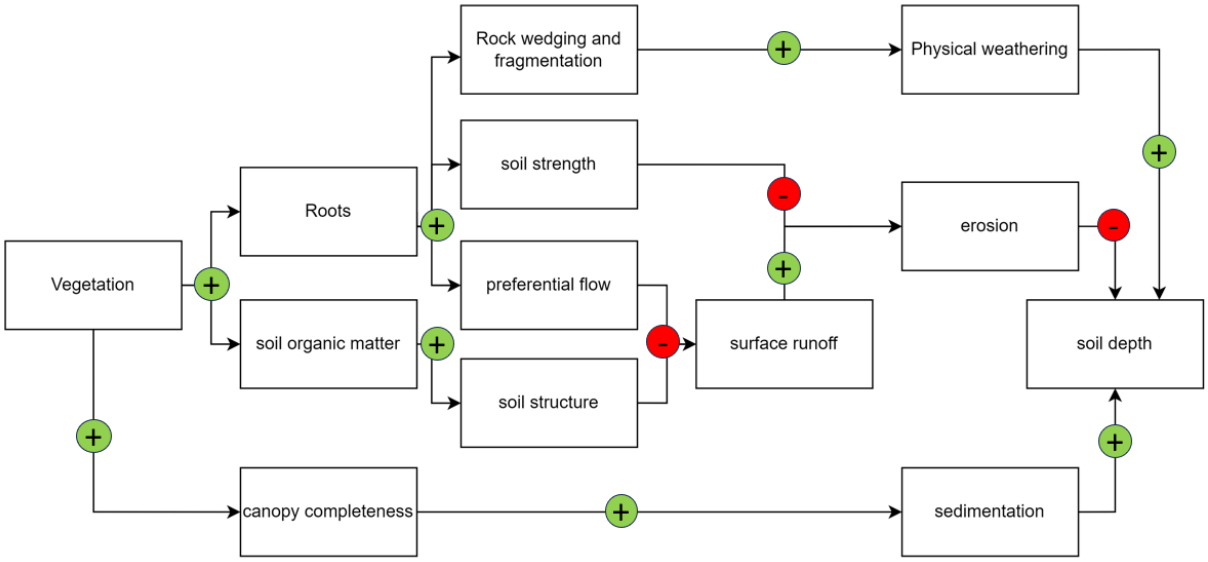

Figure 34: Overview of effects of vegetation on soil depth, where an increase in sedimentation and physical weathering, and a decrease in soil erosion cause an increase in soil depth (scheme by Dick van de Lisdonk).

6.2 Effects of topography

According to the PCA analysis, elevation has the strongest explanatory power to predict variations in soil parameters among the environmental predictors (variables). A major cause of this can be that elevation strongly affects the climatic conditions and consequently, the soil characteristics (Kirkpatrick et al., 2014; Y. Yang et al., 2018). At every 1000 m higher elevation the temperature decreases by ca. 6.5°C (Rist et al., 2020) and the UV-radiation increases by ca. 10% (Donhauser & Frey, 2018). Moreover, due to the decreasing temperature, condensation increases at increasing elevation, which affects the precipitation (Sevruk, 1997). Also wind velocity depends on elevation (Y. Yang et al., 2020). These elevation controlled climatic variables are crucial for plant growth (Y. Yang et al., 2018). This is in line with the moderate negative correlation (-0.6) between elevation and vegetation cover (Figure 16). Consequently, forests do not grow above 2300 m in the study area (Appendix 19 and 20). The other vegetation classes have more overlap in their elevation spread. Although, the median of shrubs (ca. 2400 m) is slightly lower than those of bare, pioneer and grass plots.

The elevation controlled climatic variables have also influence on biochemical reactions like photosynthesis and respiration. These biochemical reactions control the supply of organic matter to

the soil (Donhauser & Frey, 2018; van der Putten et al., 2013). Furthermore, soil temperature (Catoni et al., 2016) and soil moisture content depend on the elevation controlled climatic variables, which affect the microbial activity (Donhauser & Frey, 2018; Siles et al., 2016; Tyagi et al., 2023; Wu et al., 2016). Microbial activity has a key role in soil development, because it controls the decomposition of organic matter and the cycling of nutrients in the soil, which is crucial for plant growth (Donhauser & Frey, 2018; Hagedorn et al., 2019; Martinez-Almoyna et al., 2020; Siles et al., 2016; Wu et al., 2016; Y. Yang et al., 2018; Yimer et al., 2006). So, the organic matter supply of vegetation has a positive feedback on vegetation growth (Figure 35). For increasing elevation, the positive effect of this feedback loop will decrease.

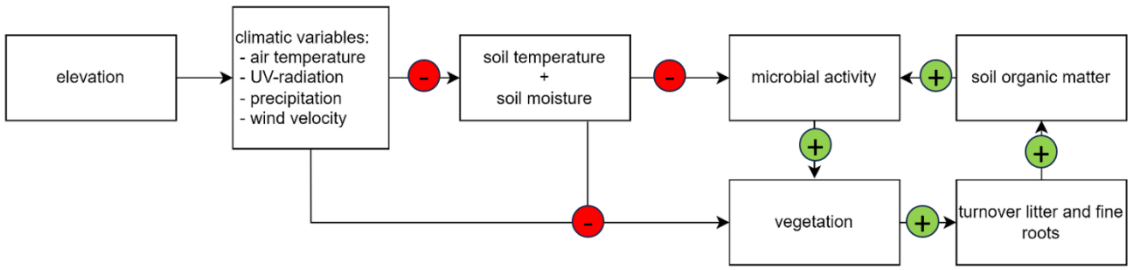

Figure 35: Overview of effects of elevation to vegetation growth, and the positive feedback of vegetation on its growth (scheme by Dick van de Lisdonk).

Thus, elevation has a large impact on the plant growth. Therefore, it indirectly influences the soil properties that depend on vegetation. This can be a reason for the strong explanatory power in comparison to the vegetation, litter and rock cover.

Climatic variation in alpine environments is not only controlled by elevation, but also by aspect and slope (Kirkpatrick et al., 2014; Wu et al., 2016). Aspect and slope influence the amount of solar radiation that can be received, which affects soil conditions like, soil temperature, soil moisture content and the nutrient cycling (Wu et al., 2016). This leads to a mosaic of microclimates (Aalto et al., 2013; Donhauser & Frey, 2018; Yimer et al., 2006). However, the explanatory power to predict variations in soil parameters of both aspect and slope angle is not significant in this research. Moreover, the correlations of aspect (-0.26) and slope angle (-0.13) with vegetation cover are both weak (Figure 16).

Topographic variables that should have influence on erosion and deposition and therefore, on the soil depth are the slope angle and slope form (Alewell et al., 2015; Donhauser & Frey, 2018; Sabzevari & Talebi, 2019). However, no correlation of slope angle with soil depth could be detected in this study (Figure 14) and the different slope forms have no significant differences in soil depth.

6.3 Cluster analysis

The cluster assignment by soil characteristics resulted in four groups of plot locations with common soil characteristics (Figure 28 and 29). Group 1 is associated with C-horizon as first horizon and no second horizon. Both parameters indicate that these soils did experience almost no pedogenic processes (FAO, 2006). This is in line with the positive association with rock cover (Figure 33) and elevation (Figure 31) and negative association with vegetation cover.

Group 2 is associated with organic layer depth, the soil texture class “organic material” and litter depth. These correlations are logical outcomes, because of the dependence of organic matter by the turnover of litter, as explained above. This group is also associated with clast sorting classes “moderate” and “very well sorted” (note that “well sorted” is not included in the NMDS ordination). This is probably caused by the fact that the vegetation in these plots creates an organic soil due to the litter turnover

instead of the deposition of eroded material from upslope locations. This reduces the variability in rock fragments (diameter > 2 mm) in the soil, which causes these soils to be moderate to very well sorted.

Group 3 is located in the center of the NMDS plot. It seems that this group has more average soil characteristics in comparison to the other groups. Although, it is associated with fine root abundance, soil depth and rooting depth, which is in line with the explanation of erosion and deposition from above.

Group 4 is associated with E-horizon as third horizon and the horizon 3 thickness, which means that these soils have developed for a relatively long period of time. Group 4 is also associated with rooting depth and coarse root abundance. As explained above, these factors stabilize the soil, which prevents erosion. These are favorable conditions for a long period of soil development, which corresponds with the association to a third horizon (Catoni et al., 2016; Donhauser & Frey, 2018).

6.4 Saturated hydraulic conductivity

The values of the k_{sat} experiments of 73 samples vary between 0.18 and 101.5 m/day. There is a significant difference between medium sand (median ca. 100 m/day) and the other values (medians between ca. 0 and 20 m/day) (Figure 21). These values are comparable with values of other studies in the Swiss Alps (Maier et al., 2020, 2023). Generally, k_{sat} decreases with finer soil textures (Gupta et al., 2021; Maier et al., 2020; Y. Yang et al., 2020). The k_{sat} increases with stoniness of a soil (Maier et al., 2020; van Wesemael et al., 2000). This corresponds to the moderate positive correlations between k_{sat} at 10 cm depth with mean rock fragment size (mm) at 10 cm depth (0.42) and with rock fragments (%) (0.39).

Besides soil texture, k_{sat} values can be influenced by the presence of vegetation. Hence, it has a positive relationship with root density due to preferential flow and soil organic matter because of improved soil structure (Li et al., 2007; Zuo & He, 2021). This corresponds with the fact that coarse root abundance has the largest positive correlation (0.33) (Figure 13) with the k_{sat} of the surface samples. The effect of organic matter cannot be seen in the correlation between the k_{sat} of the surface samples and organic matter content or organic layer depth.

6.5 Field capacity and dry bulk density

The values of the field capacity (-) vary between 0.17 and 0.64. This is comparable to the values of Gupta et al. (2021), who analyzed 7294 samples for field capacity. Coarse textured soils have generally a lower field capacity than fine textured soils (Zettl et al., 2011). The field capacity of the 10 cm depth samples were compared for the different soil texture classes at 10 cm depth. Only the soil texture classes “loamy sand” and “sandy loam” have multiple samples from which the field capacity was measured. The medians of loamy sand and sandy loam are ca. 0.3 and 0.47, respectively. These outcomes are in line with the fact that fine textured soils have a larger field capacity than coarse textured soils.

The values of the bulk density (g/cm^3) variate from 0.14 to 1.6 g/cm^3, which is different from the values of Gupta et al. (2021), based on 10487 samples analyzed for bulk density. The differences may be due to the fact that Gupta et al. (2021) did not analyze soils that mainly consist of organic matter, which decrease the bulk density of soils (Chaudhari et al., 2013). In this research several soil samples consist mainly of organic matter. The maximum value of 1.6 g/cm^3 is comparable to the data of Gupta et al. (2021).

6.6 Climate change

6.6.1 Vegetation dynamics

As described in the introduction, greening occurs all over the European Alps and is likely to increase under pressure of climate change (Hagedorn et al., 2019; Heijmans et al., 2022; Intergovernmental Panel On Climate Change (Ipcc), 2022; Rosbakh et al., 2014; Rumpf et al., 2022). Temperature rise leads to accelerated biochemical reactions of ecosystems like photosynthesis and respiration. This alters the supply of organic matter to the soil, which affects soil microbial life and the ecosystem functioning (Donhauser & Frey, 2018; Intergovernmental Panel On Climate Change (Ipcc), 2022; van der Putten et al., 2013). Furthermore, temperature rise enhances the soil temperature which results in increased microbial activity. Together, the increased organic matter supply and the increased microbial activity, leads to an accelerated nutrient cycle (Donhauser & Frey, 2018; Nicholls & Carey, 2021; van der Putten et al., 2013). Sometimes, this causes a net loss from the system (Donhauser & Frey, 2018; van der Putten et al., 2013). Simultaneously, the activity of pioneer microbes will increase due to temperature rise, which is beneficial for vegetation colonization to higher altitudes (Donhauser & Frey, 2018). The upward migration of vegetation also depends on other factors like soil stability and soil development (Rosbakh et al., 2014). So, vegetation dynamics like greening strongly depend on all these plant-soil interactions (van der Putten et al., 2013).

Besides plant-soil interactions, vegetation dynamics are also affected by climatic conditions. The annual precipitation is likely to be increased with 5-20% in 2100 and snowfall will decrease in the European Alps, which decreases the duration of snow cover (Intergovernmental Panel On Climate Change (Ipcc), 2022). This results in a longer growing season, which is also favorable for vegetation colonization to higher altitudes (Carlson et al., 2017; Intergovernmental Panel On Climate Change (Ipcc), 2022; Lamprecht et al., 2018). This causes an accelerating disappearance of cold-adapted species in certain habitats, especially in the subnival zones, but on a local scale the species richness can increase (Carlson et al., 2017; Intergovernmental Panel On Climate Change (Ipcc), 2022; Lamprecht et al., 2018).

All in all, the upward migration of vegetation due to climate change strongly depends on climatic conditions and other factors like soil stability and development (Rosbakh et al., 2014). Therefore, it is expected that especially at locations at the boundary of the snow cover extend in the winter will experience greening in the future. Besides, the locations with a large soil depth and (possibly) multiple horizons are more likely to become colonized by plants from lower elevations, because of their relatively stable slopes and developed soils. On the other hand, the pioneer and bare plots showed that vegetation can also grow at locations with relatively thin soils and large rock covers (Figure 36). Therefore, it is also possible that vegetation will shift upwards to these locations. In addition, some species can create their “own soil” on rocks (Figure 37) by sediment trapping (Isselin-Nondedeu & Bédécarrats, 2007; Talebi et al., 2016) and litter supply with succeeding decomposition (D’Amico et al., 2015; Siles et al., 2016; Y. Yang et al., 2018). In addition, physical weathering (Egli et al., 2014; Phillips et al., 2008), and decreased erosion (Alewell et al., 2015; Caviezel et al., 2014; Giupponi et al., 2023; Meusburger et al., 2010; Vannoppen et al., 2015) are also beneficial for the soil depth (Figure 34).

Figure 36: Vegetation growing on rock surfaces (picture by Dick van de Lisdonk).

Figure 37: Soil formed on a rock surface, which mainly consist of organic matter and litter (picture by Dick van de Lisdonk).

6.6.2 Hydrological effects

The magnitude and seasonality of snowmelt and glacier fed river basins will alter due to climate change (Intergovernmental Panel On Climate Change (Ipcc), 2022). Hence, the average snowmelt is expected to increase during winter, because of increased rainfall instead of snowfall. Moreover, the spring peak is expected to arise earlier in the year. This will lead to an increased winter runoff and eventually to a decrease in runoff at the end of the century (Gobiet et al., 2014; Intergovernmental Panel On Climate Change (Ipcc), 2022). The Meretschibach catchment is also a glacier and snowmelt fed basin, which is likely to experience similar effects due to of climate change.

Greening and upward migration of vegetation causes changes the soil-plant-atmosphere interaction, which alters the catchment hydrology (Nicholls & Carey, 2021). This causes increased evapotranspiration rates, which contribute on a large scale to an intensification of the hydrological cycle (Johnston et al., 2018; Nicholls & Carey, 2021). During summer, decreased precipitation and increased evapotranspiration rates are expected to cause an reduced outflow from the catchment (Gobiet et al., 2014; Nicholls & Carey, 2021). This reduction in summer precipitation can eventually lead to a decrease in productivity of vegetation, which is called browning (Rumpf et al., 2022). Browning occurs currently on a small scale in the Alps (<1%), but it is expected to increase due to the effects of climate change (Rumpf et al., 2022).

The expected increased winter runoff can be reduced by larger soil depths and increased soil water retention capacity, which are effects of greening (Carlson et al., 2017). Moreover, increased soil water retention capacity and vegetation cover cause water to be held in the catchment for a longer duration (Mueller et al., 2013).

6.7 Uncertainties

Taking the soil sample has some uncertainty, because the soil is disturbed a little due to the hammering of the metal cylinder into the soil. Moreover, some plot locations have only a few places with enough soil (5 cm deep) to take a sample. Therefore, a soil sample is not always representative for a plot, especially for bare plots, which have generally a small soil depth and large rock cover. In addition, some rock fragments that did not fit in a sample are replaced or broken to make them fit. These alternations make the sample less representative. Moreover, the 5, 10 and 30 cm depth soil samples have been taken after the pit has been dug. Despite taking the soil samples 5 to 10 cm from the 'main pit', the soil experiences disturbances from digging the pit.

The soils in the research area contain generally many rocks. In many cases the amount of rocks increased with depth, which provided problems with digging the pit for the soil measurements. The soil depth was measured as the depth of the soil pit, perpendicular to the earth's surface. The pit was dug as far as possible, which does not mean that the bottom of the soil was reached. Therefore, the data are defined as minimal soil depth.

Many uncertainties come from parameters that are estimated in the field, like surface covers (%), number of macropores, fine roots or coarse roots per dm^2, rock fragments (%), average rock fragment size (mm).

Every summer, cows are grazing in the study area. This will affect the vegetation composition and cover and consequently, the soil characteristics, erosion and deposition processes (Alewell et al., 2015; Caviezel et al., 2014; Isselin-Nondedeu & Bédécarrats, 2007; Y. Yang et al., 2018). Also, the greening of the research area may be counteracted by the grazing. However, in the research of Carlson et al. (2017) is considered that decreases in snow cover duration and temperature rise have a stronger effect on vegetation dynamics than the effects of grazing. Probably, this is also the case in the Meretschibach catchment.

6.8 Improvements

Besides, the influence of topography, climate and vegetation. Lithology and geomorphology have also effect on the soil properties, which have to be taken into account. Lithology determines the formation and development of soils. The formation depends on the weathering of the parent material, which is positively related to soil thickness (Alewell et al., 2015; D'Amico et al., 2015). The chemical composition of soils is also controlled by the lithology (Alewell et al., 2015; D'Amico et al., 2015; Egli et al., 2014).

As mentioned in the Methodology, the geomorphological unit of every plot location is described in the field, but these are not included in the analysis. However, the geomorphology has a large influence on the formation, development and preservation of soils (Masseroli et al., 2020). In addition, geomorphology is an important factor for plant community composition (Giaccone et al., 2019). Thus, it would be useful if geomorphology will be taken into account in further research.

Not all soil samples that were taken in the field were analyzed in the laboratory. As a result, some plot locations with incomplete measurements needed to be omitted from further analysis. To improve the statistical analysis, it is important that more (all) of these samples will be used to measure the k_{sat}, organic matter content, field capacity and bulk density. Moreover, this will result in a larger dataset that can be used in the PCA and NMDS. This will help to get better insights in the relationships between soil, vegetation and topography in the research area.

The vegetation composition and the surface covers per species, which were derived in the field, were not analyzed in this research. When these data will be used in the analysis instead of the five predefined vegetation classes, the insights about the effects of the vegetation will be improved. Moreover, images

were created of every plot using a drone. These images can (possibly) be used to calculate the exact percentages of the surface covers, which will be more accurate than the estimations that were done in the field.

It is also important that the soil textures of the samples will be analyzed in the laboratory using sieves and laser techniques, because this will improve the insights in the soil texture composition of the samples in comparison to the method that is executed using Appendix 9.

Slope forms play an important role of the denudation in mountain areas (Alewell et al., 2015; Donhauser & Frey, 2018; Sabzevari & Talebi, 2019). The slope forms in this research were described at plot scale and no effects were found. However, erosion and deposition of soil material operates mainly at a hillslope scale. Therefore, it can be interesting to describe the slope form on a larger scale, and try to evaluate whether a plot is located in a part of the slope that receives or loose material.

7 Conclusion

The aim of this research was to investigate the relationships between soil, vegetation and topography in an alpine environment. One of the major findings is that the predefined vegetation classes are no good predictors for soil characteristics. However, the boxplot analysis showed that some soil parameters are typically high or low for certain vegetation classes. In addition, vegetation cover has a strong explanatory power for the soil data.

From the topographic variables only elevation has a strong influence on the soil characteristics, which explanatory power is larger than those of the surface cover variables. This is possibly caused by elevation dependent climatic variables like air temperature, precipitation and solar radiation. They control plant growth and the microbial activity and consequently, various soil characteristics and development of soils. Effects of the other topographic variables (slope angle, aspect and slope form) cause a mosaic of strongly variable soil characteristics. However, the effects on soil characteristics of these variables was not found in this research.

The values of the k_{sat} depend mainly on the soil texture. Coarse root abundance has the largest positive correlation (0.33) with k_{sat} surface, which may induce the effect of preferential flow. Moreover, stoniness is positively related to k_{sat}. Although, it is important to execute the laboratory experiments (k_{sat}, field capacity, bulk density and organic matter content) for all the soil samples that are taken in the field. This will enlarge the dataset, which provides better insights in the relationships of these soil properties with the other soil, topographic and surface cover data.

Climate change will cause greening and upward migration of vegetation in the research area. The rate and extent of this migration depends on climatic conditions and plant-soil interactions. It is expected that vegetation migrates the most to locations with the most developed and stable soils.

The research area is a glacier and snow melt fed catchment. Under pressure of climate change, the runoff from the catchment is likely to increase in the winter and to decrease during summer. At the end of the century, also the winter runoff is expected to decrease. The expected greening of the area may reduce the runoff and may hold the water in the catchment for a longer period. Decreased precipitation during summer together with prolonged periods of droughts can cause browning, which is likely to happen in the Meretschibach catchment under pressure of climate change.

8 References

Aalto, J., le Roux, P. C., & Luoto, M. (2013). Vegetation Mediates Soil Temperature and Moisture in Arctic-Alpine Environments. *Arctic, Antarctic, and Alpine Research*, *45*(4), 429-439. https://doi.org/10.1657/1938-4246-45.4.429

Alewell, C., Egli, M., & Meusburger, K. (2015). An attempt to estimate tolerable soil erosion rates by matching soil formation with denudation in Alpine grasslands. *Journal of Soils and Sediments*, *15*(6), 1383-1399. https://doi.org/10.1007/s11368-014-0920-6

Armstrong, R. A. (2014). When to use the Bonferroni correction. *Ophthalmic and Physiological Optics*, *34*(5), 502-508. https://doi.org/10.1111/opo.12131

Berrick, S. (2023, november 17). *ASTER Global Digital Elevation Model V003*. ASTER Global Digital Elevation Model V003. https://cmr.earthdata.nasa.gov/search/concepts/C1711961296-LPCLOUD.html

Bodenkartierungskatalog—NABODAT. (z.d.). Geraadpleegd 21 juni 2023, van https://www.nabodat.ch/index.php/de/service/bodenkartierungskatalog

Borcard, D., Gillet, F., & Legendre, P. (2011). Canonical Ordination. In D. Borcard, F. Gillet, & P. Legendre (Red.), *Numerical Ecology with R* (pp. 153-225). Springer. https://doi.org/10.1007/978-1-4419-7976-6_6

Carlson, B. Z., Corona, M. C., Dentant, C., Bonet, R., Thuiller, W., & Choler, P. (2017). Observed long-term greening of alpine vegetation—A case study in the French Alps. *Environmental Research Letters*, *12*(11), 114006. https://doi.org/10.1088/1748-9326/aa84bd

Castelli, M. (2021). Evapotranspiration Changes over the European Alps: Consistency of Trends and Their Drivers between the MOD16 and SSEBop Algorithms. *Remote Sensing*, *13*(21), Article 21. https://doi.org/10.3390/rs13214316

Catoni, M., D'Amico, M. E., Zanini, E., & Bonifacio, E. (2016). Effect of pedogenic processes and formation factors on organic matter stabilization in alpine forest soils. *Geoderma*, *263*, 151-160. https://doi.org/10.1016/j.geoderma.2015.09.005

Caviezel, C., Hunziker, M., Schaffner, M., & Kuhn, N. J. (2014). Soil–vegetation interaction on slopes with bush encroachment in the central Alps – adapting slope stability measurements to shifting process domains. *Earth Surface Processes and Landforms*, *39*(4), 509-521. https://doi.org/10.1002/esp.3513

Chaudhari, P. R., Ahire, D. V., Ahire, V. D., Chkravarty, M., & Maity, S. (2013). Soil bulk density as related to soil texture, organic matter content and available total nutrients of Coimbatore soil. *International Journal of Scientific and Research Publications*, *3*(2), 1-8.

Cianfrani, C., Buri, A., Vittoz, P., Grand, S., Zingg, B., Verrecchia, E., & Guisan, A. (2019). Spatial modelling of soil water holding capacity improves models of plant distributions in mountain landscapes. *Plant and Soil*, *438*(1), 57-70. https://doi.org/10.1007/s11104-019-04016-x

Dai, L., Yuan, Y., Guo, X., Du, Y., Ke, X., Zhang, F., Li, Y., Li, Q., Lin, L., Zhou, H., & Cao, G. (2020). Soil water retention in alpine meadows under different degradation stages on the northeastern Qinghai-Tibet Plateau. *Journal of Hydrology*, *590*, 125397. https://doi.org/10.1016/j.jhydrol.2020.125397

D'Amico, M., Gorra, R., & Freppaz, M. (2015). Small-scale variability of soil properties and soil–vegetation relationships in patterned ground on different lithologies (NW Italian Alps). *CATENA*, *135*, 47-58. https://doi.org/10.1016/j.catena.2015.07.005

Dexter, E., Rollwagen-Bollens, G., & Bollens, S. M. (2018). The trouble with stress: A flexible method for the evaluation of nonmetric multidimensional scaling. *Limnology and Oceanography: Methods*, *16*(7), 434-443. https://doi.org/10.1002/lom3.10257

Dingman, S. L. (2015). *Physical Hydrology: Third Edition*. Waveland Press.

Donhauser, J., & Frey, B. (2018). Alpine soil microbial ecology in a changing world. *FEMS Microbiology Ecology*, *94*(9), fiy099. https://doi.org/10.1093/femsec/fiy099

Egli, M., Dahms, D., & Norton, K. (2014). Soil formation rates on silicate parent material in alpine environments: Different approaches–different results? *Geoderma*, *213*, 320-333. https://doi.org/10.1016/j.geoderma.2013.08.016

Faisal, M., Zamzami, E. M., & Sutarman. (2020). Comparative Analysis of Inter-Centroid K-Means Performance using Euclidean Distance, Canberra Distance and Manhattan Distance. *Journal of Physics: Conference Series*, *1566*(1), 012112. https://doi.org/10.1088/1742-6596/1566/1/012112

FAO (Red.). (2006). *Guidelines for soil description* (4. ed). Food and Agriculture Organization of the United Nations.

Frank, F., McArdell, B., Oggier, N., Baer, P., Christen, M., & Vieli, A. (2016). *Debris flow modeling at Meretschibach and Bondasca catchment, Switzerland: Sensitivity testing of field data-based erosion model*. https://doi.org/10.5194/nhess-2016-295

Gao, L., & Shao, M. (2012). Temporal stability of soil water storage in diverse soil layers. *CATENA*, *95*, 24-32. https://doi.org/10.1016/j.catena.2012.02.020

Giaccone, E., Luoto, M., Vittoz, P., Guisan, A., Mariéthoz, G., & Lambiel, C. (2019). Influence of microclimate and geomorphological factors on alpine vegetation in the Western Swiss Alps. *Earth Surface Processes and Landforms*, *44*(15), 3093-3107. https://doi.org/10.1002/esp.4715

Giupponi, L., Leoni, V., Pedrali, D., Zuccolo, M., & Cislaghi, A. (2023). Plant cover is related to vegetation and soil features in limestone screes colonization: A case study in the Italian Alps. *Plant and Soil*, *483*(1), 495-513. https://doi.org/10.1007/s11104-022-05760-3

Gobiet, A., Kotlarski, S., Beniston, M., Heinrich, G., Rajczak, J., & Stoffel, M. (2014). 21st century climate change in the European Alps—A review. *Science of The Total Environment*, *493*, 1138-1151. https://doi.org/10.1016/j.scitotenv.2013.07.050

Google Earth. (z.d.). Geraadpleegd 22 november 2023, van https://earth.google.com/web/search/MEretschi/@46.25824903,7.65180483,2325.5527824a,6487.40338565d,35y,-19.60439005h,44.9700518t,0.00000001r/data=CnQaShJECiUweDQ3OGYxODJjNWU1NDM5ZjM6MHg3Zjc3NzY2ODlhNDYzOTM0Gc9g-

C3fJUdAIbZrnRPWoR5AKglNRXJIdHNjaGkYAiABIiYKJAlyTaWyrTNHQBHbMpyqdQlHQBlz3po50AggQCE6U2H8Lz8eQDoDCgEw

Gupta, S., Hengl, T., Lehmann, P., Bonetti, S., & Or, D. (2021). SoilKsatDB: Global database of soil saturated hydraulic conductivity measurements for geoscience applications. *Earth System Science Data*, *13*(4), 1593-1612. https://doi.org/10.5194/essd-13-1593-2021

Hagedorn, F., Gavazov, K., & Alexander, J. M. (2019). Above- and belowground linkages shape responses of mountain vegetation to climate change. *Science*, *365*(6458), 1119-1123. https://doi.org/10.1126/science.aax4737

Hartmann, A., Weiler, M., & Blume, T. (2020). The impact of landscape evolution on soil physics: Evolution of soil physical and hydraulic properties along two chronosequences of proglacial moraines. *Earth System Science Data*, *12*(4), 3189-3204. https://doi.org/10.5194/essd-12-3189-2020

Heijmans, M. M. P. D., Magnússon, R. Í., Lara, M. J., Frost, G. V., Myers-Smith, I. H., Van Huissteden, J., Jorgenson, M. T., Fedorov, A. N., Epstein, H. E., Lawrence, D. M., & Limpens, J. (2022). Tundra vegetation change and impacts on permafrost. *Nature Reviews Earth & Environment*, *3*(1), 68-84. https://doi.org/10.1038/s43017-021-00233-0

Heiri, O., Lotter, A. F., & Lemcke, G. (2001). Loss on ignition as a method for estimating organic and carbonate content in sediments: Reproducibility and comparability of results. *Journal of Paleolimnology*, *25*(1), 101-110. https://doi.org/10.1023/A:1008119611481

Hendriks, M. (2010). *Introduction to Physical Hydrology*. OUP Oxford.

Hörsch, B. (2003). Modelling the spatial distribution of montane and subalpine forests in the central Alps using digital elevation models. *Ecological Modelling*, *168*(3), 267-282. https://doi.org/10.1016/S0304-3800(03)00141-8

Intergovernmental Panel On Climate Change (Ipcc). (2022). *The Ocean and Cryosphere in a Changing Climate: Special Report of the Intergovernmental Panel on Climate Change* (1ste dr.). Cambridge University Press. https://doi.org/10.1017/9781009157964

Israels, A. Z. (1984). Redundancy analysis for qualitative variables. *Psychometrika*, *49*(3), 331-346. https://doi.org/10.1007/BF02306024

Isselin-Nondedeu, F., & Bédécarrats, A. (2007). Influence of alpine plants growing on steep slopes on sediment trapping and transport by runoff. *CATENA*, *71*(2), 330-339. https://doi.org/10.1016/j.catena.2007.02.001

Johnston, V. E., Borsato, A., Frisia, S., Spötl, C., Dublyansky, Y., Töchterle, P., Hellstrom, J. C., Bajo, P., Edwards, R. L., & Cheng, H. (2018). Evidence of thermophilisation and elevation-dependent warming during the Last Interglacial in the Italian Alps. *Scientific Reports*, *8*(1), Article 1. https://doi.org/10.1038/s41598-018-21027-3

Jurman, G., Riccadonna, S., Visintainer, R., & Furlanello, C. (2009). *Canberra distance on ranked lists*. 81.

Karamizadeh, S., Abdullah, S. M., Manaf, A. A., Zamani, M., & Hooman, A. (2013). An Overview of Principal Component Analysis. *Journal of Signal and Information Processing*, *04*(03), 173-175. https://doi.org/10.4236/jsip.2013.43B031

Kemppinen, J., Niittynen, P., Virkkala, A.-M., Happonen, K., Riihimäki, H., Aalto, J., & Luoto, M. (2021). Dwarf Shrubs Impact Tundra Soils: Drier, Colder, and Less Organic Carbon. *Ecosystems*, *24*(6), 1378-1392. https://doi.org/10.1007/s10021-020-00589-2

Kia, A., Wong, H. S., & Cheeseman, C. R. (2017). Clogging in permeable concrete: A review. *Journal of Environmental Management*, *193*, 221-233. https://doi.org/10.1016/j.jenvman.2017.02.018

Kirkpatrick, J. B., Green, K., Bridle, K. L., & Venn, S. E. (2014). Patterns of variation in Australian alpine soils and their relationships to parent material, vegetation formation, climate and topography. *CATENA*, *121*, 186-194. https://doi.org/10.1016/j.catena.2014.05.005

Körner, C. (2004). Mountain Biodiversity, Its Causes and Function. *AMBIO: A Journal of the Human Environment*, *33*(sp13), 11-17. https://doi.org/10.1007/0044-7447-33.sp13.11

Kotlarski, S., Gobiet, A., Morin, S., Olefs, M., Rajczak, J., & Samacoïts, R. (2023). 21st Century alpine climate change. *Climate Dynamics*, *60*(1), 65-86. https://doi.org/10.1007/s00382-022-06303-3

Lamprecht, A., Semenchuk, P. R., Steinbauer, K., Winkler, M., & Pauli, H. (2018). Climate change leads to accelerated transformation of high-elevation vegetation in the central Alps. *New Phytologist*, *220*(2), 447-459. https://doi.org/10.1111/nph.15290

Legendre, P., & Legendre, L. (2012). *Numerical Ecology*. Elsevier.

Lengyel, A., & Botta-Dukát, Z. (2022). *A guide to between-community functional dissimilarity measures* (p. 2021.01.06.425560). bioRxiv. https://doi.org/10.1101/2021.01.06.425560

Li, X.-G., Li, F.-M., Zed, R., Zhan, Z.-Y., & Bhupinderpal-Singh. (2007). Soil physical properties and their relations to organic carbon pools as affected by land use in an alpine pastureland. *Geoderma*, *139*(1), 98-105. https://doi.org/10.1016/j.geoderma.2007.01.006

Ma, B., Yu, X., Ma, F., Li, Z., & Wu, F. (2014). Effects of Crop Canopies on Rain Splash Detachment. *PLOS ONE*, *9*(7), e99717. https://doi.org/10.1371/journal.pone.0099717

Maier, F., Lustenberger, F., & Van Meerveld, I. (2023). *Assessment of plot scale sediment transport on young moraines in the Swiss Alps using a fluorescent sand tracer* [Preprint]. Hillslope hydrology/Instruments and observation techniques. https://doi.org/10.5194/egusphere-2023-899

Maier, F., van Meerveld, I., Greinwald, K., Gebauer, T., Lustenberger, F., Hartmann, A., & Musso, A. (2020). Effects of soil and vegetation development on surface hydrological properties of moraines in the Swiss Alps. *CATENA*, *187*, 104353. https://doi.org/10.1016/j.catena.2019.104353

Martinez-Almoyna, C., Piton, G., Abdulhak, S., Boulangeat, L., Choler, P., Delahaye, T., Dentant, C., Foulquier, A., Poulenard, J., Noble, V., Renaud, J., Rome, M., Saillard, A., Consortium, T. O., Thuiller, W., & Münkemüller, T. (2020). Climate, soil resources and microbial activity shape the

distributions of mountain plants based on their functional traits. *Ecography*, *43*(10), 1550-1559. https://doi.org/10.1111/ecog.05269

Masseroli, A., Bollati, I. M., Proverbio, S. S., Pelfini, M., & Trombino, L. (2020). Soils as a useful tool for reconstructing geomorphic dynamics in high mountain environments: The case of the Buscagna stream hydrographic basin (Lepontine Alps). *Geomorphology*, *371*, 107442. https://doi.org/10.1016/j.geomorph.2020.107442

Matteodo, M., Grand, S., Sebag, D., Rowley, M. C., Vittoz, P., & Verrecchia, E. P. (2018). Decoupling of topsoil and subsoil controls on organic matter dynamics in the Swiss Alps. *Geoderma*, *330*, 41-51. https://doi.org/10.1016/j.geoderma.2018.05.011

MD Sahadat Hossain, P. D., Islam, M. A., Badhon, F. F., & Imtiaz, T. (2021). *Permeability Test*. https://uta.pressbooks.pub/soilmechanics/chapter/permeability-test/

Meusburger, K., Bänninger, D., & Alewell, C. (2010). Estimating vegetation parameter for soil erosion assessment in an alpine catchment by means of QuickBird imagery. *International Journal of Applied Earth Observation and Geoinformation*, *12*(3), 201-207. https://doi.org/10.1016/j.jag.2010.02.009

Mueller, M. H., Weingartner, R., & Alewell, C. (2013). Importance of vegetation, topography and flow paths for water transit times of base flow in alpine headwater catchments. *Hydrology and Earth System Sciences*, *17*(4), 1661-1679. https://doi.org/10.5194/hess-17-1661-2013

Munsell color. (2016, september 6). How to Read a Munsell Color Chart [Munsell.com]. *Munsell Color System; Color Matching from Munsell Color Company*. https://munsell.com/about-munsell-color/how-color-notation-works/how-to-read-color-chart/

Nicholls, E. M., & Carey, S. K. (2021). Evapotranspiration and energy partitioning across a forest-shrub vegetation gradient in a subarctic, alpine catchment. *Journal of Hydrology*, *602*, 126790. https://doi.org/10.1016/j.jhydrol.2021.126790

Oki, T., Entekhabi, D., & Harrold, T. (2004). The global water cycle. *Washington DC American Geophysical Union Geophysical Monograph Series*, 225-237. https://doi.org/10.1029/150GM18

Phillips, J. D., Turkington, A. V., & Marion, D. A. (2008). Weathering and vegetation effects in early stages of soil formation. *CATENA*, *72*(1), 21-28. https://doi.org/10.1016/j.catena.2007.03.020

Puth, M.-T., Neuhäuser, M., & Ruxton, G. D. (2014). Effective use of Pearson's product–moment correlation coefficient. *Animal Behaviour*, *93*, 183-189. https://doi.org/10.1016/j.anbehav.2014.05.003

Ringnér, M. (2008). What is principal component analysis? *Nature Biotechnology*, *26*(3), Article 3. https://doi.org/10.1038/nbt0308-303

Rist, A., Roth, L., & Veit, H. (2020). Elevational ground/air thermal gradients in the Swiss inner Alpine Valais. *Arctic, Antarctic, and Alpine Research*, *52*(1), 341-360. https://doi.org/10.1080/15230430.2020.1742022

Rosbakh, S., Bernhardt-Römermann, M., & Poschlod, P. (2014). Elevation matters: Contrasting effects of climate change on the vegetation development at different elevations in the Bavarian Alps. *Alpine Botany*, *124*(2), 143-154. https://doi.org/10.1007/s00035-014-0139-6

Rumpf, S. B., Gravey, M., Brönnimann, O., Luoto, M., Cianfrani, C., Mariethoz, G., & Guisan, A. (2022). From white to green: Snow cover loss and increased vegetation productivity in the European Alps. *Science*, *376*(6597), 1119-1122. https://doi.org/10.1126/science.abn6697

Sabzevari, T., & Talebi, A. (2019). Effect of hillslope topography on soil erosion and sediment yield using USLE model. *Acta Geophysica*, *67*(6), 1587-1597. https://doi.org/10.1007/s11600-019-00361-8

Schober, P., Boer, C., & Schwarte, L. A. (2018). Correlation Coefficients: Appropriate Use and Interpretation. *Anesthesia & Analgesia*, *126*(5), 1763. https://doi.org/10.1213/ANE.0000000000002864

SEVRUK, B. (1997). REGIONAL DEPENDENCY OF PRECIPITATION-ALTITUDE RELATIONSHIP IN THE SWISS ALPS. *Climatic Change*, *36*(3), 355-369. https://doi.org/10.1023/A:1005302626066

Siles, J. A., Cajthaml, T., Minerbi, S., & Margesin, R. (2016). Effect of altitude and season on microbial activity, abundance and community structure in Alpine forest soils. *FEMS Microbiology Ecology*, *92*(3), fiw008. https://doi.org/10.1093/femsec/fiw008

St»hle, L., & Wold, S. (1989). Analysis of variance (ANOVA). *Chemometrics and Intelligent Laboratory Systems*, *6*(4), 259-272. https://doi.org/10.1016/0169-7439(89)80095-4

S.U., S. L., Singh, D. N., & Shojaei Baghini, M. (2014). A critical review of soil moisture measurement. *Measurement*, *54*, 92-105. https://doi.org/10.1016/j.measurement.2014.04.007

Swiss Geoportal. (z.d.). geo.admin.ch. Geraadpleegd 26 juni 2023, van https://map.geo.admin.ch

Swiss National Basic Climatological Network—MeteoSwiss. (z.d.). Geraadpleegd 26 juni 2023, van https://www.meteoswiss.admin.ch/weather/measurement-systems/land-based-stations/swiss-national-basic-climatological-network.html

Talebi, A., Hajiabolghasemi, R., Hadian, M. R., & Amanian, N. (2016). Physically based modelling of sheet erosion (detachment and deposition processes) in complex hillslopes. *Hydrological Processes*, *30*(12), 1968-1977. https://doi.org/10.1002/hyp.10770

Tyagi, B., Takkar, S., & Kumar, P. (2023). Chapter 5 - Soil biological processes of mountainous landscapes: A holistic view. In R. Bhadouria, S. Singh, S. Tripathi, & P. Singh (Red.), *Understanding Soils of Mountainous Landscapes* (pp. 91-113). Elsevier. https://doi.org/10.1016/B978-0-323-95925-4.00008-X

van der Putten, W. H., Bardgett, R. D., Bever, J. D., Bezemer, T. M., Casper, B. B., Fukami, T., Kardol, P., Klironomos, J. N., Kulmatiski, A., Schweitzer, J. A., Suding, K. N., Van de Voorde, T. F. J., & Wardle, D. A. (2013). Plant–soil feedbacks: The past, the present and future challenges. *Journal of Ecology*, *101*(2), 265-276. https://doi.org/10.1111/1365-2745.12054

van Wesemael, B., Mulligan, M., & Poesen, J. (2000). Spatial patterns of soil water balance on intensively cultivated hillslopes in a semi-arid environment: The impact of rock fragments and

soil thickness. *Hydrological Processes*, *14*(10), 1811-1828. https://doi.org/10.1002/1099-1085(200007)14:10<1811::AID-HYP65>3.0.CO;2-D

Vannoppen, W., Vanmaercke, M., De Baets, S., & Poesen, J. (2015). A review of the mechanical effects of plant roots on concentrated flow erosion rates. *Earth-Science Reviews*, *150*, 666-678. https://doi.org/10.1016/j.earscirev.2015.08.011

Viviroli, D., Archer, D. R., Buytaert, W., Fowler, H. J., Greenwood, G. B., Hamlet, A. F., Huang, Y., Koboltschnig, G., Litaor, M. I., López-Moreno, J. I., Lorentz, S., Schädler, B., Schreier, H., Schwaiger, K., Vuille, M., & Woods, R. (2011). Climate change and mountain water resources: Overview and recommendations for research, management and policy. *Hydrology and Earth System Sciences*, *15*(2), 471-504. https://doi.org/10.5194/hess-15-471-2011

Wang, C., Zhao, C., Xu, Z., Wang, Y., & Peng, H. (2013). Effect of vegetation on soil water retention and storage in a semi-arid alpine forest catchment. *Journal of Arid Land*, *5*(2), 207-219. https://doi.org/10.1007/s40333-013-0151-5

Wild, J., Kopecký, M., Macek, M., Šanda, M., Jankovec, J., & Haase, T. (2019). Climate at ecologically relevant scales: A new temperature and soil moisture logger for long-term microclimate measurement. *Agricultural and Forest Meteorology*, *268*, 40-47. https://doi.org/10.1016/j.agrformet.2018.12.018

Wu, J., Anderson, B. J., Buckley, H. L., Lewis, G., & Lear, G. (2016). Aspect has a greater impact on alpine soil bacterial community structure than elevation. *FEMS Microbiology Ecology*, fiw253. https://doi.org/10.1093/femsec/fiw253

Xu, S., Yu, Z., Lettenmaier, D. P., McVicar, T. R., & Ji, X. (2020). Elevation-dependent response of vegetation dynamics to climate change in a cold mountainous region. *Environmental Research Letters*, *15*(9), 094005. https://doi.org/10.1088/1748-9326/ab9466

Yang, F., Zhang, G.-L., Yang, J.-L., Li, D.-C., Zhao, Y.-G., Liu, F., Yang, R.-M., & Yang, F. (2014). Organic matter controls of soil water retention in an alpine grassland and its significance for

hydrological processes. *Journal of Hydrology*, *519*, 3086-3093. https://doi.org/10.1016/j.jhydrol.2014.10.054

Yang, Y., Chen, R., Song, Y., Han, C., Liu, Z., & Liu, J. (2020). Spatial variability of soil hydraulic conductivity and runoff generation types in a small mountainous catchment. *Journal of Mountain Science*, *17*(11), 2724-2741. https://doi.org/10.1007/s11629-020-6258-1

Yang, Y., Zhang, L., Li, H., He, H., Wei, Y., Luo, J., Zhang, G., Huang, Y., Li, Y., & Zhou, H. (2018). Soil physicochemical properties and vegetation structure along an elevation gradient and implications for the response of alpine plant development to climate change on the northern slopes of the Qilian Mountains. *Journal of Mountain Science*, *15*(5), 1006-1019. https://doi.org/10.1007/s11629-017-4637-z

Yimer, F., Ledin, S., & Abdelkadir, A. (2006). Soil property variations in relation to topographic aspect and vegetation community in the south-eastern highlands of Ethiopia. *Forest Ecology and Management*, *232*(1), 90-99. https://doi.org/10.1016/j.foreco.2006.05.055

Zettl, J., Lee Barbour, S., Huang, M., Si, B., & Leskiw, L. A. (2011). Influence of textural layering on field capacity of coarse soils. *Canadian Journal of Soil Science*, *91*(2), 133-147. https://doi.org/10.4141/cjss09117

Zuo, Y., & He, K. (2021). Evaluation and Development of Pedo-Transfer Functions for Predicting Soil Saturated Hydraulic Conductivity in the Alpine Frigid Hilly Region of Qinghai Province. *Agronomy*, *11*(8), Article 8. https://doi.org/10.3390/agronomy11081581

9 Appendix

Topographic property	Unit
Slope	Degrees. Classification: (1: Flat 0–4°, 2: Sloping 4–12°, 3: Strongly sloping 12-20°, 4: Steep 20–35°, 5: Very steep 35-50°, 6: Extremely steep to vertical > 50°)
Aspect	Degrees (N (0°), E (90°), S (180°) and W (270°)
Slope form	Concave, convex, straight, complex

Appendix 1: List of topographic properties.

Topography property	How to characterize	How to measure
Slope	Use the compass to estimate the slope angle.	Estimation of slope in degrees and classify the slope.
Aspect	Use the compass to assess the aspect of the slope.	Estimation of the major wind direction of the slope.
Slope form	Assess the main slope form within the plot.	Evaluate the slope form.

Appendix 2: Protocol for the in-field measurements of the topography properties.

Soil property	Unit or classes
Soil depth	cm
Organic layer depth	cm
Matrix grading	none, fining up, coarsening up
Macropores	nr/dm^2 in the wall of the pit
Rooting depth	cm
Fine root abundance (< 1 mm)	nr/dm^2 in the wall of the pit
coarse root abundance (< 1 mm)	nr/dm^2 in the wall of the pit
Litter depth	cm

Appendix 3: List of soil properties, described for the entire soil profile.

Soil property	Unit or classes
Soil texture	sand, loam, clay, silt etc.
Musell colour	light grey, grey, black etc.
Rock fragments	%
Rock fragment size	very fine (2-4 mm), fine (4-8 mm), medium (8-16 mm), coarse (16-32 mm), very coarse (32-64 mm)
Clast sorting	Poorly, moderately, well sorted etc.

Appendix 4: List of soil properties, described at 10, 20 and 30 cm depth.

Horizons properties
Thickness (cm)
Classification (O, A, E, C)

Appendix 5: List of horizon properties (FAO, 2006).

Horizon class	Properties
O	Dominated by organic material and undecomposed litter. Mineral fraction is a small proportion.
C	Little affected by pedogenic processes. Mostly mineral layer.
A	Mineral layer at surface or below O-horizon, including accumulation of humified organic matter.

E	Main feature is loss of silicate clay iron or aluminium, which destruct some of the original rock structures.

Appendix 6: Explanation of soil horizon class properties (FAO, 2006).

Soil property	How to characterize	How to measure
Soil depth	The max soil depth is at the surface of the bedrock	Measure the depth in cm with a ruler.
Organic layer depth	The organic layer contains organic living organisms, plants, litter and also (partly) decomposed organic matter.	Identify organic layer and measure the depth of the layer in cm with a ruler.
Litter depth	Layer of litter that is not decomposed into soil organic matter.	Identify and measure litter layer in cm with a ruler.
Matrix grading	The average size of the soil grains can vary with depth. Generally, there are three possibilities: 'fining upwards', 'coarsening upwards' or 'no grading'.	Evaluate the matrix grading.
Macropores	Assess a critical value from which a pore is a macropore (diameter > 2 mm), choose a representative area of 1 dm^2 in the soil profile and count the number of macropores.	Estimate the average number of macropores per dm^3.
Rooting depth	Maximum depth of the living roots.	Measure the depth in cm.
Fine root abundance	Assess a critical value when a root is fine (diameter < 1 mm), choose a representative area of 1 dm^2 in the soil profile and count the number of fine roots.	Estimate the average number of fine roots per dm^3 in the rooted layer.
Coarse root abundance	Assess a critical value when a root is coarse (diameter > 1 mm), choose a representative area of 1 dm^2 in the soil profile and count the number of coarse roots.	Estimate the average number of coarse roots per dm^3 in the rooted layer.

Appendix 7: Protocol for determining the in-field soil characteristics that are described for the entire soil profile (FAO, 2006).

Soil property	How to characterize	How to measure
Soil texture	Classification using scheme of Appendix 9.	Sand, loam, silt, clay, sandy loam, etc.
Musell color	Classification using Munsell method (Appendix 10-14)	Match the soil color with the right hue, value and chroma.
Rock fragments size	Asses the average rock fragment size.	very fine (2-4 mm), fine (4-8 mm), medium (8-16 mm), coarse (16-32 mm), very coarse (32-64 mm).
Rock fragments (%)	Use Appendix 15 for estimation.	Estimation of percentage of rock fragments.

Clast sorting	Use Appendix 16 for classification.	Very poorly to very well sorted.

Appendix 8: Protocol for determining the in-field measurements for soil properties at 10, 20 and 30 cm depth (FAO, 2006).

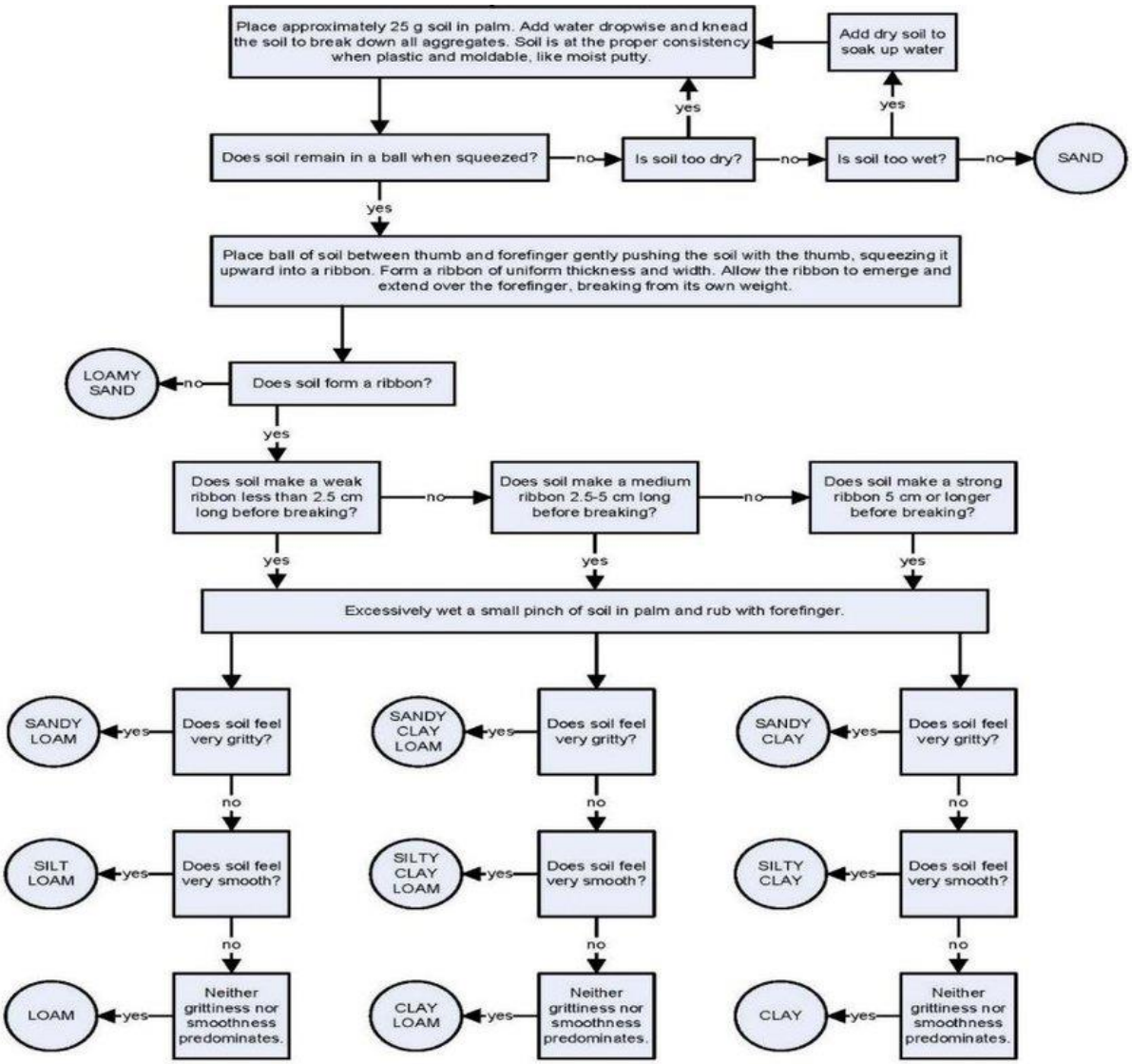

Appendix 9: Protocol to classify the soil texture in-field estimation.

Step	Component	Munsell code
Step 1	Hue: red, yellow, green etc., or a combination.	Red (R), yellow (Y), yellow-red (YR), green-yellow (GY), etc.
Step 2	Value: the lightness of the color.	The scale of value ranges from 0 for pure black to 10 for pure white.
Step 3	Chroma: degree of a color from a neutral color of the same value.	Typically range from 2 to 14, sometimes up to 30.

Appendix 10: Protocol for Munsell color classification in field (Munsell color, 2016).

Appendix 11: Munsell hue classification diagram (Munsell color, 2016).

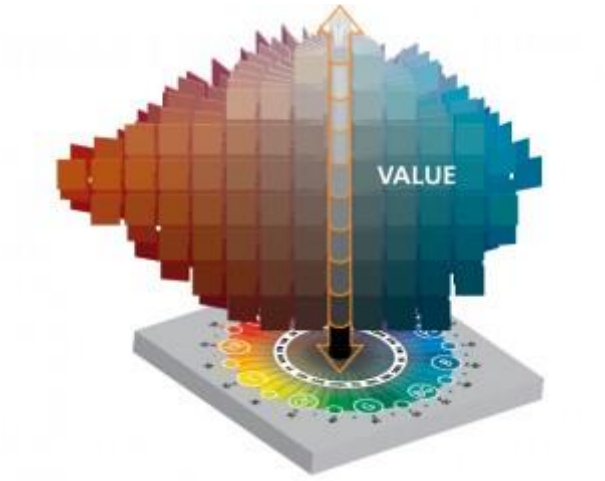

Appendix 12: Munsell value classification diagram (Munsell color, 2016).

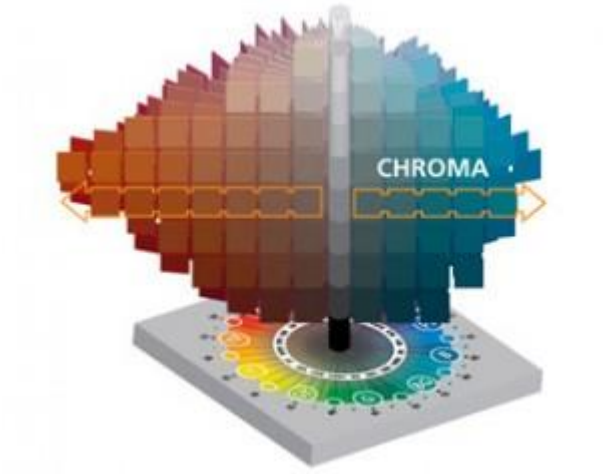

Appendix 13: Munsell chroma classification diagram (Munsell color, 2016).

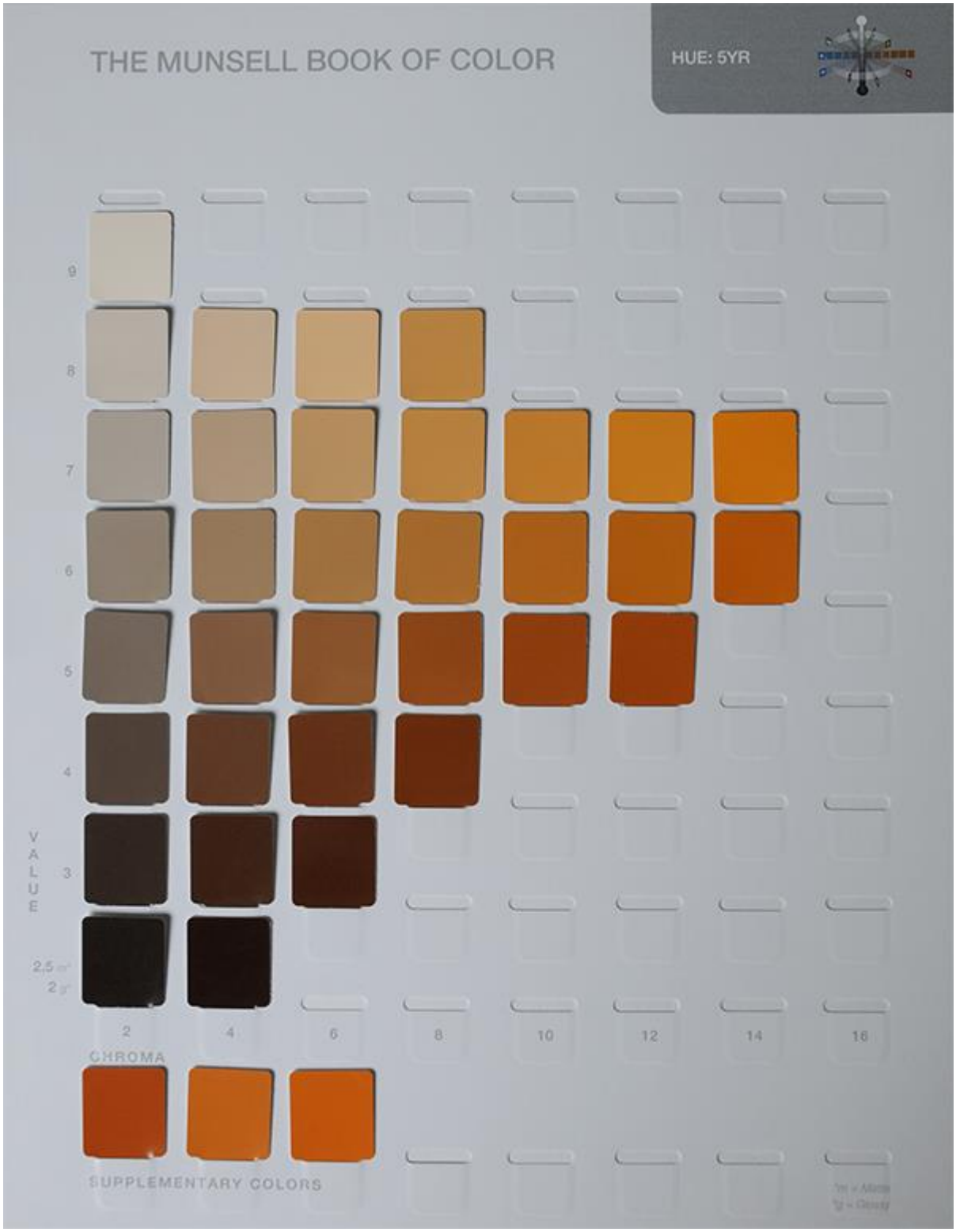

Appendix 14: Example of a Munsell color chart (Munsell color, 2016).

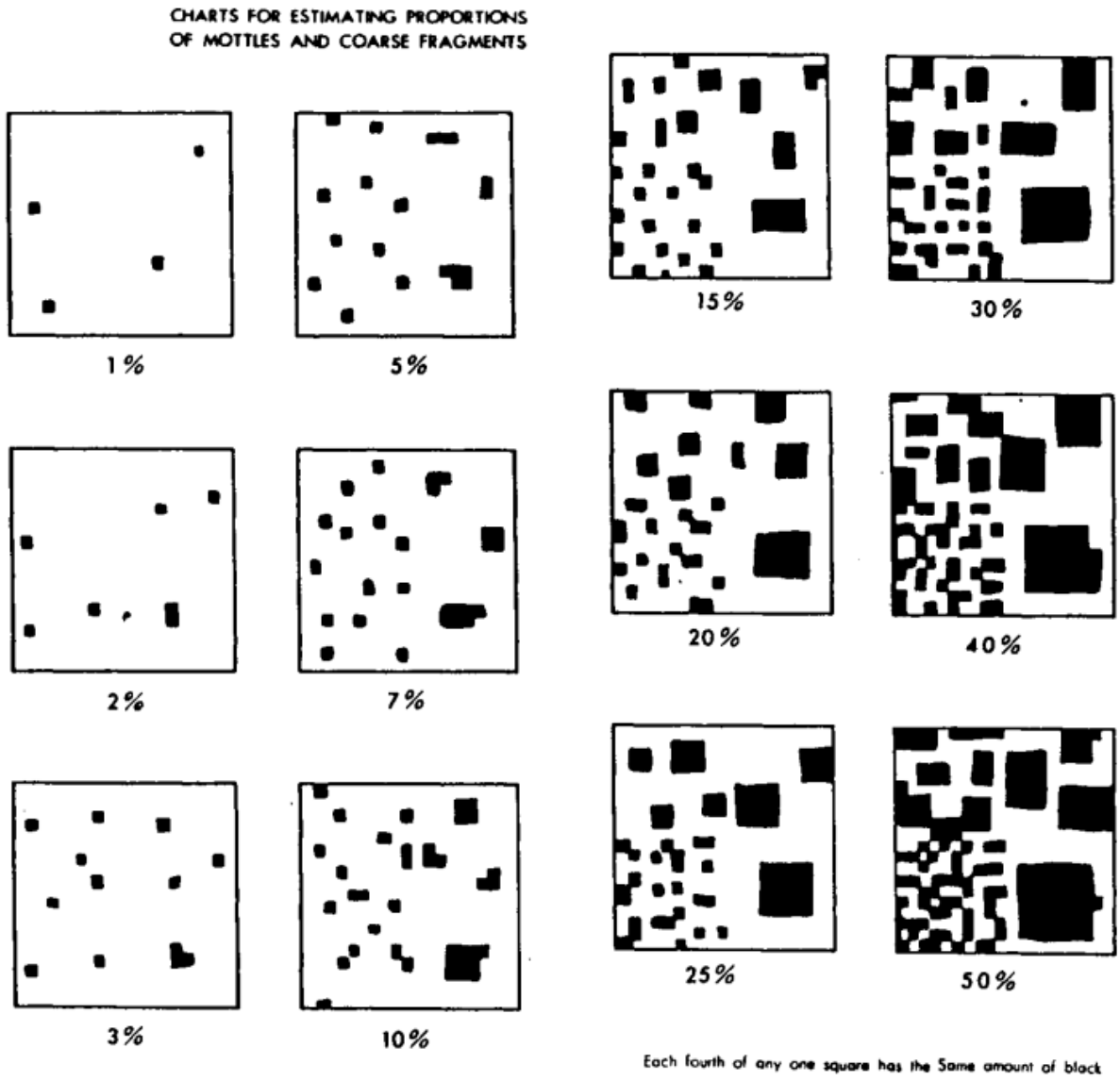

Appendix 15: Estimation diagram of rock size and percentages for in-field estimation.

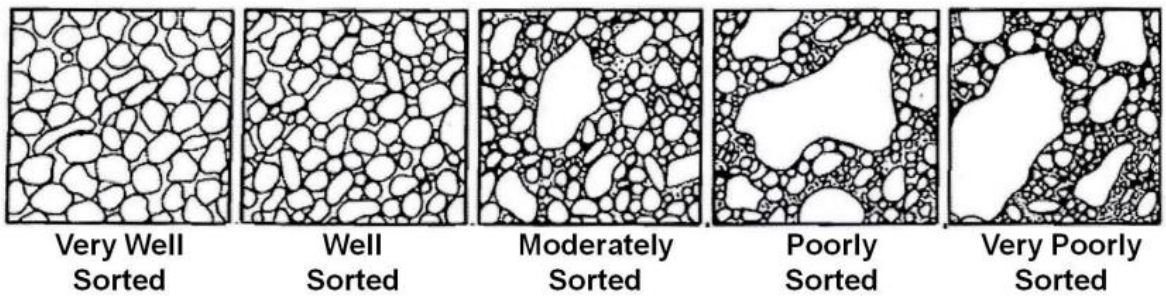

Figure A2-1 *Chart for the field estimation of sorting.*

Appendix 16: Clast sorting diagram for in-field estimation.

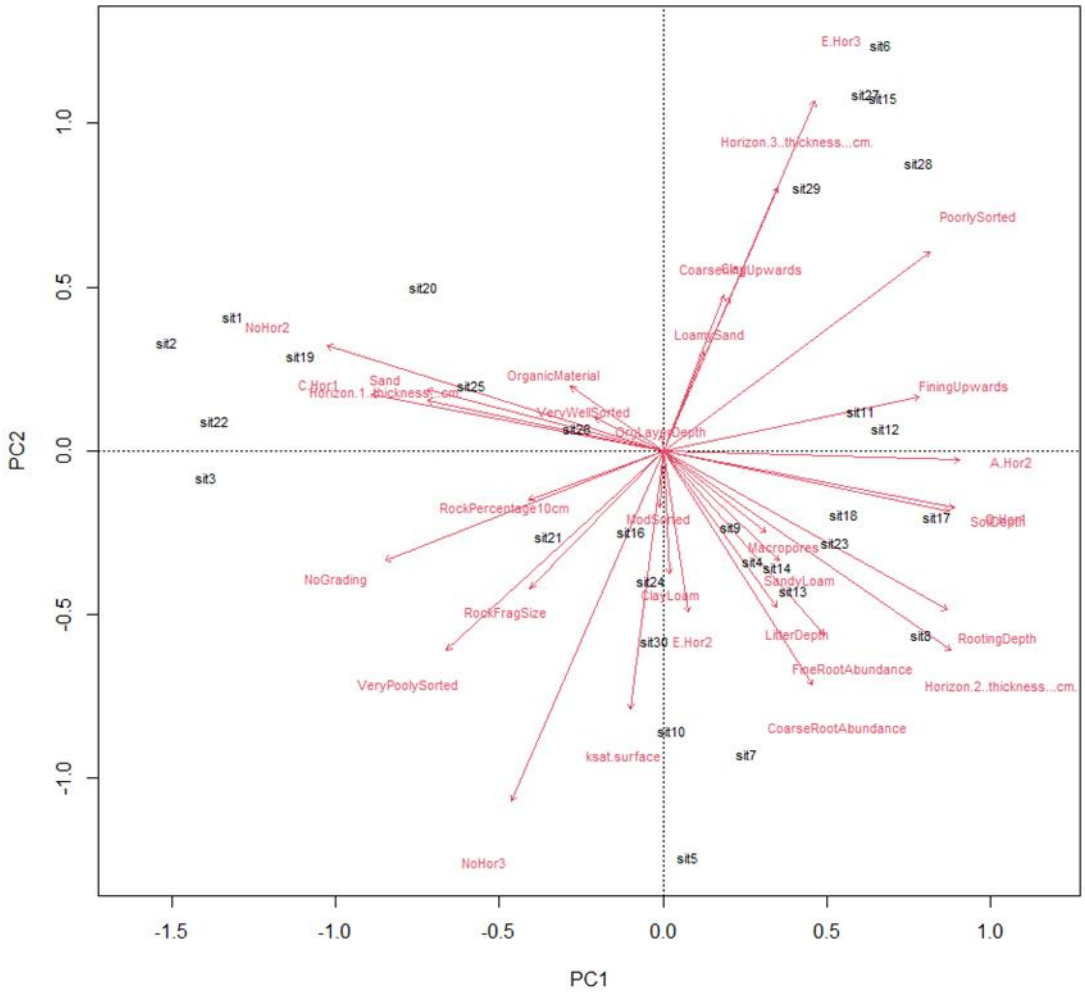

Appendix 17: PCA plot of both the numeric and ordinal soil parameters (red arrows) and plot locations (black codes (e.g. sit1) (variance explained by PC1 and PC2 = 37%).

Plot number PCA	Plot number
sit1	B5
sit2	B6
sit3	B8
sit4	F1
sit5	F3
sit6	F4
sit7	F5
sit8	F6
sit9	F7
sit10	F8
sit11	G1
sit12	G2
sit13	G3
sit14	G4
sit15	G6
sit16	G7
sit17	P2

sit18	P3
sit19	P4
sit20	P5
sit21	P6
sit22	P7
sit23	P8
sit24	S1
sit25	S2
sit26	S3
sit27	S4
sit28	S5
sit29	S6
sit30	S7
sit31	S8

Appendix 18: Plot numbers of PCA plot and the corresponding original, plot location numbers.

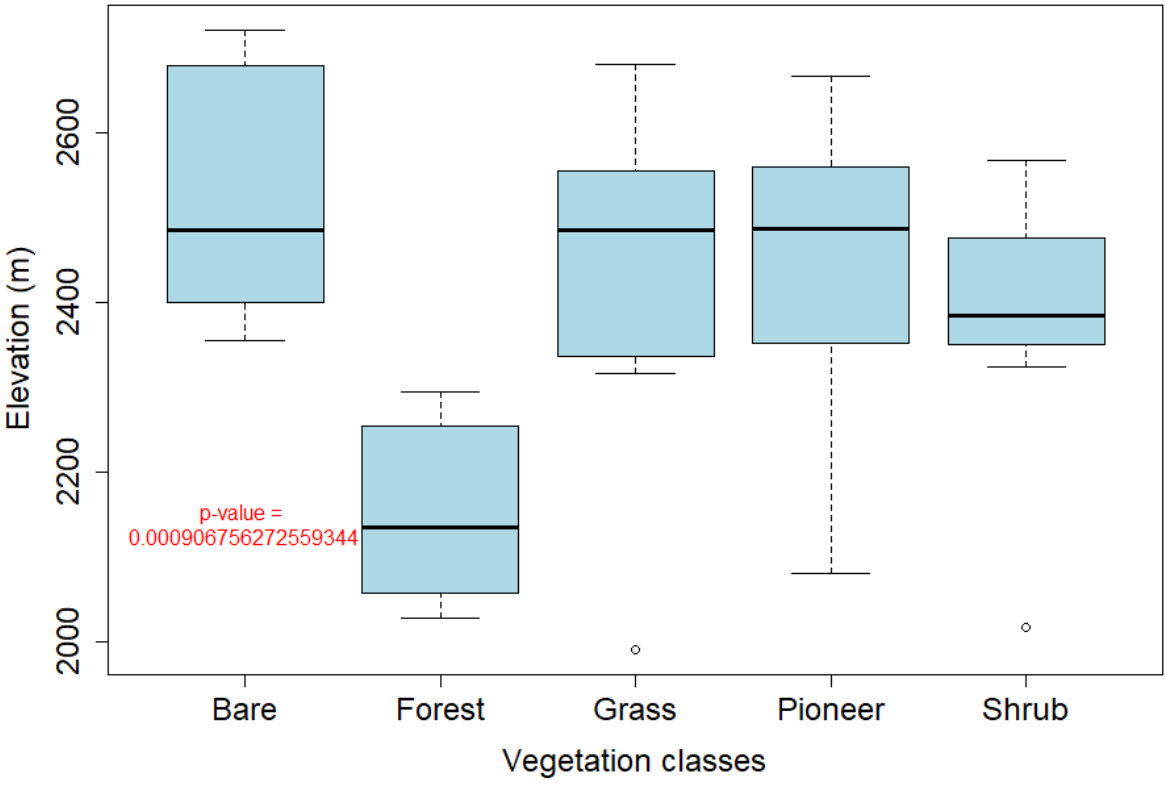

Appendix 19: : Boxplot of elevation (m) for the five vegetation classes (bare, forest, grass, pioneer and shrub), including the overall p-value (red).

	Bare	**Forest**	**Grass**	**Pioneer**
Forest	****			
Grass	-	**		
Pioneer	-	**	-	
Shrub	-	-	-	-

Appendix 20: p-values of the pairwise comparisons using a t-test between the different vegetation classes (bare, forest, grass, pioneer and shrub) for the boxplot against elevation (m).

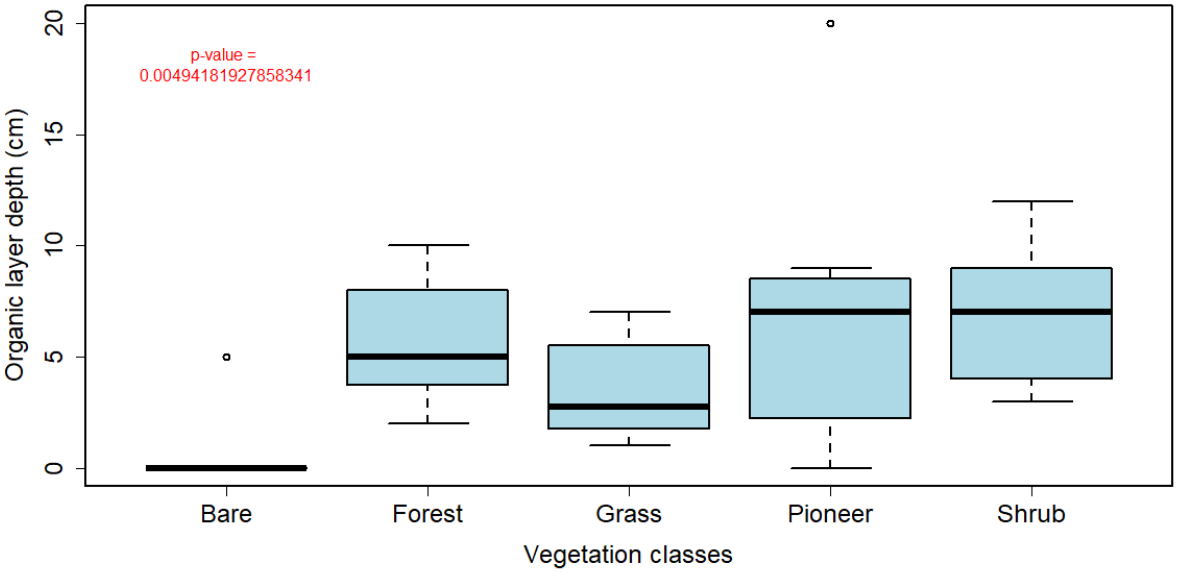

Appendix 21: Boxplot of organic layer depth (cm) for the five vegetation classes (bare, forest, grass, pioneer and shrub), including the overall p-value (red).

	Bare	**Forest**	**Grass**	**Pioneer**
Forest	-			
Grass	-	-		
Pioneer	*	-	-	
Shrub	*	-	-	-

Appendix 22: p-values of the pairwise comparisons using a t-test between the different vegetation classes (bare, forest, grass, pioneer and shrub) for the boxplot against organic layer depth (cm).

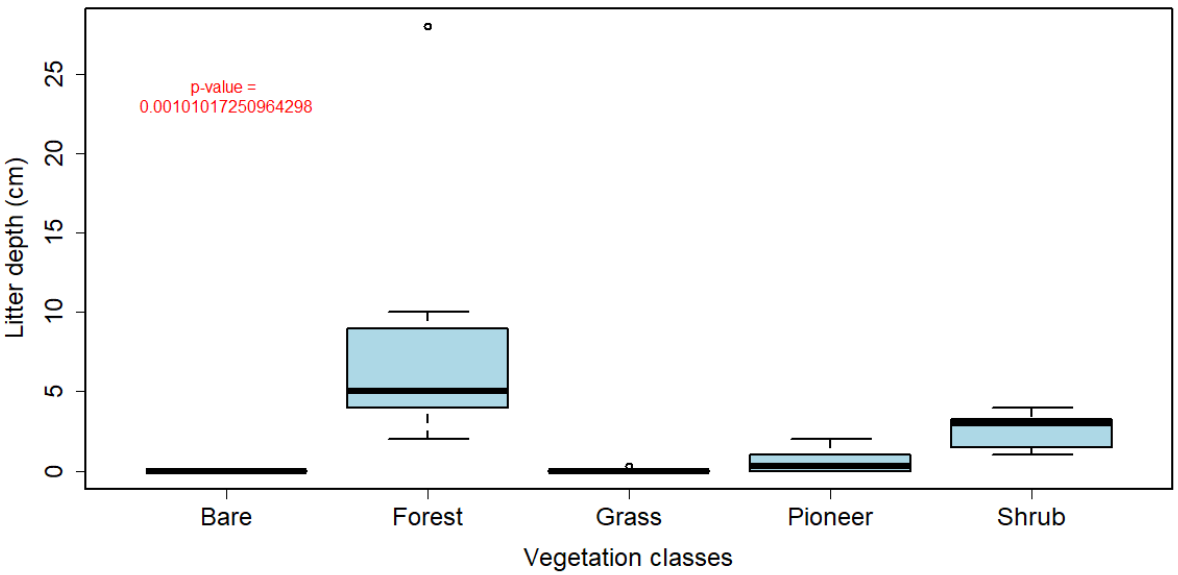

Appendix 23: Boxplot of litter depth (cm) for the five vegetation classes (bare, forest, grass, pioneer and shrub), including the overall p-value (red).

	Bare	Forest	Grass	Pioneer
Forest	***	-	-	-
Grass	-	***	-	-
Pioneer	-	**	-	-
Shrub	-	-	-	-

Appendix 24: p-values of the pairwise comparisons using a t-test between the different vegetation classes (bare, forest, grass, pioneer and shrub) for the boxplot against litter depth (cm).

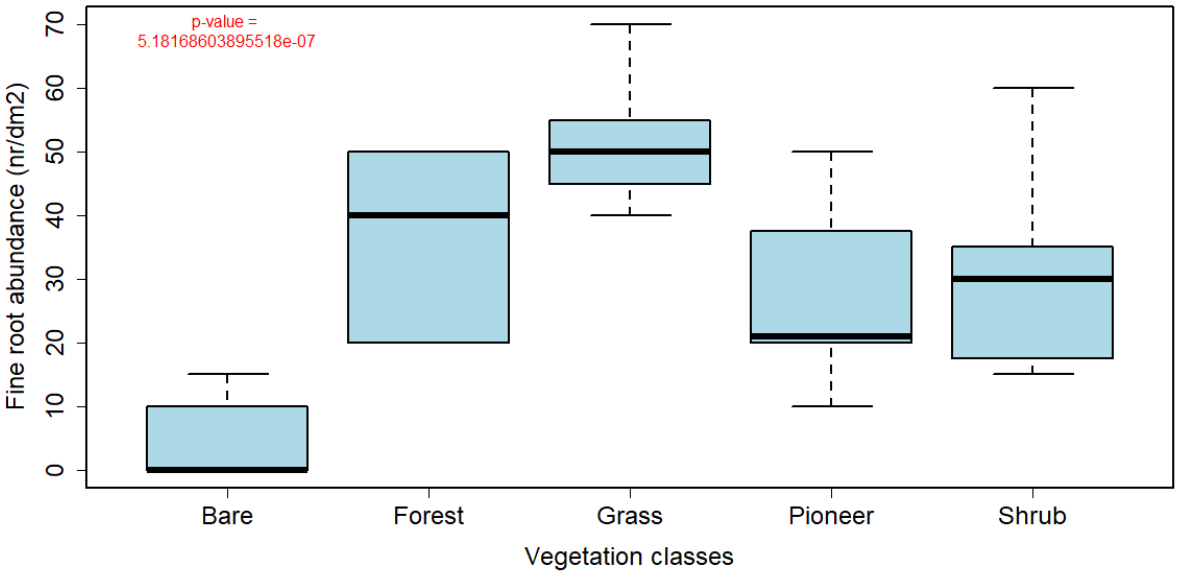

Appendix 25: Boxplot of fine root abundance (nr/dm²) for the five vegetation classes (bare, forest, grass, pioneer and shrub), including the overall p-value (red).

	Bare	Forest	Grass	Pioneer
Forest	****			
Grass	*****	-		
Pioneer	***	-	***	
Shrub	***	-	*	-

Appendix 26: p-values of the pairwise comparisons using a t-test between the different vegetation classes (bare, forest, grass, pioneer and shrub) for the boxplot against fine root abundance (nr/dm²).

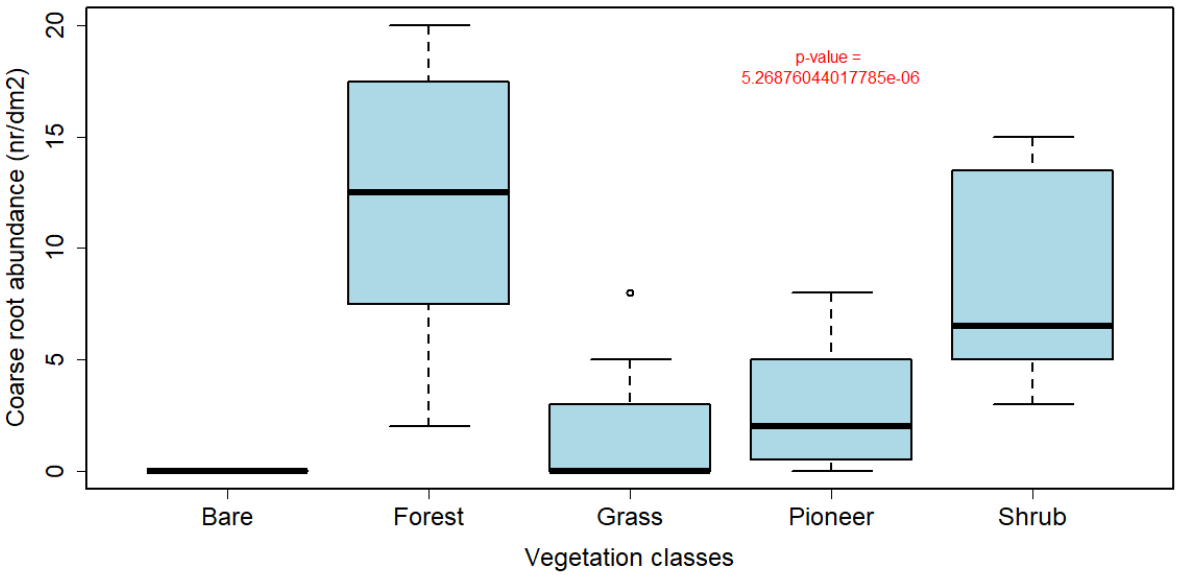

Appendix 27: Boxplot of coarse root abundance (nr/dm²) for the five vegetation classes (bare, forest, grass, pioneer and shrub), including the overall p-value (red).

	Bare	Forest	Grass	Pioneer
Forest	*****			
Grass	-	****		
Pioneer	-	****	-	
Shrub	***	-	*	-

Appendix 28: p-values of the pairwise comparisons using a t-test between the different vegetation classes (bare, forest, grass, pioneer and shrub) for the boxplot against coarse root abundance (nr/dm²).

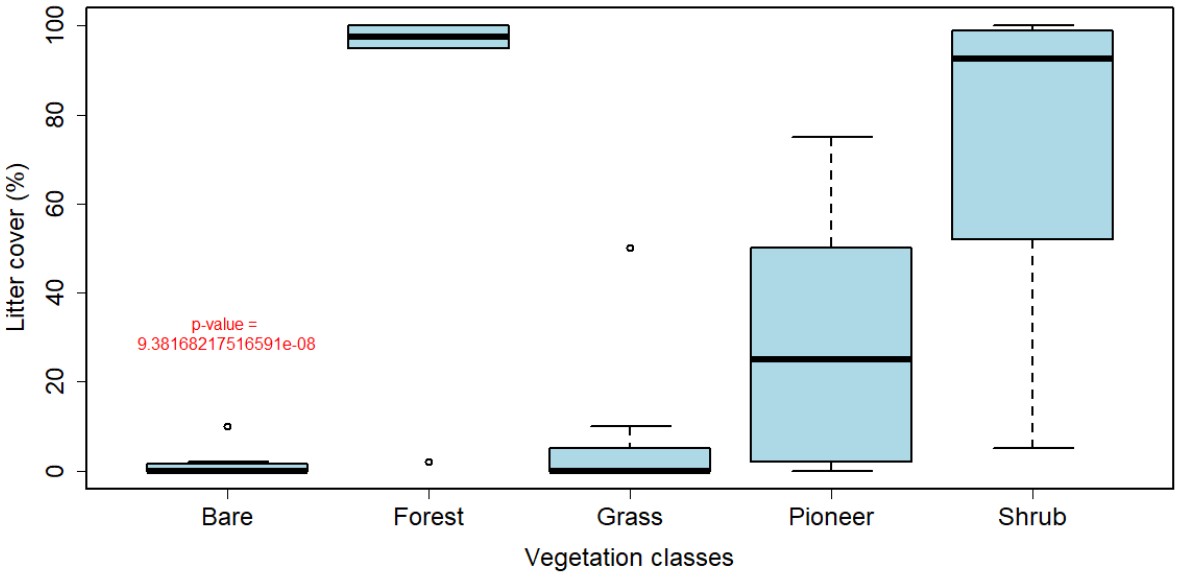

Appendix 29: Boxplot of litter cover (%) for the five vegetation classes (bare, forest, grass, pioneer and shrub), including the overall p-value (red).

	Bare	Forest	Grass	Pioneer
Forest	*****			
Grass	-	*****		
Pioneer	-	***	-	
Shrub	*****	-	****	**

Appendix 30: p-values of the pairwise comparisons using a t-test between the different vegetation classes (bare, forest, grass, pioneer and shrub) for the boxplot against litter cover (%).

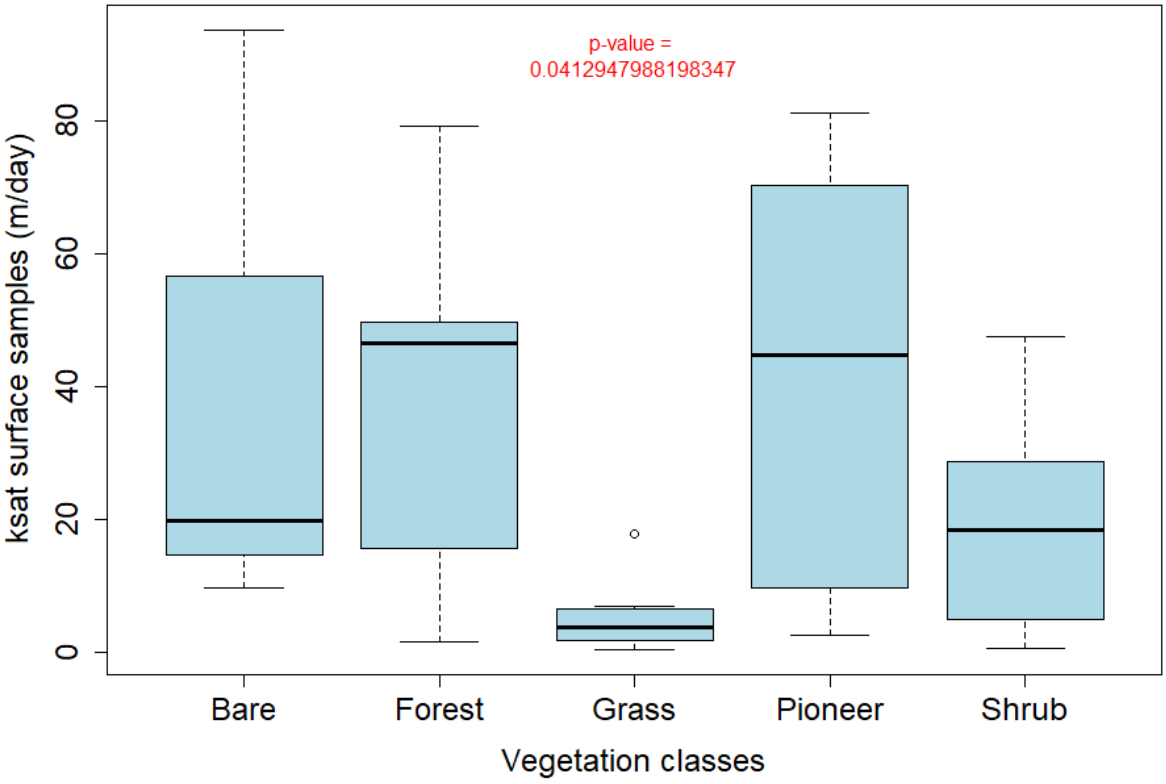

Appendix 31: Boxplot of k_{sat} surface (m/day) for the five vegetation classes (bare, forest, grass, pioneer and shrub), including the overall p-value (red).

	Bare	Forest	Grass	Pioneer
Forest	-			
Grass	-	-		
Pioneer	-	-	-	
Shrub	-	-	-	-

Appendix 32: p-values of the pairwise comparisons using a t-test between the different vegetation classes (bare, forest, grass, pioneer and shrub) for the boxplot against k_{sat} surface (m/day).